Bringing theory to life: Experimental demonstration of noise-induced transitions in biological systems

by

RajReni Beckett Kaul

(Under the Direction of John M. Drake)

Abstract

Ecologists have long been interested in understanding the causal links between environmental stochasticity and population abundance. Most theories developed to explain these dynamics use a deterministic representation of the natural world where substantial changes of a population's size occur through one of two paths as explained by alternative stable states. Either the system moves into another stable state due to an external push, or the equilibrium population size itself changes as a kinetic parameter changes. However, if the natural world is recast using a stochastic representation, a third path arises: noise-induced transitions (NITs). By taking stochasticity in the natural world into account, the location and/or number of equilibrium population sizes can change. NITs have been demonstrated in chemistry and physics but have largely been ignored in ecology. This dissertation consists of two combined theoretical/empirical studies to demonstrate NITs in biological populations. First, I demonstrate the destabilizing effects of environmental noise through a noise-induced extinction—as expected under the ecological dogma of stochasticity—using chemostats of the cyanobacteria, *Aphanizomenon flos-aqua*. Then, I present the surprising result of noise-induced persistence in stochastically harvested populations using microcosms of *Saccharomyces cerevisiae*. This dissertation is the first step in building a concept map of noise-induced outcomes given dif-

ferent combinations of nonlinear dynamics and types of environmental noise. Building upon these results, we can develop a heuristic understanding of how and when a stochastic rather than deterministic model is a more appropriate description of the natural world.

INDEX WORDS: Environmental stochasticity, Extinction, Microcosm, Noise-induced transition, Population dynamics, Transitions

Bringing theory to life: Experimental demonstration of noise-induced transitions in biological systems

by

RajReni Beckett Kaul

B.S., Michigan State University, 2007

M.S., Auburn University, 2011

A Dissertation Submitted to the Graduate Faculty

of The University of Georgia in Partial Fulfillment

of the

Requirements for the Degree

Doctor of Philosophy

Athens, Georgia

2021

Bringing theory to life: Experimental demonstration of noise-induced transitions in biological systems

by

RajReni Beckett Kaul

Major Professor: John M. Drake

Committee: Ford Ballantyne IV
Andrew Park
William C. Ratcliff

Electronic Version Approved:

Ron Walcott
Dean of the Graduate School
The University of Georgia
August 2021

Contents

List of Figures

List of Tables

Introduction

1.1 Overview

Nature presents itself in many different states. Understanding and explaining how populations, communities, and ecosystems switch between these states is an overarching problem (May, 2001; Strogatz, 2001; Cushing *et al.*, 2001; Chase, 2003). This is especially the case during catastrophic changes, such as sudden extinction caused by a disproportionately small change in the population's vital rates (Post & Forchhammer, 2002; Stenseth *et al.*, 2002; Scheffer *et al.*, 2001, 2009). These rapid extinction events are typically explained by one of two mechanisms (Nolting & Abbott, 2016).

The first is a change in kinetic parameter value. For example, in the logistic map if the kinetic parameter of intrinsic growth rate drops below zero ($r \leq 0$) the non-zero equilibrium population size (K, previously stable, now unstable) exchanges stability with the extinction equilibrium (previously unstable, now stable). The population size then moves towards the newly stable equilibrium of extinction (Fig. 1.1A). A population approaching the stability switch in equilibrium values has a unique set of characteristics, a subset of these characteristics are referred to as critical slowing down and has been experimentally demonstrated (Drake & Griffen, 2010).

The second mechanism used to explain rapid extinction is a change in the local equilibrium value. In this case, extinction and a non-zero equilibrium population size are both

stable and are buffered by an unstable intermediate equilibrium. Populations with this pattern of stable-unstable-stable equilibrium values are said to have alternative stable states (Fig. 1.1B). A population with alternative stable states can undergo rapid extinction when the population size falls below the intermediate population size equilibrium (as reviewed by Thornton *et al.*, 2014).

However, there is a third possible mechanism to explain catastrophic change (May, 1973). Rather than the population size moving towards the locally stable equilibrium size, the number and location of the equilibrium population size change (Fig. 1.1C). While sometimes more broadly defined, within this work the appearance and disappearance of equilibrium values is referred to as a phase transition, or transition. Usually we think about a macroscopic parameter (such as one of the kinetic parameters) driving the phase transition. But, in stochastic systems there is another possibility: the system noise itself may induce qualitative changes in the steady state which is now considered to be a probability distribution, rather than a deterministic limiting behavior like a point equilibrium or limit cycle. When the mechanism causing the phase transition is a change in the magnitude of environmental variability this phenomenon may be called a *noise-induced phase transition*, or shortened to *noise-induced transition* (NIT; Horsthemke & Lefever, 2006; Kabashima *et al.*, 1979a; Kawakubo *et al.*, 1973b,a; Kabashima *et al.*, 1976; Kawakubo *et al.*, 1981; Briggs & Rauscher, 1973; De Kepper & Horsthemke, 1979a; Arecchi & Harrison, 2012).

The possibility and prevalence of NITs in ecological systems has been overlooked for the last 50 years. However, advances in computational power and the move towards ecological 'big data' have made exploring this new mechanisms highly tractable (Farley *et al.*, 2018). Not only *can* this mechanism now be explored, it *should* be explored now. As we observe the 6th mass extinction in the Anthropocene age, many ecological systems are believed to be approaching their sustainability limits (Wake & Vredenburg, 2008; Barnosky *et al.*, 2011; Ceballos *et al.*, 2017). Additionally, environmental noise is expected to increase with climate change (Thornton *et al.*, 2014). It is entirely possible that as ecological systems approach

their critical points, environmental stochasticity will independently increase representing a double threat to the resilience of historically robust ecosystems. The combination of these factors requires systematically incorporating environmental noise into the understanding, modeling and forecasting of population dynamics. The remainder of this chapter reviews some general ideas about NIT, and place it in the context of current ecological work. The following chapters report on the first experimental demonstrations of a NIT in biological systems paired with a mechanistic model's predictions.

1.2 Exploring An Alternative Mechanism: Case Studies

This section reviews NITs in ecological population models. The impact of environmental noise will be highlighted by first reviewing the deterministic model, and then modifying the model to include environmental stochasticity. While comparing models, I assume that the reader is familiar with deterministic models but not necessarily stochastic models. For this reason I will occasionally introduce terminology and concepts used in stochastic models, and when possible draw connections to the deterministic counterpart. Next, I review theoretical studies of NITs in grassland ecosystems. Finally, I review a few empirical studies from other disciplines.

1.2.1 Ecological Case Studies of NIT

Case Study 1: Logistic model

A NIT can be illustrated by first exploring a continuous time logistic model in a constant environment, and then comparing to the same population in a randomly varying environment.

$$\frac{dN}{dt} = rN(K_o - N) \tag{1.1}$$

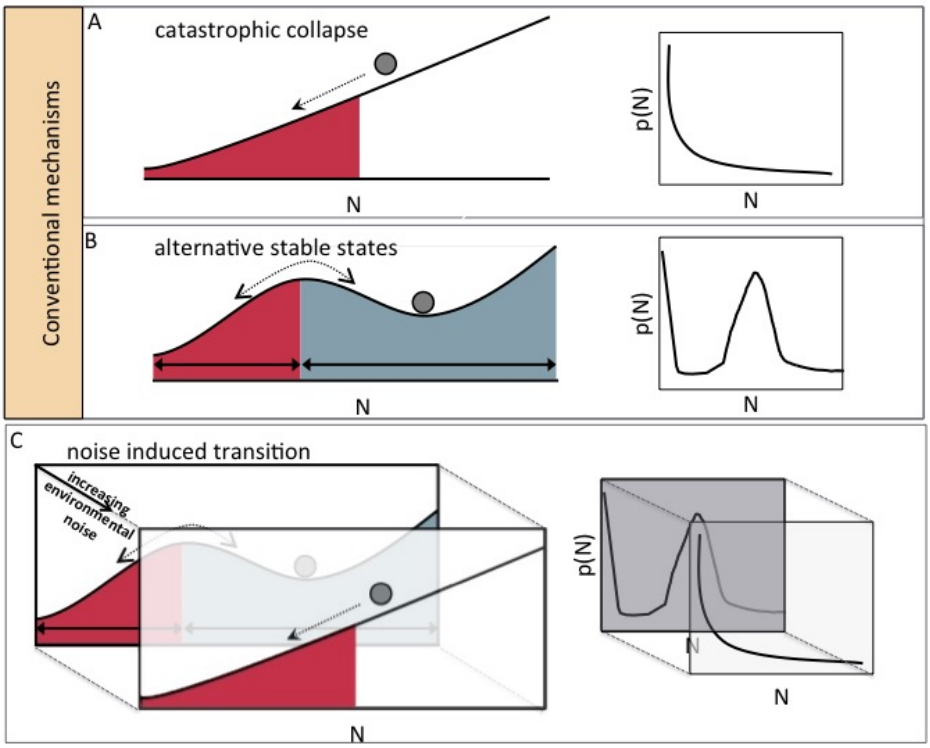

Figure 1.1: Potential diagram and corresponding histogram of population size. Panels A, and B represent conventional mechanisms leading to qualitative change, while panel C describes the mechanism explored in this work. (A) When a kinetic parameter value is below a threshold to maintain a non-zero population size, extinction colored in red is the only stable equilibrium value. This is reflected in a histogram of the population size over time, where the most likely population size is zero. If the population is perturbed (ie. an immigration event), the population size will eventually return to zero. Extinction can also be one of two alternative stable states, as in the case of populations subject to an Allee effect. If the population is perturbed such that the size drops below the minimum threshold represented by the peak between the two wells in (B), the population will go extinct. However, this is reversible by an immigration of individuals larger than the minimum threshold. In the case of a noise-induced transition, the potential diagram changes shape. Panel C is an example of a noise-induced extinction where a system with minimal environmental noise has two stable states. As the environmental noise is increased, the potential diagram undergoes a transition such that extinction becomes the only stable state. This transition can be detected by a qualitative change in the histogram.

The equilibria of this model are extinction and carrying capacity ($N^\star = (0, K_o)$). The stability of the equilibria is determined by the growth rate parameter r. For populations with a sufficiently large growth rate ($r > 0$), the carrying capacity (K) is the stable equilibrium, while extinction is an unstable equilibrium. If the growth rate falls below the threshold

($r = 0$), the stability is exchanged. The logistic model can be simplified by rescaling time ($t' = rt$). This rescaling restricts the model to the space of parameters where ($r > 0$) (Eq 1.2).

$$f(N) = N(K_o - N) \tag{1.2}$$

Now, natural populations exist in constantly changing environments, for instance with respect to the resources available to the population, causing the environment's instantaneous carrying capacity to fluctuate. This environmental stochasticity can be introduced into the system by replacing the constant carrying capacity parameter (K_o) with a random normal variable of mean K_o and variance s_{gn}.

$$\begin{aligned} f(N) &= N(K_{gn} - N) \\ K_{gn} &\sim N(K_o, s_{gn}) \end{aligned} \tag{1.3}$$

This stochastic model cannot be studied as above due to the impact of the random variable on the model's stability. However, there are direct analogs. Instead of calculating the state values at the root of the model (ie. solve for $N^\star$ when $\frac{dN}{dt} = 0$), the system's steady state value must be expressed in probabilistic terms. When the noise is very small, the most probable states are parametrically equivalent to the equilibrium values of the deterministic model. The probability density function (pdf) which is the inverse of the potential landscape for 1.3 can be derived using the Fokker-Planck equation and Ito's interpretation of a stochastic equation such that

$$p(N) = \left[\frac{s_{gn}}{2}\Gamma\Big(\frac{2k_o}{s_{gn}} - 1\Big)\right]^{-1} \Big(\frac{2N}{s_{gn}}\Big)^{(2k_o/s_{gn})-2} \exp\Big(\frac{2N}{s_{gn}}\Big). \tag{1.4}$$

This solution was first derived by May (1973) (but see Ridolfi *et al.*, 2011, for method). In cases where the pdf cannot be analytically derived as above, it can be numerically obtained.

Since 1.4 is a function of s_{gn}, it is easy to explore the impact of environmental stochasticity, or noise on the PDF shape or mode (Fig. 1.2). The stochastic and deterministic models have similar mean population sizes at small values of s_{gn}. Gradually the mean population size decreases as s_{gn} increases from zero to $K_o/2$, above this value the PDF mode has shifted to extinction. Despite exhibiting a non-zero carrying capacity, the system is likely to go extinct within a short (ecologically relevant) time. Finally, at $s_{gn} \geq K_o$ extinction is the only possible population size. Additionally, the time to extinction is also a decreasing function of the environmental stochasticity (Adler & Drake, 2008).

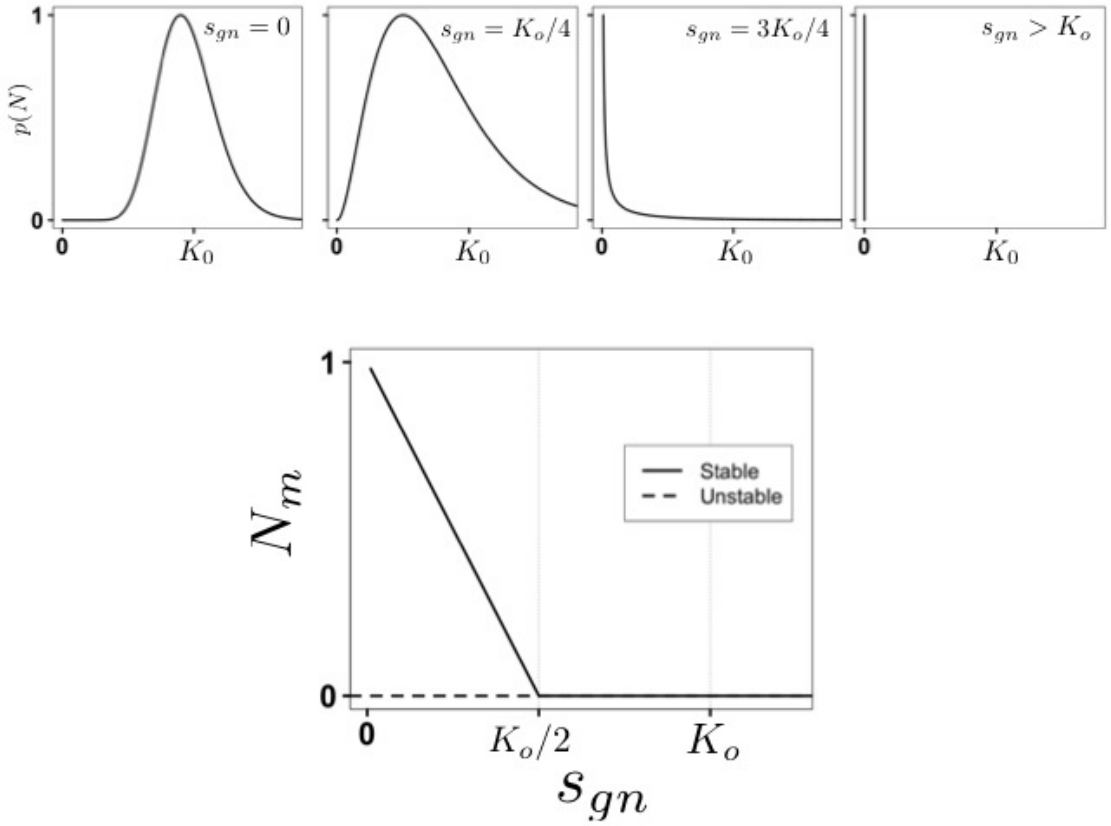

Figure 1.2: Impact of a random normally distributed carrying capacity with increasing variance (s_{gn}) on pdf and mode population size (N_m). The mode population size, N_m, is derived from Eq 1.4 and calculated as $N_m = K_o - 2s_{gn}$.

Case Study 2: Logistic model with variable harvest

NIT are not only found in a logistic system with a variable carrying capacity, and can be present in many ecological systems with non-linear relationships. Here we build on the initial logistic example by adding an additional proportional mortality rate due to harvesting (h) such that (in the deterministic case)

$$\frac{dN}{dt} = rN(K_o - N) - hN. \tag{1.5}$$

The equilibrium values are $N^\star = 0$ (unstable state), and $N^\star = K_o - h/r$ (stable state) assuming $K_o > h/r$. However, a constant harvest rate is a highly idealized abstraction and can be replaced with a Poisson harvest process such that the harvest rate (h) is modeled as white shot noise (WSN) with a mean waiting time between harvests, $1/\lambda$, and a mean proportional harvest α which are drawn from an exponential and Gaussian distribution, respectively. In other words, an instantaneous harvest that occurs at different time intervals and variable intensity. WSN is analytically tractable when normalized by the constant carrying capacity. As derived by Ridolfi *et al.* (2011, see Box 2.3, or 4.3.1) the steady state probability distribution solution to the stochastic model is

$$p\left(\frac{N}{K_o}\right) = \frac{\Gamma\left(\frac{1}{\alpha}\right)}{\Gamma\left(\frac{1}{\alpha} - \frac{\lambda}{\alpha}\right)\Gamma\left(\frac{\lambda}{\alpha}\right)} \left(\frac{N}{K_o}\right)^{\frac{1}{\alpha} - \frac{\lambda}{\alpha} - 1} \left(1 - \frac{N}{K_o}\right)^{\frac{\lambda}{\alpha} - 1} \tag{1.6}$$

where $\Gamma(\cdot)$ is the gamma function ($\Gamma(n) = (n-1)!$).While in the previous example, the shape of the PDF was dictated by a single variable (s_{gn} of K_{gn}), the PDF of a system experiencing WSN is a function of both harvest frequency (λ) and intensity (α). If the shape of the PDF is studied over this parameter space, we find distinct boundaries that correspond to rapid qualitative changes in the shape of the PDF (Fig. 1.3).

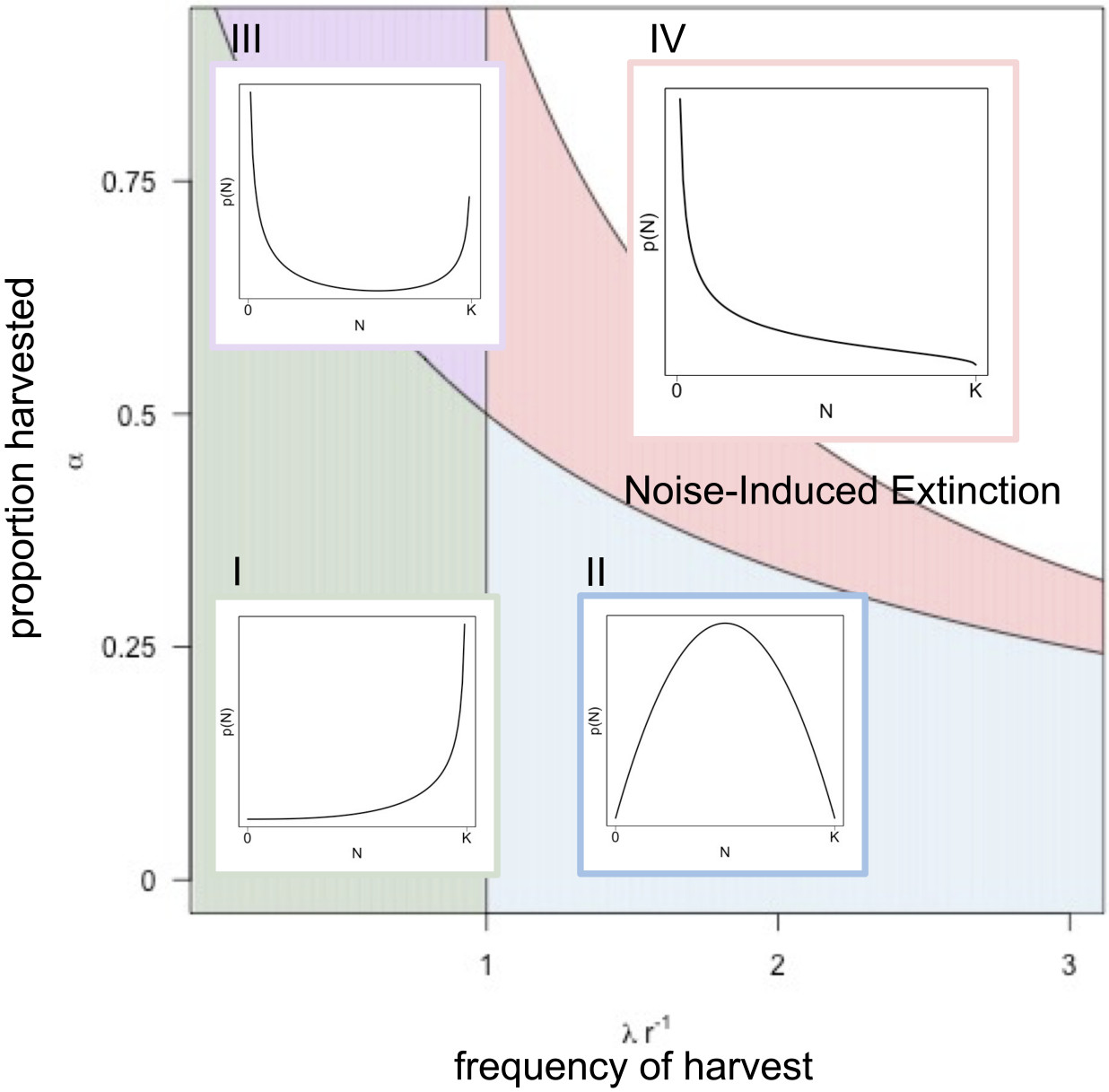

Figure 1.3: The pdf of a logistic model changes as a function of mean harvest frequency, and mean proportion harvested. The shaded regions have qualitatively different pdf shapes, and modes. In region I (green), the stochastic model has a mode of carrying capacity and the population would have dynamics similar to the equivalent deterministic model. In region II (blue), the mode population size decreases. In region III (purple), bistability appears. If observing populations in this region, the population dynamics may be described using an alternative stable state framework attributing state switching to some spurious force. Finally in region IV (pink), the system undergoes a noise-induced extinction, meaning the mode is at N=0. In the white region, extinction is the only possibility.

1.2.2 Appearance of NIT in models of grassland ecosystems

The ecological case studies presented are abstractions of ecological systems, which may or may not reflect observed dynamics in natural systems. Encouragingly, NITs appear in mechanistic models of savanna-woodland dynamics with data-derived parameters.

Grass dominated savannas are lost to shrub encroachment leading to a woodland dominated system. The switching between these two alternative stable states, grassland and shrubs, is moderated by intermittent fires D'Odorico *et al.* (2006). However, there is spatial heterogeneity in these systems which lead to mosaic patches of grasslands and shrubs at the local scale. While this patterning was originally explained through deterministic hydrologic feedback cycles, this pattern can also be explained by the variation in intermittent fires (D'Odorico *et al.*, 2007). When variation in precipitation is incorporated into the model a new stable state, bare soil, arises (Yu *et al.*, 2016). These models have also been applied to dryland plant ecosystems that alternate between bare soil and vegetative states based on rainfall. As the variance in rainfall increases a third stable state arises at an intermediate between the deterministic model's alternative stable states. By incorporating the variance in rainfall the potential landscape's hysteresis loop is replaced with a smooth, continuous increasing function (D'Odorico *et al.*, 2005).

1.2.3 NITs in other disciplines

NITs are not unique to ecological systems, and much of the foundational work pre-dates ecological work presented above. The following section reviews the models and corresponding experimental demonstrations of this behavior in other systems.

Physical systems

Some of the earliest studies of noise-induced transitions were in the physical sciences. An oscillating circuit can be pushed from an oscillating to non-oscillating state by introducing a

white noise current to the system's sinusoidal current which changes the decay constant, and aligned with the theoretical predictions. The transition between states cannot be attributed to changes in parameter values since critical slowing down indicated by increased variance was not observed prior to the transition. The lack of critical slowing down was used to assert this phase transition as noise-induced (Kabashima *et al.*, 1979b). Similar approaches pairing theoretical predictions, and experimental data have shown NIT in lasers (Arecchi & Harrison, 2012), and electrical oscillators (Kawakubo *et al.*, 1973b,a; Kabashima *et al.*, 1976; Kawakubo *et al.*, 1981).

Chemical reactions

The Briggs-Rauscher (BR) oscillating chemical reaction is another experimental system that exhibits a NIT. The closed system BR reaction is an oscillating iodine clock, that cycles through iodide, iodine, and triiodide which in the presence of starch is colorless, amber, and dark blue, respectively (Briggs & Rauscher, 1973). However, in a steady flow tank reactor (or open system) this reaction is photosensitive and exhibits many non-equilibrium phenomena including multiple steady states, limit cycles, and chaotic behavior. The open system BR reaction displays a hysteresis loop as a function of the constant light intensity resulting in initial condition dependent alternative stable states. At high light conditions the reaction is non-oscillating and triiodide is the dominant species (dark blue), while low light conditions favor an oscillating reaction. At intermediate light intensities, the reaction state can be either oscillatory or non-oscillatory. Environmental noise is introduced by replacing the constant light condition with light following a Gaussian white noise distribution. When environmental noise is introduced the bistability region is roughly doubled, and is shifted to lower mean light values such that the bistability region in a non-fluctuating and fluctuating environment do not overlap (De Kepper & Horsthemke, 1979b). In other words, if light is slowly increased the reaction becomes non-oscillatory at lower mean light values in a variable environment when compared to a constant light environment.

1.3 Detecting NITs in experimental systems

Despite being foundational to any empirical demonstration of NITs, I have not explained why the mode of the stochastic model's probability density is equivalent to the deterministic equilibrium. This section reviews the connection between the stationary probability density in a stochastic model and the deterministic model. I will walk through a generic model before moving onto the a logistic model following Horsthemke & Lefever (2006) explanation. First, we start with some deterministic model

$$dX = f_\lambda(X)dt = (h(X) + \lambda g(X))dt \tag{1.7}$$

where X is the state of the system, and λ depends on the environment. If the constant λ is replaced with a white noise term $\lambda_t = \lambda + \sigma\xi_t$, it can be written based on the Ito's stochastic differential equation (SDE Horsthemke & Lefever, 2006)

$$dX_t = [h(X_t) + \lambda g(X_t)]dt + \sigma g(X_t)dW_t. \tag{1.8}$$

From equation (1.8) we can use the Fokker-Planck equation (FPE) to find the stationary probability density of the system state X. The FPE, which describes how the probability density $p(x,t)$ changes over time,

$$\delta_t p(x,t) = -\delta_x f_\lambda(x)p(x,t) + \frac{\sigma^2}{2}\delta_{xx}g^2(x)p(x,t) \tag{1.9}$$

is used to find the stationary distribution, $p_s(x)$,by taking the limit of the FPE solution, $p(x,t)$, for time tending to infinity.

This process of defining the SDE and FPE can be repeated for a more biologically relevant, Verhulst model,

$$dX_t = \lambda X - X^2. \tag{1.10}$$

which has two stationary solutions, $x = (0, \lambda)$. Once again, we can add white noise into the model by replacing the constant λ with $\lambda_t = \lambda + \sigma\xi_t$ resulting in the SDE

$$\begin{aligned} dX_t &= [\lambda X_t - X_t^2]dt + \sigma g(X_t)dW_t \\ &= f(X_t)dt + \sigma g(X_t)dW_t \end{aligned} \tag{1.11}$$

and the corresponding FPE

$$\delta_t p(x,t) = -\delta_x[(\lambda x - x^2)p(x,t)] + \frac{\sigma^2}{2}\delta_{xx}x^2 p(x,t). \tag{1.12}$$

The FPE is used to find the stationary probability density

$$p_s(x) = Cx^{(2\lambda/\sigma^2)-2}\ \exp\left(\frac{-2x}{\sigma^2}\right), \tag{1.13}$$

where C is a normalizing constant so the integral of $p_s(x) = 1$. By examining 1.13 we can conclude that $p_s(x)$ is integrable over $[0, \infty)$, and that a solution only exists if the exponent of x is greater than zero so $\lambda > \sigma^2$. We can also calculate the extrema of $p_s(x)$ by solving for the root of the derivative of $p_s(x)$ (eq. 1.13) over $[0, \infty]$ so

$$\lambda x_m - x_m^2 - \sigma^2 x_m = 0 \tag{1.14}$$

is true when $x_{m_1} = 0$ or $x_{m_2} = \lambda - \sigma^2$ as long as $x_m \geq 0$. Looking closer at 1.14, it consists of three terms. The first two terms, $\lambda x_m - x_m^2$, are identical to the deterministic model 1.10, and the third term is multiplied by the noise intensity, σ. This shows that the mode is the stochastic analog of the equilibrium in a deterministic model. As the noise intensity approaches zero, the extrema approach the deterministic equilibria. However, as the noise increase to $\sigma^2 > \lambda$ the extremum, x_{m_2}, approaches zero until there is only a single

extrema at zero. Therefore any change in the extrema is due to noise alone.

We can repeat the same process of solving for the extrema of $p_s(x)$ for the general SDE 1.8 by using the general FPE equation 1.9 to calculate the $p_s(x)$ which can then be used the find the extrema of the probability density are by solving for the root of $dp_s(x)/dx$ which is

$$[h(x_m) + \lambda g(x_m)] - \sigma^2 g(x_m) g'(x_m) = 0. \tag{1.15}$$

As before, this expression can be broken down into two components, the first is the deterministic equilibria and the second is the effect on the extrema from the external noise, σ. The ability to decompose the extrema expression into these components demonstrates that the probability extrema (ie. modes) are an appropriate equivalent to the deterministic equilibria.

As a minor secondary point, the extrema are an appropriate metric to track transitions for two reasons. First, transitions are a change in the qualitative change to the potential meaning the extrema must change for a transition to occur. Second, other available metrics —such as the mean or higher moments —are not unique to a distribution, meaning a transition could occur with minimal change in the mean, variance, etc.

1.4 Natural systems are ideal for NITs: noisy and nonlinear

The case studies presented above demonstrated how environmental noise can dramatically change population trajectories. Environmental noise is an inherent requirement for a noise-induced transition, while nonlinearity increases the likelihood of NITs arising (but see Lewontin & Cohen, 1969). Given persistent environmental noise and prevalence of nonlinear relationships in population dynamics, they are an ideal natural system to observe the NITs phenomena in biological systems. In addition to the inherent stochasticity in natural sys-

tems, the Anthropocene has increased environmental noise indirectly and directly.

The Anthropocene is defined, in part, by our impact on the climate. Predictions about climate change include an increase in the frequency and magnitude of warm spells, or heat waves across most land areas over the period of decades to centuries (Thornton *et al.*, 2014). Expected increases or decreases in precipitation vary by region, but the proportion of precipitation occurring during heavy rainfall events is expected to increase globally. These changes in climate variability, rather than mean value, are often more meaningful for biological systems. For example, the agricultural gross domestic product of sub-Saharan countries are closely tied to the interannual rainfall variability (Thornton *et al.*, 2014). For theses reasons, I consider environmental noise associated with climate change to be an example of an indirect anthropogenic effect on environmental noise.

On one hand, indirect anthropogenic noise is a slow process that takes place over geological time. On the other hand, a direct anthropogenic effect on environmental noise will be more instantaneous. The direct harvesting, or manipulation of population sizes falls into this category. Direct anthropogenic effects on environmental noise have a much shorter time between cause and effect, and the potential to be localized. The difference in geographic (local vs global) and time (ecological vs geological) scales would require different detection methods, and stakeholders to change the anthropologically introduced noise. These differences in the scale and the appropriate response is why I have made this distinction.

1.4.1 Theory beyond the small noise assumption

Most relevant ecological theory has been developed with the assumption that environmental noise is relatively small, and merely introduces minor fluctuations around the deterministic equilibrium. This "small noise" assumption is used to justify constant mean parameter values when developing theoretical models. Exploring the limitations to this assumption can be traced to the early discrete time models of Lewontin & Cohen (1969), and has shaped the foundations of extinction theory.

Extinction theory predicts that increasing environmental noise should increase time to establishment and probability of extinction, while decreasing the time to extinction. An experimental test of these predictions did not show an effect of environmental noise on time to establishment, but did increase probability of extinction and reduced time to extinction (Drake & Lodge, 2004). However, the relationship between extinction and environmental noise depends on the organizational level of interest. While environmental noise can have a negative impact on a population's persistence, when multiple competing populations are considered, environmental noise can have a stabilizing effect by allowing co-existence (Adler & Drake, 2008; D'Odorico *et al.*, 2008). As in models of a single population, environmental noise can also increase metapopulations' probability of extinction. Increasing variation of vital rates in metapopulations require larger patch sizes to maintain the same viability level (ie. 5% extinction probability in five years). Troublingly for conservation efforts, the minimum patch size is predicted to increase exponentially with environmental stochasticity (Verboom *et al.*, 2010).

1.5 Bringing theory to life

The previous sections have reviewed our current understanding of catastrophic change in natural systems. Traditionally, mechanisms explaining catastrophic change, kinetic parameter change and alternative stable states, have been developed under the small noise assumption (Fig. 1.1A,B). Predictions arising from these small noise mechanisms have been tested using observational data and experimental microcosms (As reviewed by Schröder *et al.*, 2005; Scheffer & Carpenter, 2003; Scheffer *et al.*, 2012).

However, if we relax the small noise assumption an alternative, novel and overlooked mechanism, NITs, can explain our observations of catastrophic changes (Fig. 1.1C). To date, NITs in ecological systems have been described using theoretical models. As seen in the ecological case studies, incorporating the variance of a parameter value can identify a

previously unknown thresholds seriously impeding our predictive accuracy of future populations. The need to understand where these thresholds lie is compounded by the expected increase in climate variability with climate change, and the prevalence of currently stressed natural systems that characterize the Anthropocene.

Noise-induced transitions fundamentally change our understanding of nature's predictability. I will build on these concepts by translating the theoretical work into empirical studies to demonstrate NITs. This will be done by pairing mechanistic models with single species microbial microcosms experiments. The quantitative methods create system specific testable predictions, while microcosms allow for highly replicated counterfactual conditions (Drake & Kramer, 2012). *I predict that adding environmental noise in the experimental microcosms will result in population extinctions, while those in a constant environment will persist indefinitely.*

I demonstrate NITs in two separate microbial microcosm systems. The first microbial system uses the cyanobacteria, *Aphanizomenon flos-aqua*, and a well described mechanistic model of the species growth within a well mixed chemostat (Gerla *et al.*, 2011). Environmental noise is introduced by growing the cultures under variable light conditions. This manipulation is equivalent to the first case study, variable carrying capacity, presented. I predict that populations exposed to environmental noise will bleach due to photo-inhibition before going extinct. This work can be found in chapters 2 (model) and 3 (experiment).

The second system uses the yeast, *Saccharomyces cerevisiae* BY4741:YFP, grown on a substrate and paired with a generic logistic growth model including harvesting (Dai *et al.*, 2012; Dennis, 2002). In this case, environmental noise will be introduced by variable harvest frequency and proportion just as in the second case study. I predict that the populations subject to variable harvest will fail to produce visible colonies, while those subject to constant harvest will produce visible colonies. This work can be found in chapter 4 (model) and 5 (experiment).

Finally, I will generalize the findings in the concluding chapter.

Bibliography

Adler, P. & Drake, J. (2008). Environmental Variation, Stochastic Extinction, and Competitive Coexistence. *The American Naturalist*, 172, E186–E195.

Arecchi, F. T. & Harrison, R. G. (2012). *Instabilities and Chaos in Quantum Optics*. Springer Science & Business Media. ISBN 978-3-642-71708-6. Google-Books-ID: bzvtCAAAQBAJ.

Barnosky, A. D., Matzke, N., Tomiya, S., Wogan, G. O. U., Swartz, B., Quental, T. B., Marshall, C., McGuire, J. L., Lindsey, E. L., Maguire, K. C., Mersey, B. & Ferrer, E. A. (2011). Has the Earth's sixth mass extinction already arrived? *Nature*, 471, 51–57.

Briggs, T. S. & Rauscher, W. C. (1973). An oscillating iodine clock. *Journal of Chemical Education*, 50, 496.

Ceballos, G., Ehrlich, P. R. & Dirzo, R. (2017). Biological annihilation via the ongoing sixth mass extinction signaled by vertebrate population losses and declines. *Proceedings of the National Academy of Sciences*, 114, E6089–E6096.

Chase, J. M. (2003). Experimental evidence for alternative stable equilibria in a benthic pond food web. *Ecology Letters*, 6, 733–741.

Cushing, J. M., Henson, S. M., Desharnais, R. A., Dennis, B., Costantino, R. F. & King, A. (2001). A chaotic attractor in ecology: Theory and experimental data. *Chaos, Solitons & Fractals*, 12, 219–234.

Dai, L., Vorselen, D., Korolev, K. S. & Gore, J. (2012). Generic Indicators for Loss of Resilience Before a Tipping Point Leading to Population Collapse. *Science*, 336, 1175–1177.

De Kepper, P. & Horsthemke, W. (1979a). Experimental Evidence of Noise-Induced Transitions in an Open Chemical System. In: *Synergetics* (eds. Pacault, A. & Vidal, C.), vol. 3.

Springer Berlin Heidelberg, Berlin, Heidelberg. ISBN 978-3-642-67264-4 978-3-642-67262-0, pp. 61–63.

De Kepper, P. & Horsthemke, W. (1979b). Experimental Evidence of Noise-Induced Transitions in an Open Chemical System. In: *Synergetics* (eds. Pacault, A. & Vidal, C.), vol. 3. Springer Berlin Heidelberg, Berlin, Heidelberg. ISBN 978-3-642-67264-4 978-3-642-67262-0, pp. 61–63. URL `http://link.springer.com/10.1007/978-3-642-67262-0_10`.

Dennis, B. (2002). Allee effects in stochastic populations. *Oikos*, 96, 389–401.

D'Odorico, P., Laio, F., Porporato, A., Ridolfi, L. & Barbier, N. (2007). Noise-induced vegetation patterns in fire-prone savannas. *Journal of Geophysical Research: Biogeosciences*, 112.

D'Odorico, P., Laio, F. & Ridolfi, L. (2005). Noise-induced stability in dryland plant ecosystems. *Proceedings of the National Academy of Sciences of the United States of America*, 102, 10819–10822.

Drake, J. M. & Griffen, B. D. (2010). Early warning signals of extinction in deteriorating environments. *Nature*, 467, 456–459.

Drake, J. M. & Kramer, A. M. (2012). Mechanistic analogy: how microcosms explain nature. *Theoretical Ecology*, 5, 433–444.

Drake, J. M. & Lodge, D. M. (2004). Effects of environmental variation on extinction and establishment. *Ecology Letters*, 7, 26–30.

D'Odorico, P., Laio, F. & Ridolfi, L. (2006). A Probabilistic Analysis of Fire-Induced Tree-Grass Coexistence in Savannas. *The American Naturalist*, 167, E79–E87.

D'Odorico, P., Laio, F., Ridolfi, L. & Lerdau, M. T. (2008). Biodiversity enhancement induced by environmental noise. *Journal of Theoretical Biology*, 255, 332–337.

Farley, S. S., Dawson, A., Goring, S. J. & Williams, J. W. (2018). Situating Ecology as a Big-Data Science: Current Advances, Challenges, and Solutions. *BioScience*, 68, 563–576.

Gerla, D. J., Mooij, W. M. & Huisman, J. (2011). Photoinhibition and the assembly of light-limited phytoplankton communities. *Oikos*, 120, 359–368.

Horsthemke, W. & Lefever, R. (2006). *Noise-induced transitions: theory and applications in physics, chemistry, and biology*. No. 15 in Springer series in synergetics, 2nd edn. Springer, Berlin. ISBN 978-3-540-11359-1.

Kabashima, S., Kogure, S., Kawakubo, T. & Okada, T. (1979a). Oscillatory-to-nonoscillatory transition due to external noise in a parametric oscillator. *Journal of Applied Physics*, 50, 6296–6302.

Kabashima, S., Kogure, S., Kawakubo, T. & Okada, T. (1979b). Oscillatory-to-nonoscillatory transition due to external noise in a parametric oscillator. *Journal of Applied Physics*, 50, 6296–6302.

Kabashima, S., Yamazaki, H. & Kawakubo, T. (1976). Critical Fluctuation near Threshold of Gunn Instability. *Journal of the Physical Society of Japan*, 40, 921–924.

Kawakubo, T., Kabashima, S. & Nishimura, K. (1973a). Observation of Critical Fluctuations in Negative-Resistance Oscillation. *Journal of the Physical Society of Japan*, 34, 1460–1461.

Kawakubo, T., Kabashima, S. & Ogishima, M. (1973b). Critical Slowing-Down near Threshold of Electrical Oscillation. *Journal of the Physical Society of Japan*, 34, 1149–1152.

Kawakubo, T., Yanagita, A. & Kabashima, S. (1981). External Noise Effect on the Onset of Williams Domain in Nematic Liquid Crystals. *Journal of the Physical Society of Japan*, 50, 1451–1456.

Lewontin, R. C. & Cohen, D. (1969). On Population Growth in a Randomly Varying Environment. *Proceedings of the National Academy of Sciences*, 62, 1056–1060.

May, R. M. (1973). Stability in Randomly Fluctuating Versus Deterministic Environments. *The American Naturalist*, 107, 621–650.

May, R. M. (2001). *Stability and Complexity in Model Ecosystems*. Princeton Landmarks in Biology, 1st edn. Princeton University Press, Princeton. ISBN 0-691-08861-6.

Nolting, B. C. & Abbott, K. C. (2016). Balls, cups, and quasi-potentials: Quantifying stability in stochastic systems. *Ecology*, 97, 850–864.

Post, E. & Forchhammer, M. C. (2002). Synchronization of animal population dynamics by large-scale climate. *Nature*, 420, 168–171.

Ridolfi, L., DOdorico, P. & Laio, F. (2011). *Noise-Induced Phenomena in the Environmental Sciences*. Cambridge University Press, Cambridge. ISBN 978-0-511-98473-0. URL `http://ebooks.cambridge.org/ref/id/CBO9780511984730`.

Scheffer, M., Bascompte, J., Brock, W. A., Brovkin, V., Carpenter, S. R., Dakos, V., Held, H., van Nes, E. H., Rietkerk, M. & Sugihara, G. (2009). Early-warning signals for critical transitions. *Nature*, 461, 53–59.

Scheffer, M., Carpenter, S., Foley, J. A., Folke, C. & Walker, B. (2001). Catastrophic shifts in ecosystems. *Nature*, 413, 591–596.

Scheffer, M. & Carpenter, S. R. (2003). Catastrophic regime shifts in ecosystems: linking theory to observation. *Trends in Ecology & Evolution*, 18, 648–656.

Scheffer, M., Carpenter, S. R., Lenton, T. M., Bascompte, J., Brock, W., Dakos, V., Koppel, J. v. d., Leemput, I. A. v. d., Levin, S. A., Nes, E. H. v., Pascual, M. & Vandermeer, J. (2012). Anticipating Critical Transitions. *Science*, 338, 344–348.

Schröder, A., Persson, L. & Roos, A. M. D. (2005). Direct experimental evidence for alternative stable states: a review. *Oikos*, 110, 3–19.

Stenseth, N. C., Mysterud, A., Ottersen, G., Hurrell, J. W., Chan, K.-S. & Lima, M. (2002). Ecological Effects of Climate Fluctuations. *Science*, 297, 1292–1296.

Strogatz, S. H. (2001). *Nonlinear Dynamics and Chaos: With Applications to Physics, Biology, Chemistry, and Engineering*. Studies in Nonlinearity, 2nd edn. Perseus Books, Cambridge, Mass. ISBN 978-0-7382-0453-6.

Thornton, P. K., Ericksen, P. J., Herrero, M. & Challinor, A. J. (2014). Climate variability and vulnerability to climate change: a review. *Global Change Biology*, 20, 3313–3328.

Verboom, J., Schippers, P., Cormont, A., Sterk, M., Vos, C. C. & Opdam, P. F. M. (2010). Population dynamics under increasing environmental variability: implications of climate change for ecological network design criteria. *Landscape Ecology*, 25, 1289–1298.

Wake, D. B. & Vredenburg, V. T. (2008). Are we in the midst of the sixth mass extinction? A view from the world of amphibians. *Proceedings of the National Academy of Sciences*, 105, 11466–11473.

Yu, K., Okin, G. S., Ravi, S. & D'Odorico, P. (2016). Potential of grass invasions in desert shrublands to create novel ecosystem states under variable climate. *Ecohydrology*, 9, 1496–1506.

Mechanistic model of *Aphanizomenon* growth in a randomly fluctuating environment

2.1 Introduction

Understanding the causes of fluctuations in population abundance over time is a key aim of population ecology. These fluctuations have been attributed to climate, trophic interactions, and non-linear dynamics (Post & Forchhammer, 2002; Stenseth *et al.*, 2002; May, 1976; Cushing *et al.*, 2001). These mechanisms were described assuming that a deterministic model was an appropriate description of the natural world. Of course, a deterministic representation is not always appropriate. For example, environmental conditions may be better represented with a random variable rather than a constant parameter value (May, 1973). Despite acknowledging this, much of the theory developed around environmental stochasticity has been restricted to larger perturbations that lead to catastrophic change by pushing the system from state to another state or small perturbations that create a cloud of points around the deterministic equilibria. The challenge with this conception of environmental stochasticity, or noise, is appropriately categorizing perturbations as large or small. As an alternative framework, we can use to a stochastic model rather then a deterministic

description of populations.

The shift from a deterministic to stochastic interpretation of natural systems changes our conceptual understanding of stability within the system. I will first review stability in a deterministic model and then how stability is defined within a stochastic model. A deterministic model, with constant parameter values, has stable and unstable equilibria. Stability is conceptually based on sensitivity to perturbations, defined mathematically by eigenvalues (local stability) or a Lyapunov function (global stability). An equilibrium is stable if the system returns to that value after a small perturbation, while any perturbations at an unstable equilibrium will not result in the system returning to the state prior to perturbations. Alternatively, a ball-and-valley model, the geometric equivalent of the potential function, allows us to develop some intuition about the system stability (as reviewed by Nolting & Abbott, 2016). Here, the system state is the location of the ball, while the peaks and valleys are the unstable and stable equilibria, respectively. The ball follows gravity to the closest valley, or basin of attraction. Depending on the strength, perturbations can either wiggle the ball at the bottom of the valley or move the ball to another valley by pushing the ball uphill.

When the same phenomenological model is recast as a stochastic model, stability is described in probabilistic terms. The probability distribution of population size is derived from the Fokker-Planck equation which takes into account the "drift" caused by the stochasticity and the "friction" of the underlying deterministic processes (May, 1973). The extrema of the probability distribution are analogous to deterministic equilibria given that the distribution approaches a Dirac delta peak at the deterministic equilibrium as variance tends to zero (Horsthemke & Lefever, 2006). This is demonstrated analytically by examining the expression for the extrema of the probability density function which can be broken down into two terms. The first term always matches the deterministic equilibria regardless of external noise, while the second term is a function of the external noise represented by the noise variance. As the noise approaches zero, the stochastic equilibria approaches the deter-

ministic equilibria. Given that we are able to evaluate the stability of a stochastic system with respect to the deterministic counterpart, we can easily explore the impact of noise on stability.

Interestingly, incorporating environmental stochasticity into models can yield qualitatively different picture of stability compared with the deterministic equivalent. Returning to the ball-and-valley model, environmental stochasticity can create, destroy, move, or reshape the peaks and valleys the ball moves along. The change in number and/or location of basins of attraction is referred to as a transition, and in this case it is a noise-induced transition (NIT). Other fields, mainly chemistry and physics, interested in system dynamics have demonstrated NITs are possible in experiments (Horsthemke & Lefever, 2006). While ecology has overlooked NITs since theoretical models were presented in the 1970s, NITs can have a profound impact on our understanding of population ecology, and conservation. However, we have never attempted to recreate this phenomena in an experimental system (May, 1973).

This chapter reports on a theoretical analysis for a type of NIT, a noise-induced extinction (NIE), in an experimental system by using a mechanistic model of algal growth which accounts for photo-inhibition, and light attenuation in a well mixed chemostat. A deterministic model published by Huisman & Weissing (1994) was modified to include variable incident light. Simulations with a range of environmental noise were analyzed to make testable predictions for future chemostat experiments. First, I will present the mechanistic model without environmental noise. Secondly, I will present the same model with environmental noise added to the incident light. Finally, I will compare the simulations from the deterministic and stochastic models to identify the noise threshold where the behavior of the two models diverge indicating the region where a NIE should be observed in the experimental system.

2.2 Methods

The impact of environmental noise on *Aphanizomenon flos-aqua* population dynamics was modeled as a stochastic differential equation (SDE) where incident light is a random normal variable. The SDE model was based on a previously described, mechanistic, ordinary differential equation (ODE) model developed by Huisman & Weissing (1994). Both models assume the population is grown in a well mixed, and light-limited chemostat. From this assumption, the growth rate is a function of photosynthetically active radiation (PAR, $\lambda = [400 - 700nm]$). However, is not constant across depth in the chemostat. The incident light (I_{in}) is attenuated following the Beer-Lambert law which accounts for light pathlength or depth (z), light absorbance due to the media (K_{bg}), light absorbance of an algal cell (k), and the current algal density (A; Eq. 2.1). Additionally, the reproductive response to is non-linear. Like most cyanobacteria, *Aphanizomenon* growth is inhibited at high light intensities. Early mechanistic models of photoinhibition collapsed the cellular photosynthetic machinery into a photosynthetic factory (PSF) which could be in one of three states: resting, active, or inhibited (Eilers & Peeters, 1988). This PSF function can then be rewritten in terms of p_{max}, the maximum specific production rate, I_{opt}, the optimal light intensity, and I_k, the light intensity at p_{max} if the initial slope of the p-I curve was maintained (Eq. 2.2, Fig. 2.1, Gerla *et al.* (2011)). The population overcomes photo-inhibition through self-shading which results in an Allee effect or a minimum critical density at a given light intensity. The strength of the Allee effect increases with the difference between I_{opt} and I_k(Fig. 2.1). Eq. 2.1 and Eq. 2.2 are used to derive the per capita growth rate as the average light available to the population calculated by the integral of the light attenuation function, $I(z)$, divided by the total depth z_{max} minus cell loss in the effluent, l (Eq. 2.3). It is important to note that the unit of the population density, A, is light attenuation (m^{-1}, See Appendix A for details). This non-traditional unit was used because it is easy to measure, and match experimental data. See Tbl. 2.1 and Tbl. 2.2 for parameter units and values.

$$I(z) = I_{in} * \exp\big(- z(kA + K_{bg})\big) \tag{2.1}$$

$$P(I) = \frac{p_{max} I}{\frac{I_k}{I_{opt}^2} I^2 + \left(1 - 2\frac{I_k}{I_{opt}}\right) I + I_k} \tag{2.2}$$

$$\frac{dA}{dt} = A\left(\frac{1}{z_{max}} \int_0^{z_{max}} P(I(z))dz - l\right) \tag{2.3}$$

The symbolic solution to the ODE model was obtained using Maple 2016 (Eq. 2.3), and was used to verify the numerical results (See Appendix B). The numerical solution was obtained using R package deSolve (R Core Team, 2018; Soetaert *et al.*, 2010). The deterministic point equilibria were used to guide selection of initial conditions for SDE model simulations. Environmental noise was added to the ODE model by replacing the constant incident light parameter, $I_{in} = 600$, with a random normal variable I_{in} $N(600, \sigma^2)$ creating the SDE model. A new light condition was drawn every 28 minutes in the simulation. The state space was explored by using a factorial design of initial population densities ($A_0 = (1, 25)$), and environmental noise ($\sigma = (0, 500)$). Simulations were run in parallel using R software (R Core Team (2018); Corporation & Weston (2018); Microsoft & Weston (2017), see Appendix C for code). For each of the 12,500 initial condition by environmental noise treatments 100 simulations were run for 500 days (approx. 125 generations under ideal growth conditions). Simulations were thinned by 90% and a burn-in period of 300 days was removed prior to any analysis. Population trajectories were converted to histograms to derive the steady state distribution, and mode(s). The area under the normalized steady state distribution is equivalent to the probability of a given population size.

2.3 Results

The steady state of the deterministic system is incident light dependent, while the steady state of the stochastic system is dependent on both the mean and variance of the incident light. Based on both analytic and numeric solutions of the deterministic model, alternative stable states arise between constant incident light values of $370 - 1050$ PAR (Fig. 2.2). Populations grown with a constant incident light of 600 PAR have a minimum viable density (N_c) of 6.98 m^{-1} and an upper stable equilibrium of 21.35 m^{-1}. Based on this, the mean incident light of 600 PAR was chosen for the stochastic model simulations. As the environmental noise (σ) was increased, the stochastic and deterministic model behavior diverged (Fig. 2.3). The effect of environmental noise on the most probable population size was determined by tracking the mode(s) of the steady state distribution. Populations simulated with low to moderate environmental noise ($0 < \sigma \leq 200$) were likely to approach the local stable equilibrium (extinction or 21.35 m^{-1}) as determined by the initial population size. Additionally, sufficiently large initial populations ($A_0 >> N_c$) were unlikely to go extinct within 100 days of the simulation post burn-in period (Fig. 2.5).

Populations simulated with large environmental noise ($200 < \sigma \leq 300$) were more likely to go extinct despite sufficiently large initial populations. This is due to a narrowing of the initial conditions that could lead to persistence due to an increased unstable equilibrium and a decreased upper stable equilibrium (Fig. 2.4). Populations that were able to persist had a suppressed mode, never reaching the deterministic upper equilibrium value. All populations simulated with extreme environmental noise ($\sigma \geq 320$) went extinct within the simulation period regardless of initial population size.

In between $300 < \sigma < 320$ the last hints of the deterministic behavior disappear even for sufficiently large initial populations and noise-induced extinctions prevail. This can be seen in the increase in the left tail of the steady state distribution (Fig. 2.6). Additionally, the speed of extinction increased with environmental noise. The collapse of the upper equilibrium

branch resulting in a single equilibrium value at extinction is recovered in the stochastic bifurcation diagram (Fig. 2.4).

2.4 Discussion

I modified a mechanistic growth model of *Aphanizomenon* published by Huisman & Weissing (1994) to incorporate stochastic incident light conditions. The stochastic conditions were drawn from a random normal variable with a mean of 600 PAR, and a range of noise intensities ($\sim N(600PAR, \sigma^2)$). Population simulations with stochastic incident light were compared to simulations with a constant ideal incident light of 600 PAR. The simulations were used to calculate the equilibria under varying initial state and noise conditions. When the environmental noise was increased past $\sigma = 325$, the stochastic stability profile underwent a qualitative change with respect to the deterministic stability profile resulting in a single equilibrium at extinction. This is a theoretical demonstration of environmental variability causing population extinctions despite an ideal mean environmental condition, also known as a noise-induced extinction.

Most prior work on noise-induced extinctions and more generally noise-induced transitions has been done outside the field of ecology (Kabashima *et al.*, 1979; Kawakubo *et al.*, 1973b,a; Kabashima *et al.*, 1976; Kawakubo *et al.*, 1981; Briggs & Rauscher, 1973; De Kepper & Horsthemke, 1979). For example, Arecchi & Harrison (2012) paired stochastic models with experimental data to demonstrate noise-induced transitions leading to bistability in lasers. While ecology and statistical physics are disparate, the transition process to bistability in lasers overlaps with the transition to extinction in populations. The path to extinction in ecological populations is often initiated by an initial transition to bistability. Populations with two deterministic equilibria grown under stochastic environmental conditions often pass through a bimodal phase with extinction and the upper equilibrium becoming equally probable population sizes before transitioning to extinction as the only outcome. This is the case

for at least state-dependent dichotomous noise, white shot noise in the logistic harvest model, and Gaussian white noise in the genetic model (D'Odorico *et al.*, 2007, 2006; Horsthemke & Lefever, 2006).

Within the ecological disciplines, NITs were introduced by May (1973) through noise-induced extinction using the logistic model with a stochastic carrying capacity. In trying to assess if our findings of a noise-induced extinction are expected under previously developed theory, we must take the underling deterministic stability and the type of noise into account. Like much of the theoretical work describing grassland ecosystems, the *A. flos-aqua* system also has alternative stable states in the deterministic skeleton (Yu *et al.*, 2016; D'Odorico *et al.*, 2007). Noise in the grassland systems gives rise to an intermediate stable state within the stochastic system, in essence the noise enhances the system's stability by flattening the hysteresis loop to a continuous monotonic relationship between environmental condition and system state (D'Odorico *et al.*, 2005). This flattening also occurs in the algal system demonstrated by the downward curve of the upper equilibrium of the stochastic bifurcation between an environmental noise of $\sigma = (150, 325)$ (Fig.2.4). However, the algal system still undergoes a discontinuous or first-order transition to extinction at $\sigma \sim 325$. This difference in transition outcomes, stability and extinction, between the grassland and algal systems is a bit surprising but also stresses the need to take the type of noise into account when making predictions on the type of noise-induced transition. The algal growth model incorporates continuous Gaussian white noise, as opposed to the grassland ecosystems subjected to discrete noise (dichotomous or shot) (Ridolfi *et al.*, 2011). In other instances of Gaussian white noise, most notably, May (1973) logistic model with a stochastic carrying capacity, extinction is the end point for the phase transition induced by the stochastic noise. In summary, a noise-induced extinction is unexpected based on the underlying deterministic non-linearity, but expected based on the type of noise incorporated into the deterministic dynamics. These contrasting hypotheses for the transition outcome in this system stresses the need to develop a better heuristic understanding of when and how the non-linear system

properties and noise influence the type of phase transition expected.

The likelihood of a system experiencing an extreme value increases with environmental noise. This might lead some to ask if the observed critical dynamics are truly system properties or arise from the sampling process used to create the environmental noise. There are three different ways to respond to this critic. First, we can infer the NITs are due to the environmental noise rather than the sampling processes by measuring the probability of a small population size at different noise treatments. If the observed extinctions in model simulations are the result of the sampling process, we would expect a non-monotonic relationship between the probability of a small population size and the noise treatment. Whereas a monotonic relationship would be observed if extinction arose from the dynamical properties of the system experiencing noise as is the case for this work (Fig. 2.6). Additionally, time to extinction continuously decreases with increasing noise treatments which had been predicted by (Drake & Lodge, 2004). Secondly, the possibility of the sampling process driving the observations has been rigorously tested by comparing systems experiencing dichotomous Markov noise where the environment switches between two value with a random variable permanence time, and those experiencing the two environmental values at a fixed permanence time. NITs only appear in the systems experiencing the variable switching rate, and not in the constant switching rate environment (Ridolfi *et al.*, 2011; Horsthemke & Lefever, 2006). Finally, the last response to critics surrounding the mechanism that gives rise to the transitions draws on the connection between the deterministic and stochastic equilibria. The expression for the extrema of the probability density function of the stochastic model, which are treated as equivalents to the deterministic equilibria, can be broken down into two terms (Horsthemke & Lefever, 2006). The first term is merely the deterministic equilibria, and the second is multiplied by the noise term. As the noise term approaches zero, stochastic equilibria approaches the deterministic equilibria. From this, we can conclude any deviation between the deterministic and stochastic equilibria is a sole function of the noise term.

Fluctuations in population abundances overtime have been attributed to multiple factors

including climate, trophic interactions, and non-linear dynamics (Post & Forchhammer, 2002; May, 1976; Cushing *et al.*, 2001). These mechanisms all assume a deterministic representation of the system is sufficient, even as our understanding of the importance of stochasticity increases (Connell & Slatyer, 1977; Lewontin, 1969; May, 1977; Nolting & Abbott, 2016; Dennis *et al.*, 1991; Tuljapurkar & Orzack, 1980). This work incorporates environmental stochasticity into a deterministic growth model of *Aphanizomenon flos-aqua* and reports the theoretical analysis of a noise-induced extinction by predicting the intensity of environmental noise needed for the deterministic and stochastic models to qualitatively differ in stability. These predictions can now be experimentally tested to determine the plausibility of NITs in biological systems which is the first step to developing a heuristic understanding of NITs in ecology.

2.5 Figures

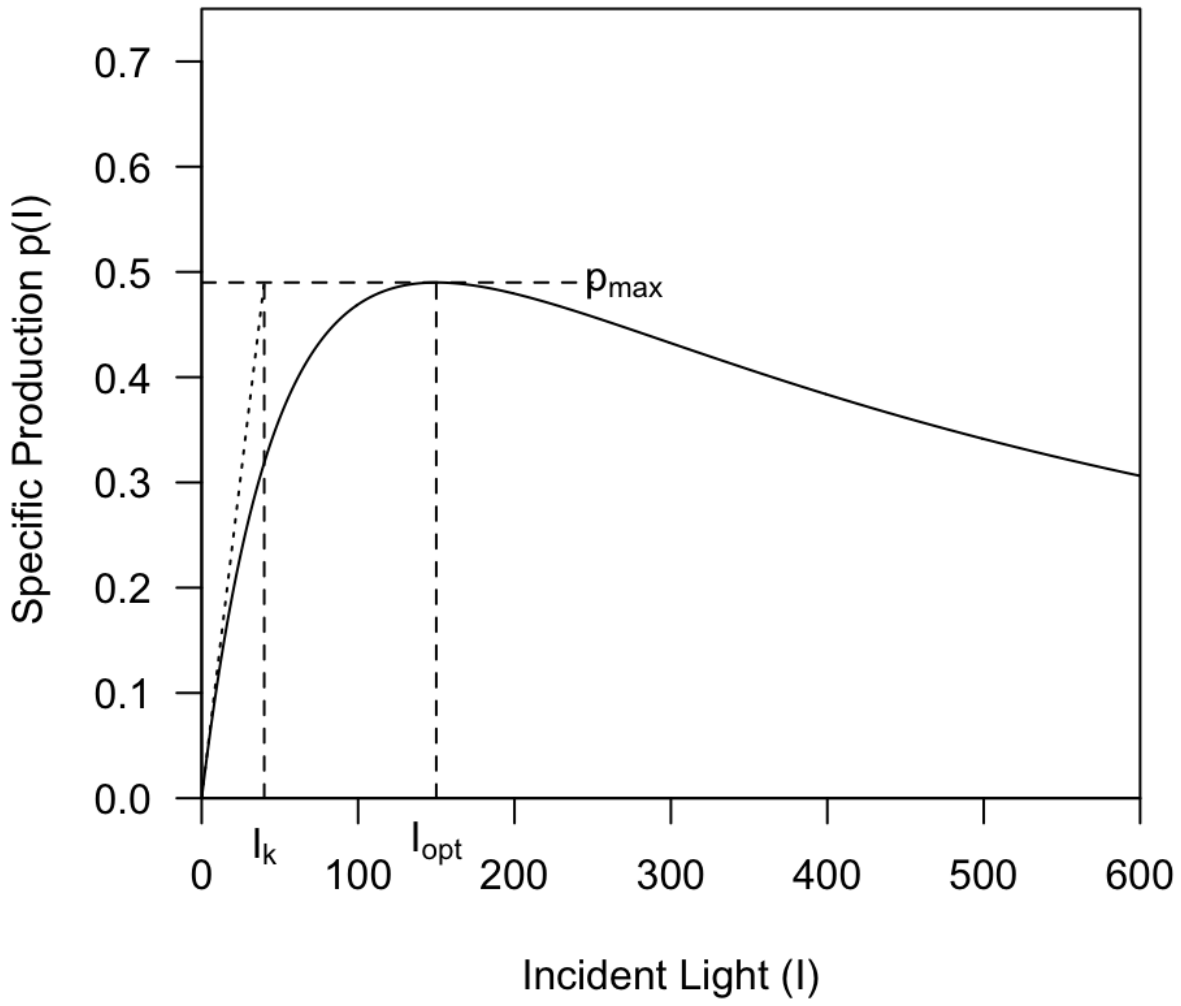

Figure 2.1: Specific production of *Aphanizomenon flas-aqua* as a function of incident light. The relationship is described by Eq. 2.2 and is a function of the maximum growth rate (p_{max}), the light intensity at the maximum growth rate (I_{opt}), and the light intensity of the maximum growth rate in the absence of photoinhibition (I_k).

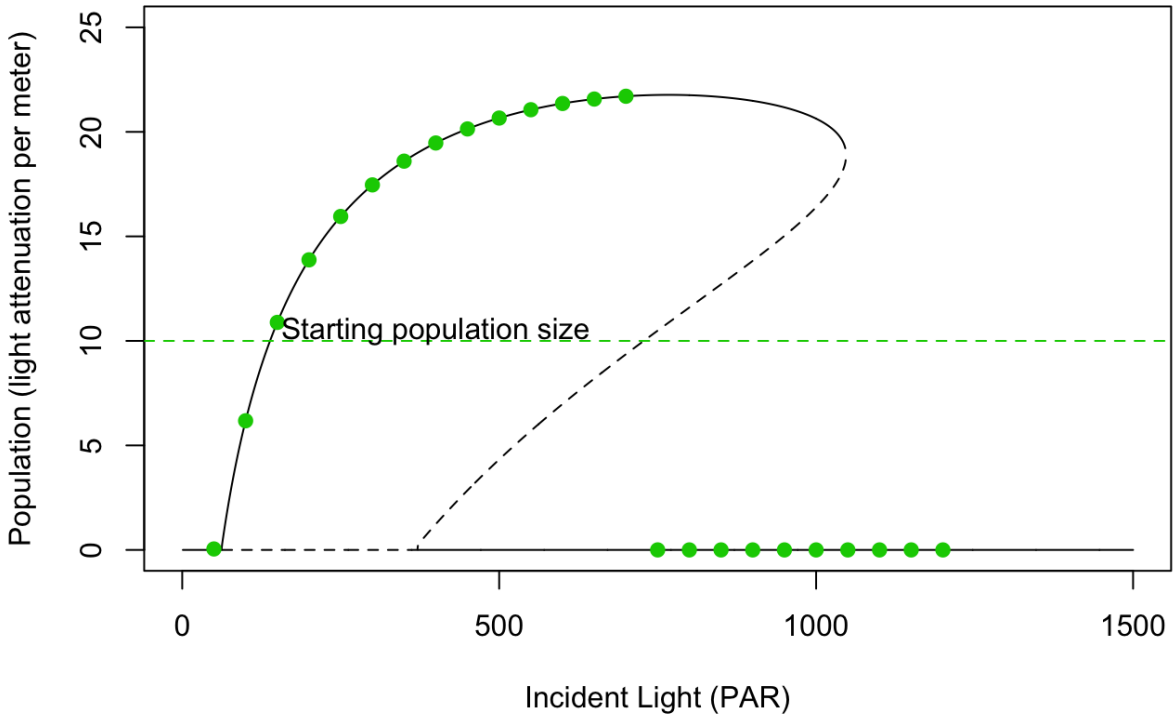

Figure 2.2: Analytical and numeric solution of the ODE model. The analytical solution is in black. The stable equilibrium is a solid line, and unstable equilibrium is the dashed line. The region of alternative stable states is between $370 - 1050$ PAR. The R code for the numeric solution was tested against the analytical solution. The numeric solution is plotted as the green points. These equilibrium values were based on a starting population of 10 m^{-1}.

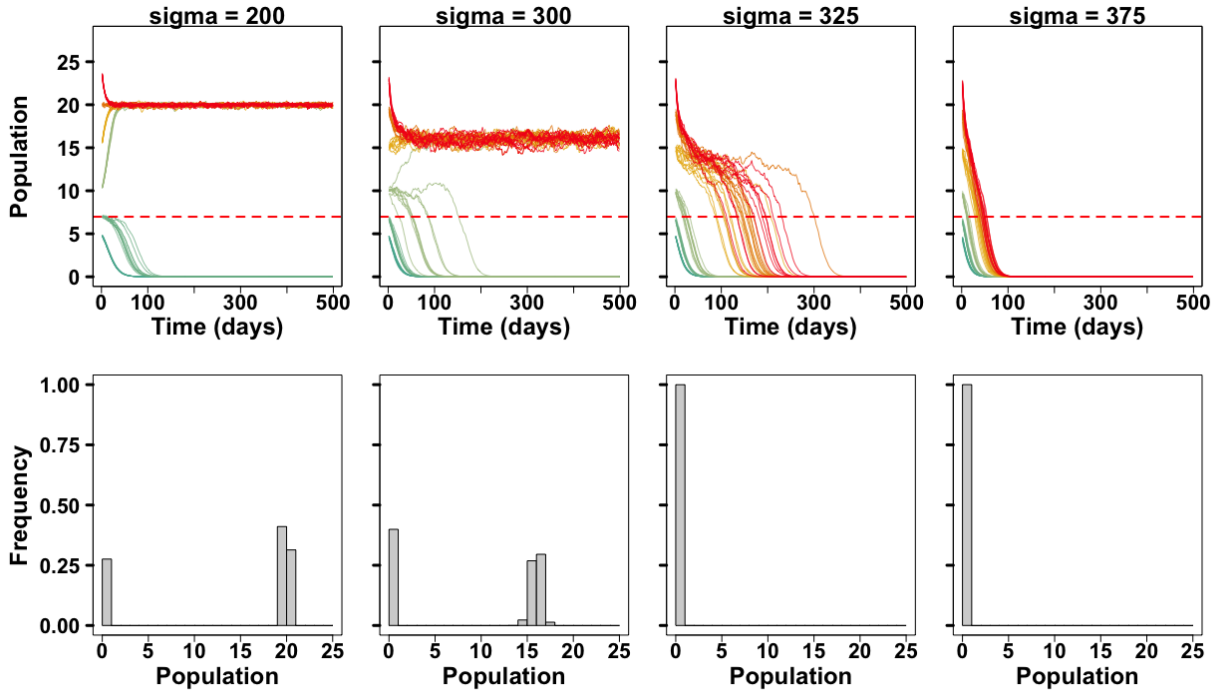

Figure 2.3: The top row are examples of simulated populations subject to light with a mean intensity of 600 PAR, and increasing environmental noise (sigma = 200,300,325, and 375, from left to right). The red dashed line is the deterministic critical threshold (N_c). Simulations were initialized with a range of population densities, and were used to calculate the steady state of the stochastic model shown in the bottom row after removing a 400 day burn-in period.

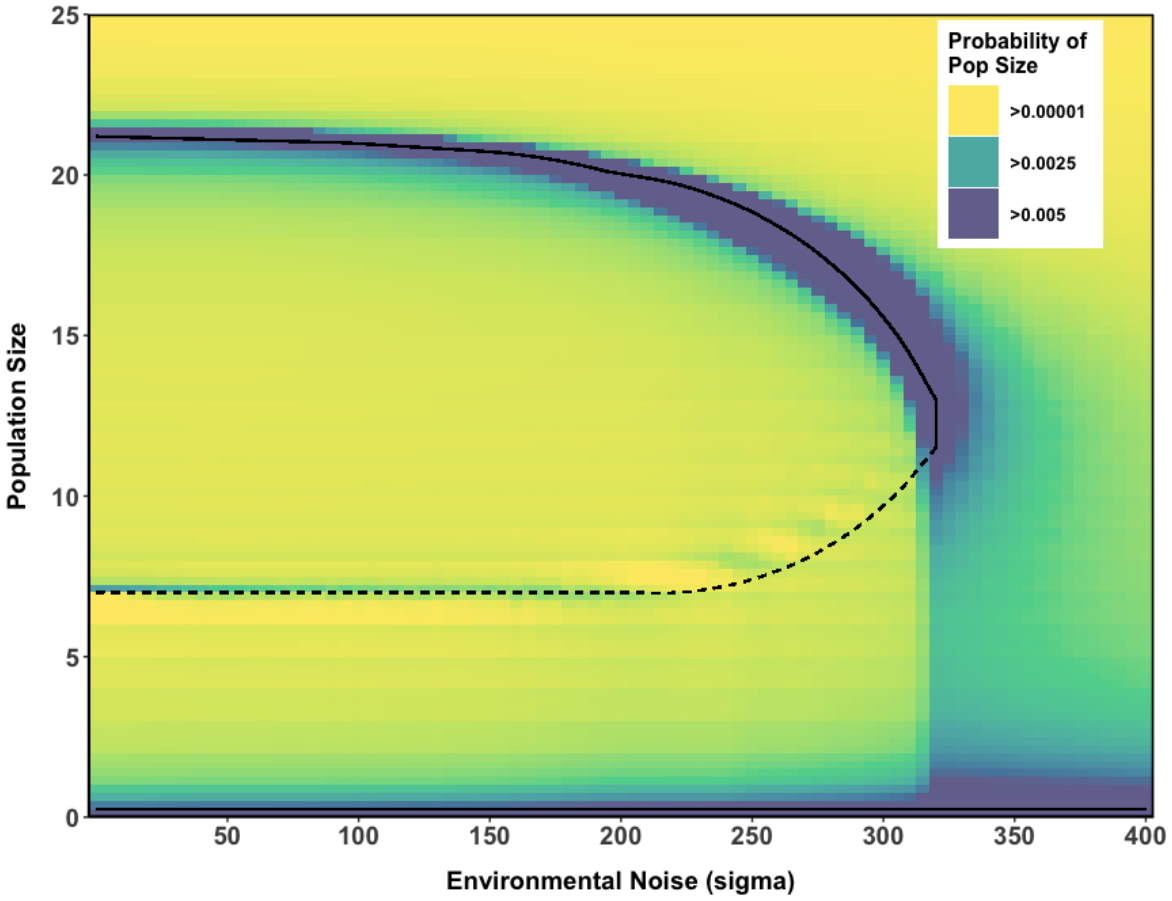

Figure 2.4: Stochastic bifurcation diagram and heatmap. The deterministic equivalent steady (solid line) and unsteady (dashed line) equilibrium are plotted as a function of environmental noise (σ, $\mu = 600\ PAR$).The equilibrium values were estimated from the modes and anti-modes of the density distribution calculated for each environmental noise. These distributions were used to create the heatmap. The hot and cool colors indicate a mode and anti-mode, respectively.

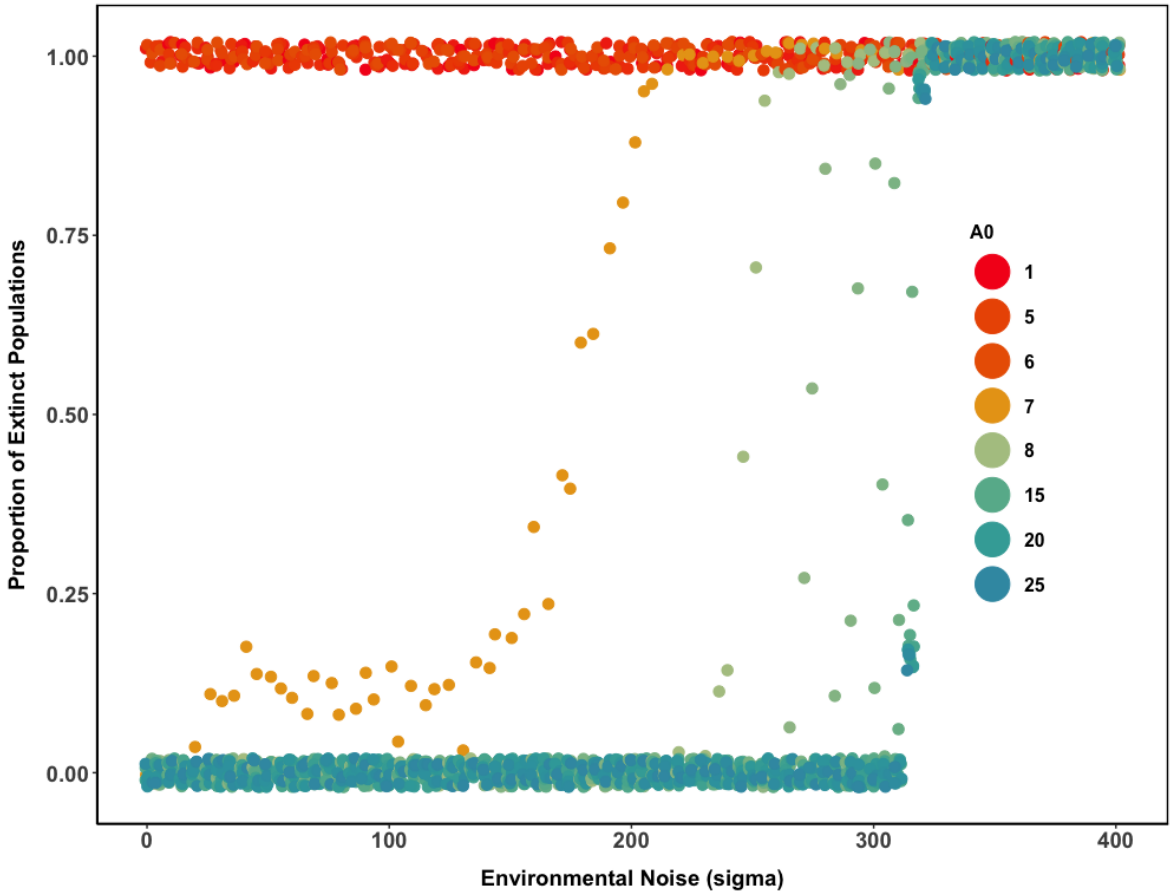

Figure 2.5: The proportion of 100 simulated populations that went extinct within 100 days. The extinction rate is a function of environmental noise ($\sim N(600\ PAR, \sigma^2)$) and initial population size (A_0). The critical threshold for the deterministic model is $N_c = 6.98\ m^{-1}$.

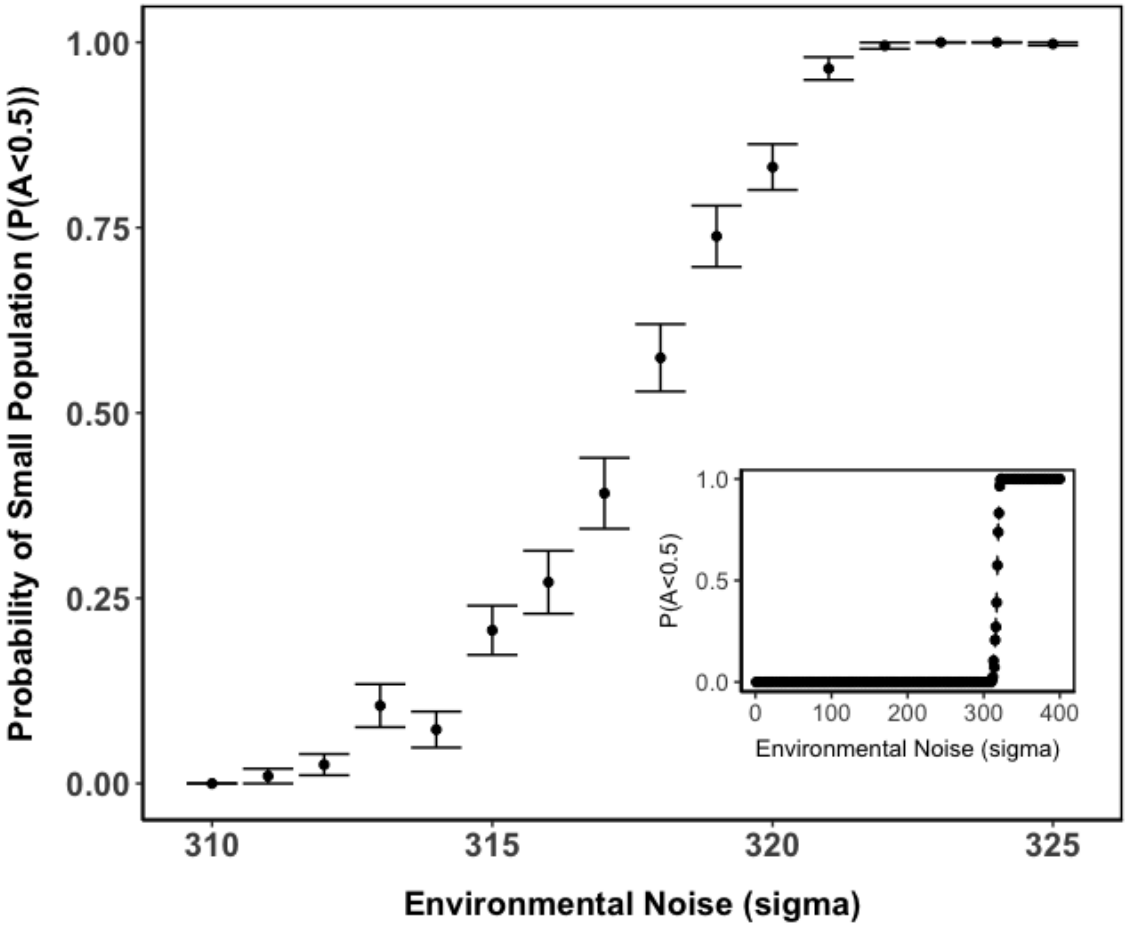

Figure 2.6: The probability of a simulated population being less than $0.5m^{-1}$ when started near the deterministic upper equilibrium value ($A_0 = 22m^{-1}$). Probability and standard error was calculated from 100 simulated populations for 100 days after a burn-in period of 400 days, and is the area for $P(A < 0.5m^{-1})$ of the steady state distribution. The probability of a very small population increases monotonically with environmental noise ($\sim N(600\ PAR, \sigma^2)$).

2.6 Tables

Table 2.1: Constant Parameter Values. Parameter values were either directly measured, calculated from their relationship to measurable values, or estimated from the population growth rate.

Parameter	Fixed Value	Interpretation	Units	Variable Type
z_{max}	0.035	total water column depth (mixing depth)	m	measured, fixed
K_{bg}	0.0011	total attenuation due to nonphytoplankton componenets (background turbidity)	m^{-1}	measured, fixed
k	1	specific attenuation coefficient of phytoplankton	$m^2 g^{-1}$	derived, fixed
$I^{\star}_{opt}$	150	light intensity where p_{max} is observed*	PAR	estimated, fixed
$I^{\star}_{k}$	40	light intensity where p_{max} would be observed in absence of photoinhibition*	PAR	estimated, fixed
$p^{\star}_{max}$	0.49	max growth rate of culture*	day^{-1}	estimated, fixed
l	0.4	specific loss rate	day^{-1}	measured, varies with time due to experimental error

* Estimated by Veraart *et al.* (2012).

Table 2.2: Variable Parameter Values. These values varied between simulations to capture the impact of initial condition dependent steady states.

Parameter	Value Range	Interpretation	Units
A_0	(1,25) by 5	initial population density (light attenuation)	$g\ m^{-1}$
I_{in}	$\sim N(600, (0-600)^2)$	light intensity*	$\mu mol\ photons\ m^2\ sec^{-1} \equiv PAR$
τ_n	$(6 \times 10^{-3}, 4 \times 10^{-}2)$	integral time step passed to lsoda	day^{-1}
τ_e	$(6 \times 10^{-3}, 4 \times 10^{-}2\ )$	environmental noise time step, duration of noise	day^{-1}

* The model expects units of PAR, however the lights are programmed using duty cycle (0,255). A standard curve will be used to convert PAR to duty cycle for experimental treatments.

Bibliography

Arecchi, F. T. & Harrison, R. G. (2012). *Instabilities and Chaos in Quantum Optics*. Springer Science & Business Media. ISBN 978-3-642-71708-6.

Briggs, T. S. & Rauscher, W. C. (1973). An oscillating iodine clock. *Journal of Chemical Education*, 50, 496.

Connell, J. H. & Slatyer, R. O. (1977). Mechanisms of succession in natural communities and their role in community stability and organization. 111, 1119–1144.

Corporation, M. & Weston, S. (2018). *doParallel: Foreach Parallel Adaptor for the 'parallel' Package*. URL `https://CRAN.R-project.org/package=doParallel`. R package version 1.0.14.

Cushing, J. M., Henson, S. M., Desharnais, R. A., Dennis, B., Costantino, R. F. & King, A. (2001). A chaotic attractor in ecology: Theory and experimental data. *Chaos, Solitons & Fractals*, 12, 219–234.

De Kepper, P. & Horsthemke, W. (1979). Experimental Evidence of Noise-Induced Transitions in an Open Chemical System. In: *Synergetics* (eds. Pacault, A. & Vidal, C.), vol. 3.

Springer Berlin Heidelberg, Berlin, Heidelberg. ISBN 978-3-642-67264-4 978-3-642-67262-0, pp. 61–63.

Dennis, B., Munholland, P. L. & Scott, J. M. (1991). Estimation of Growth and Extinction Parameters for Endangered Species. *Ecological Monographs*, 61, 115–143.

D'Odorico, P., Laio, F., Porporato, A., Ridolfi, L. & Barbier, N. (2007). Noise-induced vegetation patterns in fire-prone savannas. *Journal of Geophysical Research: Biogeosciences*, 112.

D'Odorico, P., Laio, F. & Ridolfi, L. (2005). Noise-induced stability in dryland plant ecosystems. *Proceedings of the National Academy of Sciences of the United States of America*, 102, 10819–10822.

D'Odorico, P., Laio, F. & Ridolfi, L. (2006). A Probabilistic Analysis of Fire-Induced Tree-Grass Coexistence in Savannas. *The American Naturalist*, 167, E79–E87.

Drake, J. M. & Lodge, D. M. (2004). Effects of environmental variation on extinction and establishment. *Ecology Letters*, 7.

Eilers, P. H. C. & Peeters, J. C. H. (1988). A model for the relationship between light intensity and the rate of photosynthesis in phytoplankton. *Ecological Modelling*, 42, 199–215.

Gerla, D. J., Mooij, W. M. & Huisman, J. (2011). Photoinhibition and the assembly of light-limited phytoplankton communities. *Oikos*, 120, 359–368.

Horsthemke, W. & Lefever, R. (2006). *Noise-Induced Transitions: Theory and Applications in Physics, Chemistry, and Biology*. No. 15 in Springer Series in Synergetics, 2nd edn. Springer, Berlin. ISBN 978-3-540-11359-1.

Huisman, J. & Weissing, F. J. (1994). Light-Limited Growth and Competition for Light in Well-Mixed Aquatic Environments: An Elementary Model. *Ecology*, 75, 507–520.

Kabashima, S., Kogure, S., Kawakubo, T. & Okada, T. (1979). Oscillatory-to-nonoscillatory transition due to external noise in a parametric oscillator. *Journal of Applied Physics*, 50, 6296–6302.

Kabashima, S., Yamazaki, H. & Kawakubo, T. (1976). Critical Fluctuation near Threshold of Gunn Instability. *Journal of the Physical Society of Japan*, 40, 921–924.

Kawakubo, T., Kabashima, S. & Nishimura, K. (1973a). Observation of Critical Fluctuations in Negative-Resistance Oscillation. *Journal of the Physical Society of Japan*, 34, 1460–1461.

Kawakubo, T., Kabashima, S. & Ogishima, M. (1973b). Critical Slowing-Down near Threshold of Electrical Oscillation. *Journal of the Physical Society of Japan*, 34, 1149–1152.

Kawakubo, T., Yanagita, A. & Kabashima, S. (1981). External Noise Effect on the Onset of Williams Domain in Nematic Liquid Crystals. *Journal of the Physical Society of Japan*, 50, 1451–1456.

Lewontin, R. C. (1969). The meaning of stability. 22, 13–24.

May, R. M. (1973). Stability in Randomly Fluctuating Versus Deterministic Environments. *The American Naturalist*, 107, 621–650.

May, R. M. (1976). Simple mathematical models with very complicated dynamics. *Nature*, 261, 459–467.

May, R. M. (1977). Thresholds and breakpoints in ecosystems with a multiplicity of stable states. 269, 471–477.

Microsoft & Weston, S. (2017). *foreach: Provides Foreach Looping Construct for R.* URL `https://CRAN.R-project.org/package=foreach`. R package version 1.4.4.

Nolting, B. C. & Abbott, K. C. (2016). Balls, cups, and quasi-potentials: Quantifying stability in stochastic systems. *Ecology*, 97, 850–864.

Post, E. & Forchhammer, M. C. (2002). Synchronization of animal population dynamics by large-scale climate. *Nature*, 420, 168–171.

R Core Team (2018). *R: A Language and Environment for Statistical Computing*. R Foundation for Statistical Computing, Vienna, Austria. URL `https://www.R-project.org/`.

Ridolfi, L., DOdorico, P. & Laio, F. (2011). *Noise-Induced Phenomena in the Environmental Sciences*. Cambridge University Press, Cambridge. ISBN 978-0-511-98473-0. URL `http://ebooks.cambridge.org/ref/id/CBO9780511984730`.

Soetaert, K., Petzoldt, T. & Setzer, R. W. (2010). Solving differential equations in r: Package desolve. *Journal of Statistical Software*, 33, 1–25.

Stenseth, N. C., Mysterud, A., Ottersen, G., Hurrell, J. W., Chan, K.-S. & Lima, M. (2002). Ecological Effects of Climate Fluctuations. *Science*, 297, 1292–1296.

Tuljapurkar, S. & Orzack, S. H. (1980). Population dynamics in variable environments I. Long-run growth rates and extinction. *Theoretical Population Biology*, 18, 314–342.

Veraart, A. J., Faassen, E. J., Dakos, V., van Nes, E. H., Lürling, M. & Scheffer, M. (2012). Recovery rates reflect distance to a tipping point in a living system. *Nature*, 481, 357–359.

Yu, K., Okin, G. S., Ravi, S. & D'Odorico, P. (2016). Potential of grass invasions in desert shrublands to create novel ecosystem states under variable climate. *Ecohydrology*, 9, 1496–1506.

2.7 Appendix A: Model Units

The incident light decays with depth according to the Beer-Lambert law. The light intensity at a given depth, $I(z)$, is in units of PAR.

$$
\begin{aligned}
I(z) &= I_{in} * \exp\big(- zkA + zK_{bg})\big) \\
&= *\exp\left(- cm\frac{cm^2}{cell}\frac{cells}{cm^3} + cm\frac{1}{cm}\right) \\
&= PAR
\end{aligned}
\tag{2.4}
$$

The specific production function is

$$
P(I) = \frac{I}{\frac{I_k}{I_{opt}^2}I^2 + \left(1 - 2\frac{I_k}{I_{opt}}\right)I + I_k} \ , \tag{2.5}
$$

and is unit free. All incident light, I_*, has a unit of and cancel each other out. Therefore $P(I(z))$ is also unit free.

$$
\begin{aligned}
\frac{dA}{dt} &= A\ p_{max}\frac{1}{z_{max}}\int_0^{z_{max}} P(I(z))dz - lA \\
&= A\Big(\ p_{max}\frac{1}{z_{max}}\int_0^{z_{max}} P(I(z))dz - l\Big) \\
&= \frac{1}{m}\Big(\frac{1}{day}\frac{1}{m}\int_0^{z_{max}} P(I(z))\ m - \frac{1}{day}\Big) \\
&= \frac{1}{m}\frac{1}{day}
\end{aligned}
\tag{2.6}
$$

2.8 Appendix B: Symbolic Solution

The symbolic solution to the ODE model (Eq. 2.3) was obtained using Maple 2016. The parameters of the primary productivity at a given light intensity ($P(I)$, Eq. 2.2) were condensed so

$$P(I) = \frac{I}{\frac{I_k}{I_{opt}^2} I^2 + \left(1 - 2\frac{I_k}{I_{opt}}\right) I + I_k} = \frac{I}{a * I^2 + b * I + c} \tag{2.7}$$

where

$$a = \frac{I_k}{I_{opt}^2} \quad b = \left(1 - 2\frac{I_k}{I_{opt}}\right) \quad c = I_k.$$

With these substitutions, the solution is

$$\int_0^{z_{max}} P(I(z))dz = 2AI_{in}p_{max} \left[\frac{\begin{array}{r}\arctan\left(\frac{2aI_{in}^2 \exp[(z_{max}(-Ak - K_{bg})] + bI_{in}}{d}\right) \\ + \arctan\left(\frac{2aI_{in}^2 + bI_{in}}{d}\right)\end{array}}{dz_{max}(Ak + K_{bg})} \right] - lA \tag{2.8}$$

where

$$d = \sqrt{I_{in}^2(4ac - b^2)}.$$

2.9 Appendix C: R Code

Below are the functions, and objects used to simulate *Aphanizomenon* growth.

2.9.1 Global Parameter Values

These values are from Veraart *et al.* (2012).

```
Ik <- 40 # Light intensity at p_max if p(I) slope was linear (PAR)
Iopt <- 150 # Optimal light for photosynthesis (PAR)
```

```
loss <- 0.4 #Dilution Rate (day ^-1)
prod.max <- 0.49 # maximium specific production rate when plotted as a
   function of light intensity (day ^-1)
media.atten <- 10^-6 #Light extinction of media (m ^-1)
algal.atten <- 3 # Light extinction coefficient of biomass (m ^-1)
depth <- .05 #chamber depth (m)
```

2.9.2 Dynamical Model

All simulations call on `PIz.growth` as the func argument in the `lsoda` function as part of the **deSolve**

```
PIz.growth <- function(t, y, params){
  A <- y #algal biomass density (g/m^3) OR total biomass of water col (g/
     cm^2)
  #parameters needed
  # A, (mg/mL)
  # Iin,  incident light (PAR)
  # Ik = Iink # Light intensity at p_max if p(I) slope was linear (PAR)
  # l = loss, #Dilution Rate (hour ^-1)
  # pmax = prod.max, #max specific production rate (hour ^-1)
  # kd = media.atten,  background light attentuation (cm^-1)
  # k = algal.atten, algal light attenutation (cm^2/mg)
  # zmax = depth, depth (cm)
  # Imm = immigration (mg/mL),

  with(as.list(c(params)), {
    dA <-  Imm + A * (-l + pmax * (2 * Iin *
    (atan(Iin*(2*Iin*(Ik / ((Ik+Idiff) ^ 2))+(1 - 2 * (Ik / (Ik+Idiff))))
       / sqrt(Iin^2 * (-(1 - 2 * (Ik / (Ik+Idiff)))^2 + 4*(Ik / ((Ik+Idiff
       ) ^ 2))*Ik)))
    - atan(Iin*(2*(Ik / ((Ik+Idiff) ^ 2))*Iin*exp(-zmax*A*k - zmax*kd) +
       (1 - 2 * (Ik / (Ik+Idiff)))) / sqrt(Iin^2 *(-(1 - 2 * (Ik / (Ik+
```

```
      Idiff)))^2 + 4*(Ik / ((Ik+Idiff) ^ 2))*Ik)))) / (zmax*(A*k+kd) *
      sqrt(Iin^2 * (-(1 - 2 * (Ik / (Ik+Idiff)))^2+4*(Ik / ((Ik+Idiff) ^
      2))*Ik))))) #everything after pmax is the light integrated, density
       dep growth rate
    return(list(dA))
  })
}
```

2.9.3 Simulate Environmental Conditions

The environmental conditions were simulated separately than the population trajectories to easy computational load, and allowed for reproducibility when changing the underlying deterministic model.

```
#function to return matrix with ncol(n.sim * length(light.sd)) and nrows(t
   .max/delta.t). Each col has mean light.mean and standard deviation
   light.sd

light.series=function(t.max, n.sim=20, light.mean=600, light.sd=0, delta.t
    = 0.02, delta.ratio=1, rep.seed=9782435){
  #delta.t: integral step size for lsoda (Days)
  #delta.ratio: length of environmental noise time step vs system time
     step. MUST BE WHOLE NUMBER
  #t.max: max time in series/ length of time series (Days)
  #n.sim: number of replicates or simulations for given light.sd condition
  #light.mean: mean light of normal distribution
  #light.sd: sd of light from a normal distribution, can be a vector

  light.treatment <- NULL

  if(delta.ratio==1){
```

```
    tau <- round(t.max/delta.t) #determine number of light conditions in a
        simulation times long with interval delta.t
  }else{
    tau <- round(t.max/(delta.t*delta.ratio))
  }

  for( k in light.sd){ #for multiple sd treatments if wanted

    for(j in (1:n.sim)){ #j cols for each light.sd (k) treatment
      rep.j <- rnorm(tau, light.mean, k) #light regime for single
          simulation
      rep.j[rep.j<0] <- 0.01 #negative light is replaced with zero PAR
      light.treatment <- cbind(light.treatment, rep.j) #save it in a
          matrix
    }
  }
  if(delta.ratio!=1){light.treatment <- apply(light.treatment,2,rep, each=
     delta.ratio)}

  return(light.treatment)
}
```

2.9.4 Simulate Populations with Light Conditions

The single light condition function `aphani.sim` is called in the parallel function `aphani.para.sim`.

```
#Function to run simulations with varying light
aphani.sim=function(A0,light.treatment, light.sd="", delta.t=0.02, n.sim
   =20,pmax=prod.max, l=loss,Iink =Ik ,Iind=Idiff ,zmax=depth,k=algal.
   atten,kd=media.atten, immigration=1*10^-10, colnm = TRUE){

  #Updated with PIz.growth in RatePIz.R
```

```
PIz.growth <- function(t, y, params){
  A <- y #light attenuation (m^-1)
  #parameters needed
  # A, light attenuation (m^-1)
  # Iin,  incident light (PAR)
  # Ik = Iink # Light intensity at p_max if p(I) slope was linear (PAR)
  # l = loss, #Dilution Rate (day ^-1)
  # pmax = prod.max, #max specific production rate (day^-1)
  # kd = media.atten,  background light attentuation (m^-1)
  # k = algal.atten, algal light attenutation (m^-1)
  # zmax = depth, depth (m)
  # Imm = immigration,
  # a = a1,  (Iink / ((Iink+Idiff) ^ 2))
  # b = b1,  (1 - 2 * (Iink / (Iink+Idiff)))

  with(as.list(c(params)), {
    dA <-  Imm + A * (-l + pmax * (2 * Iin *
    (atan(Iin*(2*Iin*(Ik / ((Ik+Idiff) ^ 2))+(1 - 2 * (Ik / (Ik+Idiff)))
       ) / sqrt(Iin^2 * (-(1 - 2 * (Ik / (Ik+Idiff)))^2 + 4*(Ik / ((Ik+
       Idiff) ^ 2))*Ik)))
  - atan(Iin*(2*(Ik / ((Ik+Idiff) ^ 2))*Iin*exp(-zmax*A*k - zmax*kd) +
     (1 - 2 * (Ik / (Ik+Idiff)))) / sqrt(Iin^2 *(-(1 - 2 * (Ik / (Ik+
     Idiff)))^2 + 4*(Ik / ((Ik+Idiff) ^ 2))*Ik))))  / (zmax*(A*k+kd) *
     sqrt(Iin^2 * (-(1 - 2 * (Ik / (Ik+Idiff)))^2+4*(Ik / ((Iink+Idiff)
     ^ 2))*Ik))))) #everything after pmax is the light integrated,
     density dep growth rate
    return(list(dA))
  })
}

require(deSolve)
#A0 starting population
#light.treatment: matrix of incident light created by light.series()
```

```
#delta.t: delta.t used to make light.treatment
#light.sd: sd used to make light.series(), used for naming col
#n.sims: number of sim at each sd in light_series, used for naming col

w.solution  <- c()
for(r in c(1:ncol(light.treatment))) { #loop through light sequence for
   each replicate population
  w.series <-c() #for first time step in simulation
  I.treatment <- as.numeric(light.treatment[1,r]) #pull out starting
     incident light

  ode.params  <- c(pmax=pmax, Ik=Iink, Idiff=Iind, Iin=I.treatment, zmax
     =zmax, k=k, kd=kd, l=l, Imm=immigration) #parameters for ode solver
  ode.times  <- c(0,delta.t) #time for ode solver
  w.series <- lsoda(A0, ode.times, PIz.growth, parms=ode.params) #ode
     solve from t=0 to delta.t

  for(t in 2:nrow(light.treatment)){ # loop through remaining time steps
      of replicate population
    A  <- w.series[nrow(w.series),2] #set population density based on
       last ode solution
    #if NA set to 0
    #if(w.series[nrow(w.series),2]=="NaN") {A <- 0} else {A <- w.series[
       nrow(w.series),2]}
    I.treatment <- as.numeric(light.treatment[t,r]) #pull out incident
       light of current time step

    ode.params  <- c(pmax=pmax, Ik=Iink, Idiff=Iind, Iin=I.treatment,
       zmax=zmax, k=k, kd=kd, l=l, Imm=immigration) #parameters for ode
       solver, update I.treatment
    ode.times  <- c(w.series[nrow(w.series),1],w.series[nrow(w.series)
       ,1]+delta.t ) #time for ode solver
    w.temp <- lsoda(A, ode.times, PIz.growth, parms=ode.params)[2,] #
```

```
        save time, and w at next time step
      w.series <- rbind(w.series,w.temp)#save it
      }
  if(r==1) {w.solution  <- w.series} else {w.solution <-cbind(w.solution,w
     .series[,2])} #for first simulation
  }
rownames(w.solution)<-NULL
if(colnm == TRUE){colnames(w.solution) <- c("time", paste("A0",A0, "sd",
   rep(light.sd, each=n.sim),".rep",1:n.sim, sep=""))} #name each
   population (col) with treatment conditions
return(w.solution)
}
```

2.9.5 Parallel Simulation Functions

The function `light.series.list` is used to create the environmental noise. This is then fed into `aphani.para.sim` to create simulations.

```
#function to return list of matrix with ncol(n.sim * length(light.sd)) and
    nrows(t.max/delta.t). Each col has mean light.mean and standard
   deviation light.sd, each list entry has a different light.sd

light.series.list=function(t.max, n.sim=100, light.mean=600, light.sd=0,
   delta.t = 0.02, delta.ratio=1){
  #delta.t: integral step size for lsoda (Days)
  #delta.ratio: length of environmental noise time step vs system time
     step. MUST BE WHOLE NUMBER
  #t.max: max time in series/ length of time series (Days)
  #n.sim: number of replicates or simulations for given light.sd condition
  #light.mean: mean light of normal distribution
  #light.sd: sd of light from a normal distribution, can be a vector
```

```
  light.list <- list()
  if(delta.ratio==1){
    tau <- round(t.max/delta.t) #determine number of light conditions in a
        simulation times long with interval delta.t
  }else{
    tau <- round(t.max/(delta.t*delta.ratio))
  }


  for( k in 1:length(light.sd)){ #for multiple sd treatments if wanted
    light.treatment <- NULL
    for(j in (1:n.sim)){ #j cols for each light.sd (k) treatment
      rep.j <- rnorm(tau, light.mean, light.sd[k]) #light regime for
          single simulation
      rep.j[rep.j<0] <- 0.01 #negative light is replaced with zero PAR
      light.treatment <- cbind(light.treatment, rep.j) #save it in a
          matrix
    }
    if(delta.ratio!=1){light.treatment <- apply(light.treatment,2,rep,
        each=delta.ratio)}
    light.list[[k]] <- light.treatment
  }


  return(light.list)
}
```

```
#Function to run many sims with different initial conditions but same set
   of light treatments in parallel (ie. vertical slice of stochastic
   bifurcation plot)
#updated with Idiff instead of Iopt based on new PIz.growth ode function
aphani.para.sim = function(cores = 2,
```

```
                          A0.seq,
                          treat.list,
                          treat.names,
                          aphani.sim1 = aphani.sim,
                          delta.t = 0.02,
                          pm = prod.max,
                          ls = loss,
                          Ik1 = Ik ,
                          Id1 =Idiff,
                          dp = depth,
                          aa = algal.atten,
                          ma = media.atten,
                          immi = 1 * 10 ^ -10) {
# cores: number of cores to use in parallel
# A0.seq: initial conditions to simulate for each light.list entry
# treat.list: made by light.series.list; list of light treatments with
   length unique(light.sd)
#treat.names:  vector of light.sd used to make treat.list

#model parameter values held constant
# delta.t=0.02
# pmax=prod.max
# l=loss
# Iink =Ik
# Iinopt=Iopt
# zmax=depth
# k=algal.atten
# kd=media.atten
# immigration=1*10^-10

require(dplyr)
require(doParallel)
require(foreach)
```

```
merge.by.time <- function(a, b) {
  merge(a, b, by="time")
}

# make cluster
cl <- makeCluster(cores)
registerDoParallel(cl)


results <-
  foreach(i = 1:length(treat.list), .packages = "foreach") %dopar% { #
     default returns each iteration as an entry in a list
    foreach(A = A0.seq, .combine = merge.by.time) %do% {
      aphani.sim1(
        A0 = A,
        light.treatment = treat.list[[i]],
        light.sd = treat.names[i],
        delta.t = 0.02,
        n.sim = ncol(treat.list[[i]]),
        pmax = pm,
        l = ls,
        Iink = Ik1 ,
        Iind = Id1 ,
        zmax = dp,
        k = aa,
        kd = ma,
        immigration = immi
      )
    }
  }
stopCluster(cl)
```

```
  return(results)
}
```

2.9.6 R Session Details

```
sessionInfo()
R version 3.6.1 (2019-07-05)
Platform: x86_64-pc-linux-gnu (64-bit)
Running under: Ubuntu 18.04.5 LTS

Matrix products: default
BLAS:   /usr/lib/x86_64-linux-gnu/openblas/libblas.so.3
LAPACK: /usr/lib/x86_64-linux-gnu/libopenblasp-r0.2.20.so

locale:
 [1] LC_CTYPE=en_US.UTF-8
 [2] LC_NUMERIC=C
 [3] LC_TIME=en_US.UTF-8
 [4] LC_COLLATE=en_US.UTF-8
 [5] LC_MONETARY=en_US.UTF-8
 [6] LC_MESSAGES=en_US.UTF-8
 [7] LC_PAPER=en_US.UTF-8
 [8] LC_NAME=C
 [9] LC_ADDRESS=C
[10] LC_TELEPHONE=C
[11] LC_MEASUREMENT=en_US.UTF-8
[12] LC_IDENTIFICATION=C

attached base packages:
[1] parallel  stats     graphics
[4] grDevices utils     datasets
[7] methods   base
```

```
other attached packages:
[1] doParallel_1.0.14 iterators_1.0.12
[3] foreach_1.4.7     dplyr_0.8.3
[5] deSolve_1.24

loaded via a namespace (and not attached):
 [1] Rcpp_1.0.2        codetools_0.2-16
 [3] crayon_1.3.4      assertthat_0.2.1
 [5] R6_2.4.0          magrittr_1.5
 [7] pillar_1.4.2      rlang_0.4.10
 [9] rstudioapi_0.11   tools_3.6.1
[11] glue_1.3.1        purrr_0.3.2
[13] compiler_3.6.1    pkgconfig_2.0.2
[15] tidyselect_1.1.0 tibble_2.1.3
```

Experimental demonstration of a noise-induced transition

3.1 Introduction

Natural systems continuously change and take on new states. Ecologists have developed theories to explain these changes in population abundance over time such as community succession, competitive exclusion, predator-prey limit cycles and alternative stable states (abbreviated as ASS; Connell & Slatyer, 1977; Lewontin, 1969; May, 1977; Nolting & Abbott, 2016). Within the ASS framework, the system changes states either due to external disturbances or a change in the stability landscape. This landscape is created by plotting the system's potential against the system value such that the minima and maxima are stable and unstable equilibria, respectively (Strogatz, 2001). Stability can be intuitively determined by imagining the current system state is a ball sitting on the plotted potential surface (as reviewed by Nolting & Abbott, 2016). The ball follows gravity to the closest valley or stable equilibrium. Changes in the state of the system arise in one of two paths (Beisner *et al.*, 2003). In the first path, the stability landscape changes with a change in a parameter value. As an example, we can think about the logistic model which has equilibria at zero, and carrying capacity (K). Given the growth rate (r) is greater than one, the potential function will have a valley centered at the carrying capacity and a peak at zero. As the carrying capacity

is decreased, the valley in the potential function shifts towards extinction until $K = 0$. When the carrying capacity is zero, the potential function has a peak at carrying capacity and a valley at extinction. Changes in the parameter value do not always map one-to-one onto changes in the potential function (Scheffer *et al.*, 2001, 2009). If we repeated this process by slowly decreasing the growth rate, the potential function would not change until the rate is equal to one. In the second path, perturbations can change the system state by pushing the ball from one valley or basin of attraction to another, rather than shifting the location of the valley. Examples of sufficiently large perturbations include species introduction, climate oscillations, and sea-level rise (Chase, 2003; McGlathery *et al.*, 2013; Jia *et al.*, 2015; Scheffer *et al.*, 2001) Despite acknowledging the role of external forces, most theory about alternative stable states focuses on a shift in a mean environmental parameter value while ignoring parameter variance (Beisner *et al.*, 2003).

The theories described above, for the most part, assume that a deterministic model of the system is an appropriate approximation for understanding the dynamics. However, in cases with strong non-linear feedback and noise on a similar time scale as the deterministic system a stochastic model is more appropriate (May, 1973; Tuljapurkar & Orzack, 1980; Horsthemke & Lefever, 2006; Ridolfi *et al.*, 2011a). As an example, May (1973) compared a logistic model with either a fixed or varying carrying capacity (K vs $K_{sg} \sim N(\mu, \sigma^2)$). When the variance in the carrying capacity was small, the equilibria of the deterministic and stochastic model were similar. In other words, in the ball-and-valley model a small variance wobbles the ball at the bottom of the valley, in this case at the carrying capacity. As the variance increases the upper equilibrium decreases or the valley shifts from the carrying capacity towards extinction. At $\sigma \leq K/2$ the system undergoes a transition and the most probable population size is extinction. This qualitative change in the shape of the potential function is called a transition, and in this case it is a noise-induced transition (NIT). The noise-induced extinction (NIE) described by May (1973) is a subset of transitions that can result in a change in the number and/or location of valleys in the potential landscape (Ridolfi

et al., 2011b).

While equilibria are point or limit-cycles in deterministic models, equilibria in a stochastic model are defined in probabilistic terms. Here, the extrema of the stationary probability distribution (SPD) of population size is the stochastic equivalence of deterministic equilibria; modes correspond to stable equilibria while anti-modes correspond unstable equilibria (Horsthemke & Lefever, 2006). The NIT can be shown analytically by solving for the SPD extrema which breaks down into two terms (Horsthemke & Lefever, 2006). The first term is the extrema in the noise-free model, and the second term of the SPD extrema expression is multiplied by the variance, so as the variance tends to zero the extrema approach the deterministic, noise-free equilibria. The ability to breakdown the expression for the extrema into two terms is critical for two reasons. First, the extrema change with a transition making it an appropriate metric to detect the occurrence of NITs. Second, the change in extrema is dependent only on the variance or noise in the system making it a specific metric for detecting NITs. These characteristics support the use of a single metric, extrema, to detect NITs in empirical systems.

While this novel mechanism leading to alternative states was proposed over 50 years ago, it has been understudied in ecology (but see Ridolfi *et al.*, 2011b). To date, NIT has been explored in ecological models but to our knowledge it has not been empirically demonstrated in a biological system. Outside of ecology, NITs have been successfully modeled and experimentally demonstrated in electric and chemical systems (Horsthemke & Lefever, 2006).

To investigate the possibility of NIT in biological systems, I conducted experiments using chemostats of the cyanobacteria *Aphanizomenon flos-aquae*. Based on simulations of the system, I expect to observe a noise-induced extinction (NIE) when light variability passes a given threshold, while maintaining a constant mean light intensity. First, I present the constant light experiments which are used to parameterize the model with system specific parameter values. Then, I present the results from the chemostat experiments where popu-

lations were grown under variable light.

3.2 Methods

The possibility of a NIE was examined using eight 500mL chemostats of *Aphanizomenon flos-aquae* based on the design developed by Huisman *et al.* (1999, see Appendix A for details). White environmental noise was introduced by changing the output of the LED grow lights which also modified the photosynthetically active radiation (PAR).

Populations were subject to a two-by-two factorial of mean light conditions ($\mu = (83, 300PAR)$), and environmental noise ($\sigma = (0, \mu/2)$). When presenting information about light variability, I will use standard deviation rather than variance so the all units are in PAR, rather than PAR and PAR^2.

3.2.1 Model Parameterization & Treatment Selection

The stochastic model had a deterministic skeleton developed by Huisman & Weissing (1994). The deterministic model using the light intensity at a given depth (3.1), and the productivity at a given light intensity (3.2) to calculate the algal density's (A) rate of change at a given cell density (3.3). See Tbl. 3.1 for parameter definition and units.

$$I(z) = I_{in} * \exp\big(- z(kA + K_{bg})\big) \tag{3.1}$$

$$P(I) = \frac{p_{max} I}{\frac{I_k}{I_{opt}^2} I^2 + \left(1 - 2\frac{I_k}{I_{opt}}\right) I + I_k} \tag{3.2}$$

$$\frac{dA}{dt} = A\left(\frac{1}{z_{max}} \int_0^{z_{max}} P(I(z))dz - l\right) \tag{3.3}$$

Simulating the deterministic dynamics require 6 parameters, half of which can be directly measured, while the other half were estimated by simultaneously fitting the dynamical model

to multiple populations grown under a range of constant light conditions. The parameters max depth (z_{max}), algal light attenuation (k), and background light attenuation (k_d) were directly measured, while the maximum specific production rate (p_{max}), the optimal light intensity (I_{opt}), and the light intensity at p_{max} if the initial slope of the p-I curve was maintained (I_k) were estimated by trajectory matching in R using package deSolve (R Core Team, 2018; Soetaert *et al.*, 2010)(See Appendix B for R code). The system specific parameters were used to simulate populations subject to constant or variable light. In the case of variable light the I_{in} constant parameter was replaced with a random normal variable I_{wn} $N(\mu, \sigma^2)$. A 4-point light deviation gradient that spanned the NIT to extinction was selected (Ch. 2). Two of the eight chambers were randomly assigned to each treatment, light conditions were drawn from a normal distribution with the treatment standard deviation for each replicate. Enough conditions were drawn to allow the experiment to run for 30 days with the light condition changing every minute. This table of chamber x light condition was used by the Arduino Mega 2560 REV3 to change the light intensity of the LEDs through pulse-width modulation.

3.2.2 Culture & Chemostat Methods

A culture of *A. flos-aquae* CCMP2764 was obtained from the Bigelow National Center for Marine Algae and Microbiota (https://ncma.bigelow.org/). The algal cultures were maintained in BG-11 media without trace metals at 20∘ C with a 16:8 hour light dark cycle (Tbl. 3.2 Vanderploeg *et al.*, 2001).

All chemostats within an experimental block were started with 500mL from a well mixed 4L culture with an $\approx OD_{600-blank} = 0.15$. A 4 x 10W LED light grid attached to a heat sink was placed 3.5cm from the chamber. This design was efficient at diffusing heat and did not require a water jacket for cooling. The dilution rate was set at 0.2 day^{-1}. However, the rate varied over time and chamber so all effluent was measured for an accurate rate. Populations were sampled every 12 hours by collecting effluent from the twelfth hour. This

effluent was used to measure turbidity and in vivo chlorophyll-a and phycocyanin florescence using a plate reader and a 96 well plate (Biotek H1 Synergy ; Nunc part no. 265301). The use of turbidity and florescence allowed us to distinguish between increased turbidity due to cell growth or death. Florescence was not used alone as a measure of population size due to plate reader sensitivity not being able to detect extinction. The experiment was ended either when all populations went extinct, or settled to a constant density ($\pm$ 5% over 48 hours). Extinction was defined as no visible cells in a 1ml sub-sample.

Significant differences in the end point of the time series were detected by an ANOVA, and if needed, a Bonferroni corrected t-test.

3.3 Results

Populations grown under different constant light conditions different in their dynamics (Fig. 3.1) The estimated parameters were qualitatively similar to previously published values, and indicated the mean light treatment should be 300 PAR (Tbl. 3.3). However, attempts to culture *A. flos-aquae* near the previously published, and estimated optimal light, $\sim$ 150 PAR, had failed due to cell bleaching which is a sign of high light stress. Given that I knew the estimated parameters and resulting simulations were not representative of the system, I added a mean light experimental treatment of $\mu = 83$ PAR that I was able to successfully grow *A. flos-aquae* in the past. I chose to use one non-zero standard deviation treatment of half of the mean assuming that the true stochastic bifurcation would scale similarly with the simulated bifurcation diagram (Ch.2 Fig.2.4). This treatment selection created a 2x2 factorial design and was run within a single block so that each mean light (83, 300 PAR) by standard deviation (0, 0.5 $\times$ mean) was replicated twice. I was not interested in the interaction between the two factors, as is the norm with factorial designs, so each mean light treatment was analyzed separately. All populations with a mean light of 300 PAR went declined, while within the mean PAR of 83 only those subject to variable light con-

dition declined (Fig 3.2). The populations grown with and without variable light at mean of 300 PAR went extinct. Due to lost replicates, no statistical analysis was done on this group. Within the lower mean light treatment, the growth in the variable environment was significantly different than in the constant environment (Welch two sample t-test t(1.94) = 22.14, p=0.002; t(1.00)=17.41,p=0.037;t(1.07)=47.37,p=0.011 for turbidity, chlorophyll, and phycocyanin, respectively).

3.4 Discussion

Ecologists have long sought to understand mechanisms that lead to shifts in population sizes (Lewontin & Cohen, 1969; May, 1976; Cushing *et al.*, 2001; Scheffer, 2020). Most developed theory rely on a deterministic representation of the world (Nicholson, 1957; Durrett & Levin, 1994; Kendall *et al.*, 1999; Henson *et al.*, 2001; Coulson *et al.*, 2004). This is despite theoretical analysis predicting stochastic forces can reshape stability in ecological systems (May, 1973; Horsthemke & Lefever, 2006; Ridolfi *et al.*, 2011a). The presented work highlights the importance of environmental stochasticity by experimentally demonstrating a noise-induced extinction, a type of noise-induced transition using chemostats of the cyanobacteria, *A. flos-aquae*. Chemostats where grown under constant light, or variable light with a mean intensity of 83 PAR ($\sim N(\mu, \sigma^2)$ where $\sigma = (0, \mu/2)$, respectively). To the best of my knowledge, this is the first experimental demonstration of a NIE in a biological system.

For this particular study system, I found our strain of *A. flos-aquae* to be substantially more light sensitive than other work using the same species. Veraart *et al.* (2012) reported observing the maximum growth rate at a constant incident light greater than 700 PAR; our constant light model also predicted a similar range. However, when I attempted to grow cultures under these predicted ideal conditions the cultures bleached or washed out with 300 PAR, less than half of the predicted ideal incident light. Initially, I suspected the cultures were starting below the unstable equilibrium in the region of bistability (Fig. 2.2). However

in most cases, the populations declined from the starting density regardless of that initial density. This could imply that there is something not captured in our system design that is incorporated into the mechanistic model or our design differs in some significant way from the more recently published designs (Veraart *et al.*, 2012). I believe it to be the later, given the discrepancies in ideal incident light between the model predictions and experimental results. The original design by Huisman *et al.* (1999) used incandescent lights which are a significant heat source when ran constantly. A 1.2cm water jacket was used to absorb and disperse the heat away from the culture but also had a side effect of reducing the incident light experienced by the culture through scattering. The water jacket is, I believe mistakenly, omitted in later design descriptions which use more efficient LEDs (Veraart *et al.*, 2012).

The mismatch between the model predictions and observed growth does not detract from the strength of evidence for the NIE. The model predictions and experimental outcomes matched qualitatively. This work clearly demonstrated the ability for populations grown under a constant light condition of 83 PAR to persist while those experiencing variable light did not. Ideally, I would have been able to execute the initial experimental design testing a range of variances in higher replication to determine the region of the phase transition. However, this system is extremely sensitive to experimental conditions; as such, we were unable to achieve such a high level of replication, in spite of years of trials.

This demonstration of a noise-induced extinction used single species mesocosms, and a contrived source of environmental variability. This type of simplification have lead some to question the generality of mesocosm work (Carpenter, 1996; Schindler, 1998). However, this approach allows for the demonstration of yet to be observed ecological phenomena by creating a model system (Drake & Kramer, 2012). The essential properties of a model used to detect NITs, non-linear dynamics and an understanding of how the environmental noise propagates through the system, are captured in this experimental design. This meets the criteria for model-based reasoning and reasoning by analogy which asserts that a variable and response in a mesocosms is analogous to a variable and response in nature (Drake &

Kramer, 2012).

The established alternative stable states theory dictates that a system's stability changes through one of two mechanisms. Demonstrating a NIE provides a third path to stability changes, along with a kinetic parameter change or a large environmental perturbation (Nolting & Abbott, 2016). ASS has been an active research field since its introduction, this is particularly true given an outcome of ASS is a disproportionately large change in the system state as a response to a small environmental change past a threshold (Lewontin, 1969; Holling, 1973; Sutherland, 1974; May, 1977; Beisner *et al.*, 2003; Scheffer, 2020). Despite this, there have been numerous studies and meta-analyses to identify the threshold between stable states for a given environmental condition (Hillebrand *et al.*, 2020). However, these general thresholds are unlikely to be detected (Hillebrand *et al.*, 2020). Focusing on laboratory and field experiments looking for evidence of ASS, 38% of the studies demonstrated an absence of ASS (8 out of 21 studies Schröder *et al.*, 2005). The identification of ASS related thresholds are even more muddled by stochastic models that mimic deterministic models with ASS (Abbott & Nolting, 2017; Fukami & Nakajima, 2011). Clear thresholds between alternative stable states could arise if the variance of the environmental condition was also included as a predictor in addition to pulse perturbations. This is the case for grassland primary productivity when precipitation means are constant but variance in precipitation increases. The increased precipitation variance decreases net primary productivity by up to 50% (Ratajczak *et al.*, 2018).

The experimental demonstration of a noise-induced transition, in addition to the mixed evidence for alternative stable states, suggests to me that it is time to move from a deterministic representation of the world to one which incorporates stochasticity and thinks of stability in quasi-stationary terms. This transition needs to be led by experimentalists using study systems with well defined nonlinearity, short generation times, and characterized environmental stochasticity in natural populations. Through this work, we can develop a heuristic understanding of how and when a stochastic rather than deterministic model is a

more appropriate description of the natural world.

3.5 Tables

Table 3.1: Model Parameter Values. Parameter values were either directly measured, calculated from their relationship to measurable values, or estimated from the population growth rate.

Parameter	Interpretation	Units	Variable Type
A	population density	gm^{-1}	measured response
z_{max}	total water column depth (mixing depth)	m	measured, fixed
K_{bg}	total attenuation due to background turbidity	m^{-1}	measured, fixed
k	specific attenuation coefficient of phytoplankton	m^2g^{-1}	derived, fixed
I	incident light at surface	PAR	variable based on treatment
I_{opt}	light intensity where p_{max} is observed	PAR	estimated, fixed
I_k	light intensity where p_{max} would be observed in absence of photoinhibition	PAR	estimated, fixed
p_{max}	max growth rate of culture	day^{-1}	estimated, fixed
l	specific loss rate	day^{-1}	measured, varies with time due to experimental error

Table 3.2: Completed BG-11 media compounds and concentrations per liter. The pH was adjusted to 6.8 before heat sterilization.

Compound	Concentration (μM)
$CaCl_2 \bullet 2H_2O$	250
$MgSO_4 \bullet 7H_2O$	300
$NaHCO_3$	10,000
$K_2HPO_4 \bullet 3H_2O$	180
$NaNO_3$	2,000
Na_2CO_3	190
citric acid	30
ferric ammonium citrate	30
EDTA (disodium magnesium)	3

Table 3.3: Parameter values that were estimated for the constant light growth rate experiment, and those that have been published by Veraart *et al.* (2012).Parameters marked with a star (*) can be directly measured from the experimental set up.

Parameter	Estimated	Previously Published
$z^\star_{max}$	0.035	0.05
$K^\star_{bg}$	0.047	10^{-6}
$k^\star$ 2.02		3
I_{opt}	261	150
I_k	68.8	40.0
p_{max}	0.023	0.490
$l^\star$	0.2	0.4

3.6 Figures

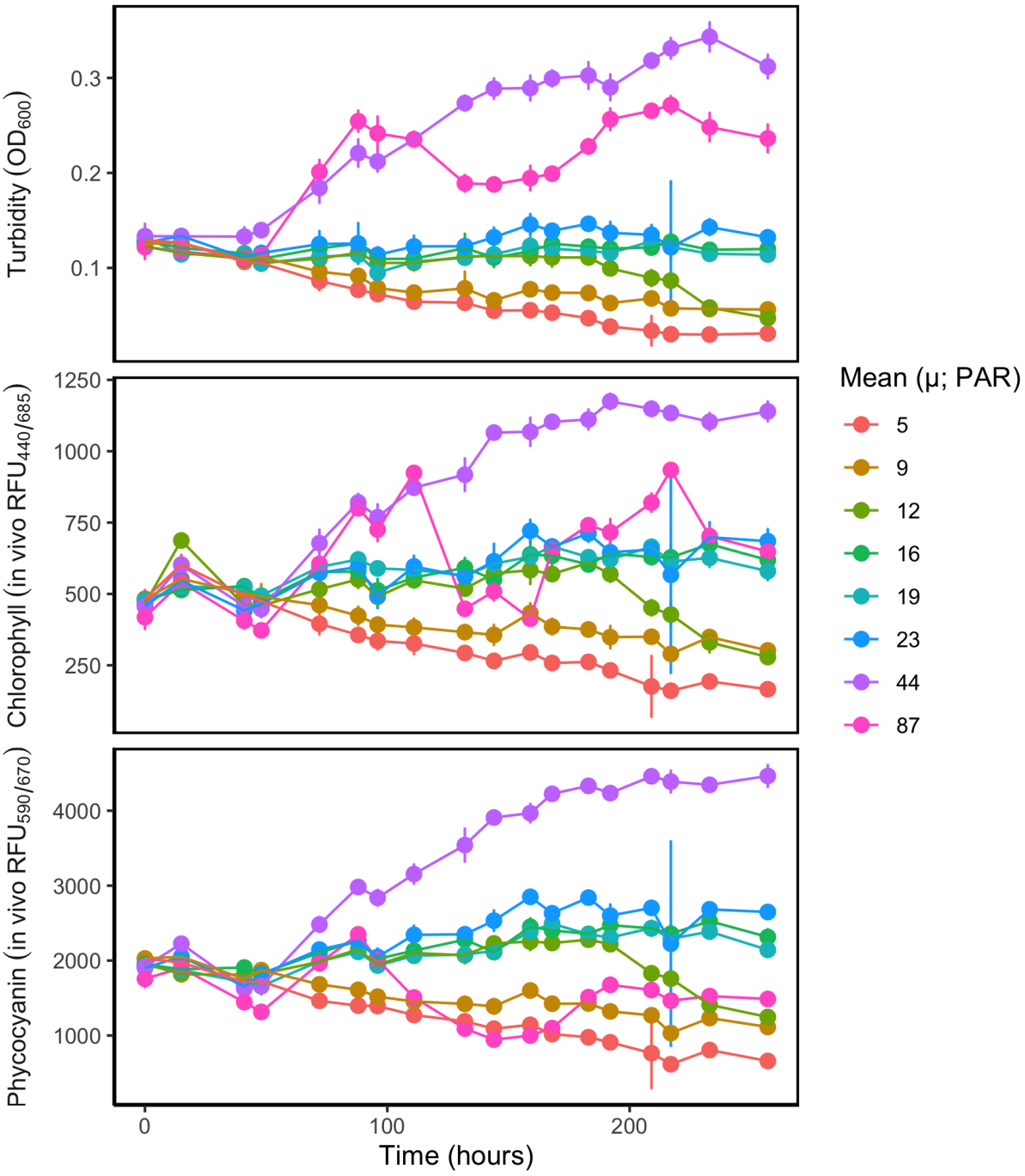

Figure 3.1: Growth under constant light was used to estimate model parameters p_{max},I_k,and I_{opt}. The different response to a range of light intensity shows the non-linear, non-monotonic relationship between light and growth rate. The need to use multiple types of population measurements is exemplified in the 87 PAR treatment which has a high turbidity, but low florescence indicating the culture was bleaching and on the way to extinction.

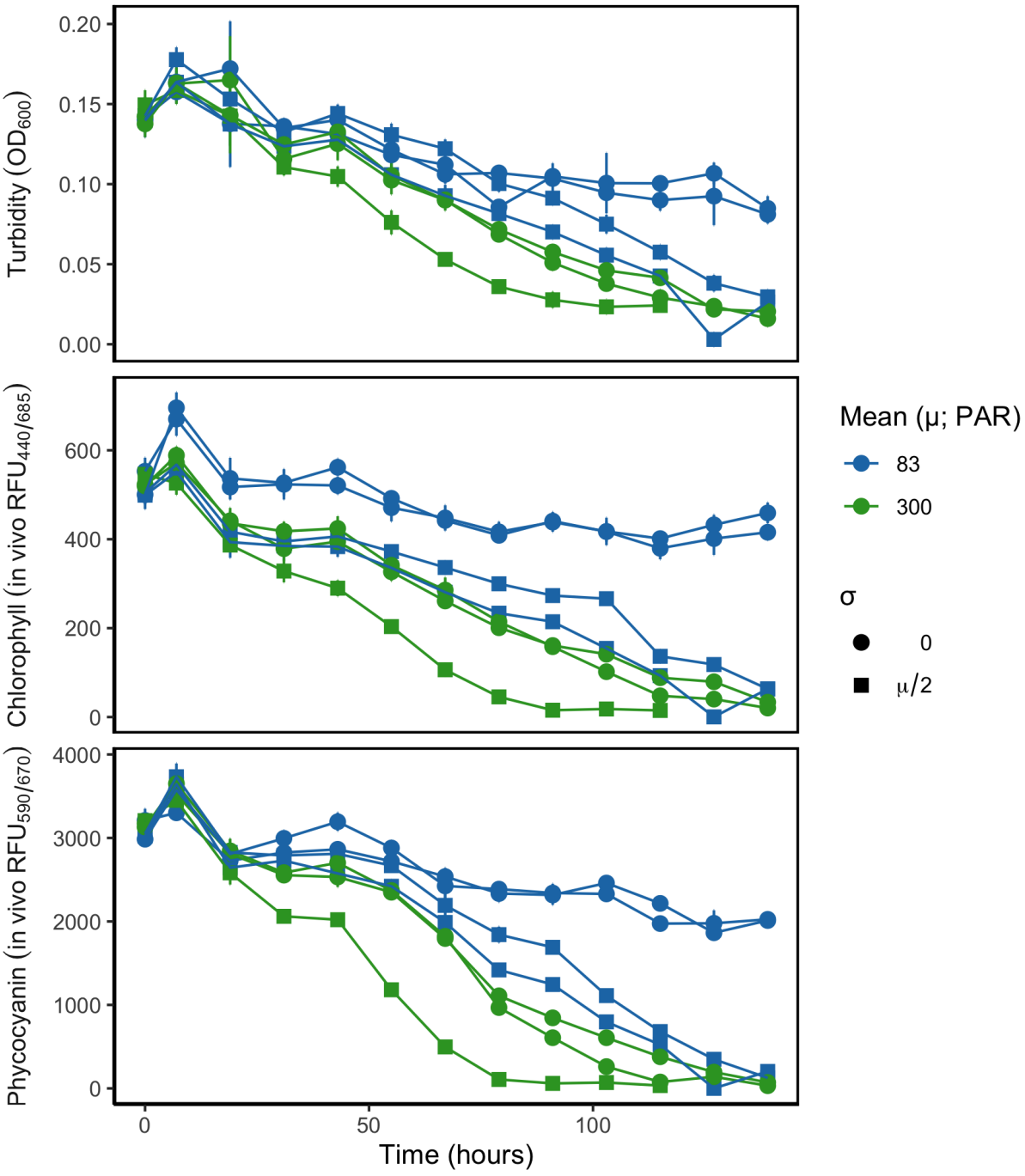

Figure 3.2: A 2X2 comparison of growth under constant and variable light at two mean values. The control of constant light (○) is used to determine the effect of the variable light treatment which follows a normal distribution with the given mean (color), and standard deviation of half of the mean (□). The experimental apparatus malfunctioned resulting in the loss of replicates in the mean PAR of 300 treatment. The populations subject to constant light at 83 PAR are significantly different from the variable light treatment with a mean PAR of 83 in all three measures of population density (t-test; p-value= 0.002,0.037,0.011 for turbidity, chlorophyll, and phycocyanin, respectively.

Bibliography

Abbott, K. C. & Nolting, B. C. (2017). Alternative (un)stable states in a stochastic predator–prey model. *Ecological Complexity*, 32, 181–195.

Beisner, B. E., Haydon, D. T. & Cuddington, K. (2003). Alternative stable states in ecology. *Frontiers in Ecology and the Environment*, 1, 376–382.

Carpenter, S. R. (1996). Microcosm Experiments have Limited Relevance for Community and Ecosystem Ecology. *Ecology*, 77, 677–680.

Chase, J. M. (2003). Experimental evidence for alternative stable equilibria in a benthic pond food web. *Ecology Letters*, 6, 733–741.

Connell, J. H. & Slatyer, R. O. (1977). Mechanisms of succession in natural communities and their role in community stability and organization. 111, 1119–1144.

Coulson, T., Rohani, P. & Pascual, M. (2004). Skeletons, noise and population growth: The end of an old debate? *Trends in Ecology & Evolution*, 19, 359–364.

Cushing, J. M., Henson, S. M., Desharnais, R. A., Dennis, B., Costantino, R. F. & King, A. (2001). A chaotic attractor in ecology: Theory and experimental data. *Chaos, Solitons & Fractals*, 12, 219–234.

Drake, J. M. & Kramer, A. M. (2012). Mechanistic analogy: How microcosms explain nature. *Theoretical Ecology*, 5, 433–444.

Durrett, R. & Levin, S. (1994). The Importance of Being Discrete (and Spatial). *Theoretical Population Biology*, 46, 363–394.

Fukami, T. & Nakajima, M. (2011). Community assembly: Alternative stable states or alternative transient states? *Ecology Letters*, 14, 973–984.

Henson, S. M., Costantino, R. F., Cushing, J. M., Desharnais, R. A., Dennis, B. & King, A. A. (2001). Lattice Effects Observed in Chaotic Dynamics of Experimental Populations. *Science*, 294, 602–605.

Hillebrand, H., Donohue, I., Harpole, W. S., Hodapp, D., Kucera, M., Lewandowska, A. M., Merder, J., Montoya, J. M. & Freund, J. A. (2020). Thresholds for ecological responses to global change do not emerge from empirical data. *Nature Ecology & Evolution*, 4, 1502–1509.

Holling, C. S. (1973). Resilience and Stability of Ecological Systems. *Annual Review of Ecology and Systematics*, 4, 1–23.

Horsthemke, W. & Lefever, R. (2006). *Noise-Induced Transitions: Theory and Applications in Physics, Chemistry, and Biology*. No. 15 in Springer Series in Synergetics, 2nd edn. Springer, Berlin. ISBN 978-3-540-11359-1.

Huisman, J., Jonker, R., Zonneveld, C. & Weissing, F. (1999). Competition for light between phytoplankton species: Experimental tests of mechanistic theory. *Ecology*, 80, 211–222.

Huisman, J. & Weissing, F. J. (1994). Light-Limited Growth and Competition for Light in Well-Mixed Aquatic Environments: An Elementary Model. *Ecology*, 75, 507–520.

Jia, Q., Anufriieva, E., Liu, X., Kong, F. & Shadrin, N. (2015). Intentional introduction of Artemia sinica (Anostraca) in the high-altitude Tibetan lake Dangxiong Co: the new population and consequences for the environment and for humans. *Chinese Journal of Oceanology and Limnology*, 33, 1451–1460.

Kendall, B. E., Briggs, C. J., Murdoch, W. W., Turchin, P., Ellner, S. P., McCauley, E., Nisbet, R. M. & Wood, S. N. (1999). Why Do Populations Cycle? A Synthesis of Statistical and Mechanistic Modeling Approaches. *Ecology*, 80, 1789–1805.

Lewontin, R. C. (1969). The meaning of stability. 22, 13–24.

Lewontin, R. C. & Cohen, D. (1969). On Population Growth in a Randomly Varying Environment. *Proceedings of the National Academy of Sciences*, 62, 1056–1060.

May, R. M. (1973). Stability in Randomly Fluctuating Versus Deterministic Environments. *The American Naturalist*, 107, 621–650.

May, R. M. (1976). Simple mathematical models with very complicated dynamics. *Nature*, 261, 459–467.

May, R. M. (1977). Thresholds and breakpoints in ecosystems with a multiplicity of stable states. 269, 471–477.

McGlathery, K., Reidenbach, M., D'Odorico, P., Fagherazzi, S., Pace, M. & Porter, J. (2013). Nonlinear Dynamics and Alternative Stable States in Shallow Coastal Systems. *Oceanography*, 26, 220–231.

Nicholson, A. J. (1957). The Self-Adjustment of Populations to Change. *Cold Spring Harbor Symposia on Quantitative Biology*, 22, 153–173.

Nolting, B. C. & Abbott, K. C. (2016). Balls, cups, and quasi-potentials: Quantifying stability in stochastic systems. *Ecology*, 97, 850–864.

R Core Team (2018). *R: A Language and Environment for Statistical Computing*. R Foundation for Statistical Computing, Vienna, Austria. URL `https://www.R-project.org/`.

Ratajczak, Z., Carpenter, S. R., Ives, A. R., Kucharik, C. J., Ramiadantsoa, T., Stegner, M. A., Williams, J. W., Zhang, J. & Turner, M. G. (2018). Abrupt Change in Ecological Systems: Inference and Diagnosis. *Trends in Ecology & Evolution*, 33, 513–526.

Ridolfi, L., DOdorico, P. & Laio, F. (2011a). *Noise-Induced Phenomena in the Environmental Sciences*. Cambridge University Press, Cambridge. ISBN 978-0-511-98473-0. URL `http://ebooks.cambridge.org/ref/id/CBO9780511984730`.

Ridolfi, L., DOdorico, P. & Laio, F. (2011b). *Noise-Induced Phenomena in the Environmental Sciences*. Cambridge University Press, Cambridge. ISBN 978-0-511-98473-0.

Scheffer, M. (2020). *Critical Transitions in Nature and Society*. Princeton University Press. ISBN 978-1-4008-3327-6.

Scheffer, M., Bascompte, J., Brock, W. A., Brovkin, V., Carpenter, S. R., Dakos, V., Held, H., van Nes, E. H., Rietkerk, M. & Sugihara, G. (2009). Early-warning signals for critical transitions. *Nature*, 461, 53–59.

Scheffer, M., Carpenter, S., Foley, J. A., Folke, C. & Walker, B. (2001). Catastrophic shifts in ecosystems. *Nature*, 413, 591–596.

Schindler, D. W. (1998). Whole-Ecosystem Experiments: Replication Versus Realism: The Need for Ecosystem-Scale Experiments. *Ecosystems*, 1, 323–334.

Schröder, A., Persson, L. & Roos, A. M. D. (2005). Direct experimental evidence for alternative stable states: A review. *Oikos*, 110, 3–19.

Soetaert, K., Petzoldt, T. & Setzer, R. W. (2010). Solving differential equations in r: Package desolve. *Journal of Statistical Software*, 33, 1–25.

Strogatz, S. H. (2001). *Nonlinear Dynamics and Chaos: With Applications to Physics, Biology, Chemistry, and Engineering*. Studies in Nonlinearity, 2nd edn. Perseus Books, Cambridge, Mass. ISBN 978-0-7382-0453-6.

Sutherland, J. P. (1974). Multiple Stable Points in Natural Communities. *The American Naturalist*, 108, 859–873.

Tuljapurkar, S. & Orzack, S. H. (1980). Population dynamics in variable environments I. Long-run growth rates and extinction. *Theoretical Population Biology*, 18, 314–342.

Vanderploeg, H. A., Liebig, J. R., Carmichael, W. W., Agy, M. A., Johengen, T. H., Fahnenstiel, G. L. & Nalepa, T. F. (2001). Zebra mussel (*Dreissena polymorpha*) selective

filtration promoted toxic *Microcystis* blooms in Saginaw Bay (Lake Huron) and Lake Erie. *Canadian Journal of Fisheries and Aquatic Sciences*, 58, 1208–1221.

Veraart, A. J., Faassen, E. J., Dakos, V., van Nes, E. H., Lürling, M. & Scheffer, M. (2012). Recovery rates reflect distance to a tipping point in a living system. *Nature*, 481, 357–359.

3.7 Appendix A: Experimental apparatus design

3.7.1 Chemostat

The chemostat chambers were custom made out of acrylic. The 4 ports were used for media input, effluent output, air for mixing, and an air release. The volume of the chamber was set by the height of the effluent output line. The in-going air line connected to a custom made glass y-splitter so air was forced into each rounded corner which created a mixing current. All luer fittings, and connecting components were stock parts from scientific supply companies.

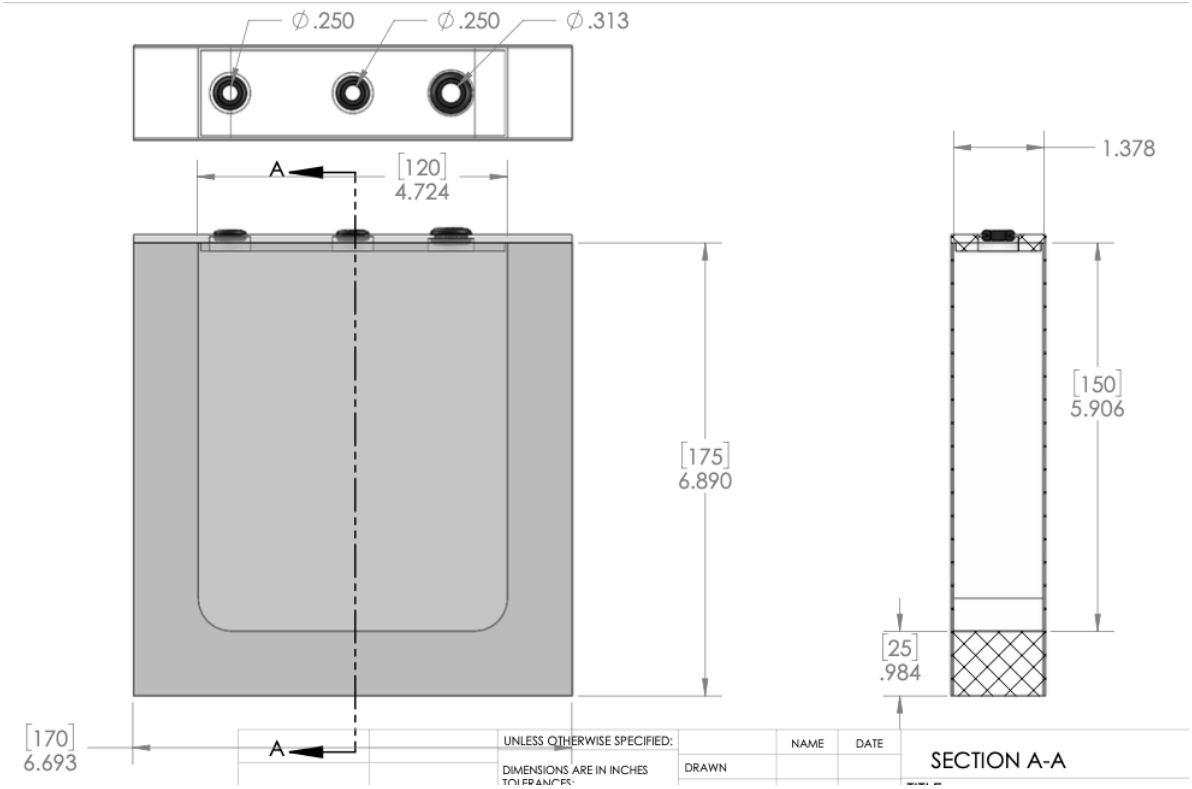

Figure 3.3: Initial design for the acrylic chambers built for the experiment. The total volume of the chamber was 525mL. The u-shape piece was cut from a solid block before panels were glued to either side to create the sides. Measurements in square brackets are in cm, otherwise units of inches are used.

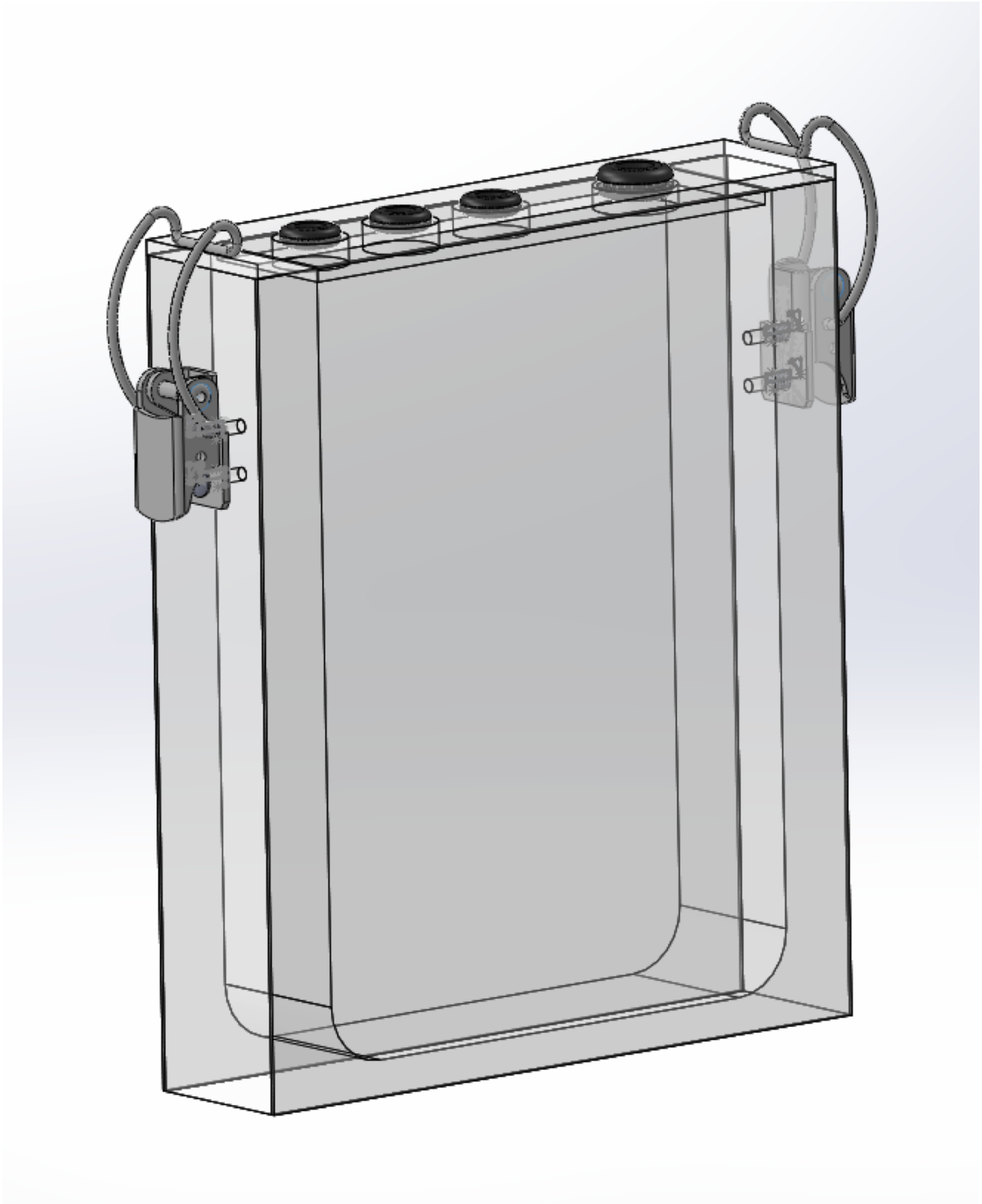

Figure 3.4: The final design for the chambers included an additional port on top, deepening the u-shape well for a total volume of 700mL, and clamps to keep the lid in place. The additional volume allowed for a working volume of 500mL with head space between the culture and media in port.

3.7.2 Lights

The light apparatus for each chemostat was built by mounting 4 LED lights to an aluminum heat sink block cooled with a computer fan. The lights were powered by a standard 45W AC adapter computer power supply, and dimmed by the LED driver based on the Arduino signal. The unique parts for this build are listed below.

- Mean Well LDD-700H DC/DC constant current LED driver
- SatisLED 5W High Power LED part number HPL5W10BW (warm White 2700-3500 deg K, 7.0-7.5V-700mA, water clear lens color, 650 700 lumens, 120 angle) archived web page
- Arduino Mega 2560 REV3
- CHENBO Micro SD SDHC TF Card Adapter reader module with SPI interface ASIN B06Y581CWF

Arduino Code

The code was written such that the light was set for each chamber every minute. This was done by sequentially reading lines from a text file on an mini-SD card attached to the Arduino. Each line contained 8 comma separated values corresponding to the 8 chambers' duty cycle for that minute.

```
//for pattern matching txt file to pin value
#include <Regexp.h>
//for SD card
#include <SPI.h>
#include <SdFat.h>
#include "sdios.h"
```

```
SdFat sd;
File file;
// print error code
#define errorHalt(msg) {Serial.println(F(msg)); SysCall::halt();}

// define pins to be used for lights, sd card, etc.
const uint8_t chipSelect = 53;
const int   lightPins[] = {2,3,4,5, 6, 7, 8, 9};
int j = 0;
int k = 0;
int i = 0; //counter for line
int linecount = 1;

unsigned long previousMillis = 60000; // will store last time LRD was read
const long interval = 60000; //time between readings (ms), 1 minutes =6000
   0, 5min = 300000

// create a serial stream
ArduinoOutStream cout(Serial);
//ifstream sdin("dutycycle.txt");

//------------------------------
void setup() {
 // begin serial to print error messages

 Serial.begin(9600);

 // Initialize at the highest speed supported by the board that is
 // not over 50 MHz. Try a lower speed if SPI errors occur.
 if (!sd.begin(chipSelect, SD_SCK_MHZ(50))) {
  sd.initErrorHalt();
 }
```

```
//Set up LED PWMpins
 for   ( k = 0; k < 8; k = k + 1) {
  pinMode(lightPins[k], OUTPUT ); //set LED pin mode to output
   }

}

void loop() {
 const int line_buffer_size = 32; // each file row is 32 characters that
    ends with line return /n
 char buffer[line_buffer_size];

//timer to keep track of when to change light PMW
 unsigned long currentMillis = millis(); //note the time
 if (currentMillis - previousMillis >= interval) {
  // save the last time you changed the LED
  previousMillis = currentMillis;

 //Read lines till you get the one that you want
 ifstream sdin("FILE_NAME.txt"); // open file;
 for ( i = 0; i < linecount ; i = i + 1) {
 sdin.getline(buffer, line_buffer_size, '\n'); // store file line into
    buffer
 }

 // parse the buffer by commas and assign to LED pins
   MatchState ms;
   ms.Target(buffer); //tell ms what the target is

   unsigned int index = 0;

 // what we are searching (the target)
 char buf[100];
```

```
int lightDC = 0;
while (true)
{
  char results = ms.Match("(%d+),(%d+),(%d+),(%d+),(%d+),(%d+),(%d+),(%d
     +)", index);
   if (results == REGEXP_MATCHED)
   {
    for (j = 0; j < ms.level; j++) {
     lightDC = atoi(ms.GetCapture(buf, j)); //read as the correct format
        for the analogWrite function
     analogWrite(lightPins[j], lightDC); // set DC for each pin
    cout << lightDC << endl;
    }
    index = ms.MatchStart + ms.MatchLength;
   }
   else
    break;
  }

//Update line counter
linecount = linecount + 1;



}
```

R Code

The R code used to simulate environmental noise text file read by the Arduino.

```
#Arduino is expecting 8 3-digit numbers separated by commas per line.

#prep to convert data from PAR -> duty cycle
```

```
#load look up table
load("../Constants/data_out/DCPARlookUpTable.Rdata")
#easiest to round DC in look up and then use join function
LU <- lookUpDC %>%
  rename(PAR = value) %>%
  mutate(Duty.Cycle = round(dc))


#Some math to figure out how many environmental conditions needed per
   experiment
exp.length <- 60*24*30 #minutes
t.enviro <- 1 #how long each condition lasts
n.total <- exp.length/t.enviro #total number of noise conditions
#Set treatment information; half of previous experiment
PARmean <- 86/2
sd.treatment <- c(0,PARmean*.2, PARmean*.4, PARmean*.8 )
n.reps <- 2
sd.seq <- rep(sd.treatment, each=n.reps)


#Block 1

#randomly assign treatment to chambers
chamber <- sample(c(1:8), size=8)

#pull noise values and convert to duty cycle
noise.seq <- foreach(i=c(1:length(sd.seq))) %do% {
                data.frame(cbind(time=c(1:n.total),PAR=rnorm(n=n.total,
                   mean = PARmean, sd= sd.seq[i]))) %>%
                mutate(PAR = ifelse(PAR > 0, round(PAR),0)) %>%
                left_join(LU, by="PAR") %>% #convert to DC
                mutate(Duty.Cycle = ifelse(Duty.Cycle > 255, 255,Duty.
                   Cycle)) %>%  #if greater than max, put max
```

```
                select(-dc)
              }
#check mean and sd- looks good
noise.check <- foreach(i=c(1:length(sd.seq)), .combine='rbind') %do% {
                    cbind(sdtreat=sd.seq[i],mean = mean(noise.seq[[i]]$PAR)
                       , sd=sd(noise.seq[[i]]$PAR), Negatives = sum(ifelse(
                       noise.seq[[i]]$PAR <0,1,0)))}


#put duty cycle into format expected by Arduino
block1 <- matrix(data=NA, nrow=n.total, ncol= 8)
for(i in 1:8){
  block1[,chamber[i]] <- sprintf("%03d",noise.seq[[i]]$Duty.Cycle) #add
     leading zero
}



#save noise
write.table(block1,sep=",", file = "data_raw/treatments/gut2_52021.txt",
   row.names = FALSE, col.names = FALSE)
```

3.8 Appendix B: R Code

```
#dynamical model; estimating Ik, Iopt, and pmax. All other values are
   known.
dAdt.model = function(t, x, params) {
  A <- x #local var A
  with(as.list(c(params)), {
    loss <- lfunc(t) #define l as a function of t, left-cont piecewise
       function, needs to be defined outside of objective function
```

```
    dA <- A*(pmax*(2*I*(atan(I*(2*I*(Ik/Iopt^2)+(1-2*Ik/Iopt))/sqrt(I^2*
       (-(1-2*Ik/Iopt)^2+4*(Ik/Iopt^2)*Ik))) - atan(I*(2*(Ik/Iopt^2)*I*exp
       (-zmax*A*k-zmax*kd)+(1-2*Ik/Iopt))/sqrt(I^2*(-(1-2*Ik/Iopt)^2+4*(Ik
       /Iopt^2)*Ik))))/(zmax*(A*k+kd)*sqrt(I^2*(-(1-2*Ik/Iopt)^2+4*(Ik/
       Iopt^2)*Ik))))-loss)
    list(c(dA), obsloss = loss) #return list of results
  })
}


#Constrained Objective Functions for biologically possible values
  #Biological requirements
    ##parameter search space to only positive values by parameterizing log
       (parameter)
    ##penalty added to SSE if Ik >= Iopt

  ##minimize SSE for all trajectories at once
constrained.sse.dAdt = function(params0, alldata, constants=c(3.5, k.est,
   kd.est)) {
  #constants <- c(zmax, k, kd)
  #data is long table of observations
  library(foreach)
  sse <- NULL

  #fit parameters that minimize sse of all trajectories simultaneously
  foreach(i = unique(alldata$pop.no)) %do% {

    data <- alldata %>% filter(pop.no == i)
    #time dep loss rate
    obsloss <- cbind(time=data$time, l=data$l) #create df of measured loss
        rate
    lfunc <<- approxfun(obsloss,rule=2, method="constant", f=1) #define l
       as a function of t, left-cont piece-wise function, needs to be
```

```
      defined outside of objective function, use double arrow to put
      function into global environment

    t <- data$time #hour of experiment
    A <- data$TSS #observed value of population size in **mg/mL**
    A0 <- data$TSS[1] #starting value of population
    I.treatment <- data$light.PAR[1] #incident light condition
    out <-  as.data.frame(ode(A0, times=t,dAdt.model, c(pmax=exp(params0
      [1]), Iopt=exp(params0[2]), Ik=exp(params0[3]), I=I.treatment, zmax
      =constants[1], k=constants[2], kd=constants[3])))

    #Penalty for violating biological sense
    if(params0[2] < params0[3]) {  #biological sense: Iopt (params0[2]) >
      Ik (params0[3])
      sse[i] <- sum((out[2]-A)^2)+1000 #sum of sq error penalty
    } else  if(params0[1] > 1) {  #biological sense: pmax is proportion
      sse[i] <- sum((out[2]-A)^2)+1000 #sum of sq error penalty
    } else
      sse[i] <- sum((out[2]-A)^2) #sum of sq error
  }
  sum(sse)
}

params0 <- c(-0.69,3.5,3.6) #initial log transformed values for pmax, Iopt
    and Ik
tmp.fit <- optim(params0, constrained.sse.dAdt, alldata=block.OD) #
   estimate parameters based on all trajectory; OD data converted to mg/mL
    using standard curve
```

```
sessionInfo()
R version 4.0.4 (2021-02-15)
Platform: x86_64-apple-darwin17.0 (64-bit)
```

```
Running under: macOS Catalina 10.15.7

Matrix products: default
BLAS:   /System/Library/Frameworks/Accelerate.framework/Versions/A/
   Frameworks/vecLib.framework/Versions/A/libBLAS.dylib
LAPACK: /Library/Frameworks/R.framework/Versions/4.0/Resources/lib/
   libRlapack.dylib

locale:
[1] en_US.UTF-8/en_US.UTF-8/en_US.UTF-8/C/en_US.UTF-8/en_US.UTF-8

attached base packages:
[1] stats     graphics  grDevices utils     datasets  methods   base

other attached packages:
[1] dplyr_1.0.5       colorspace_2.0-0  rootSolve_1.8.2.1 foreach_1.5.1
[5] deSolve_1.28      gplots_3.1.1

loaded via a namespace (and not attached):
 [1] Rcpp_1.0.6         knitr_1.31         magrittr_2.0.1     tidyselect_1
    .1.0
 [5] R6_2.5.0           rlang_0.4.10       fansi_0.4.2        stringr_1.4.
    0
 [9] plyr_1.8.6         caTools_1.18.1     tools_4.0.4        xfun_0.22
[13] KernSmooth_2.23-18 utf8_1.2.1         iterators_1.0.13   htmltools_0.
   5.1.1
[17] ellipsis_0.3.2     gtools_3.8.2       yaml_2.2.1         digest_0.6.2
   7
[21] tibble_3.1.0       lifecycle_1.0.0    crayon_1.4.1       reshape2_1.4
   .4
[25] purrr_0.3.4        codetools_0.2-18   vctrs_0.3.8        bitops_1.0-6
[29] glue_1.4.2         evaluate_0.14      rmarkdown_2.7      stringi_1.5.
   3
```

```
[33] compiler_4.0.4     pillar_1.5.1       generics_0.1.0     pkgconfig_2.
   0.3
```

Figure 3.5: Picture of LEDs used. This design (as opposed to starboard allowed for easier mounting of the LED to the heat sink. The solid back also made it easier to create a uniform layer of silver thermal grease.

Model of *Saccharomyces cerevisiae* growth exposed to noisy harvesting

4.1 Introduction

Understanding the causal links between environmental stochasticity and population abundance, especially with respect to extinction, is a long-standing question in ecology (Dennis *et al.*, 1991; Tuljapurkar & Orzack, 1980; Lewontin & Cohen, 1969). Traditionally, environmental stochasticity is linked to an increased extinction risk, and a reduced time to extinction via increased variance in the population size (as reviewed by Griffen & Drake, 2008). Humans directly influence the variation in population abundance through direct removal of individuals or harvesting. As in the well studied case of fisheries, harvested stocks fluctuate more than unharvested populations (Anderson *et al.*, 2008; Jonzén *et al.*, 2002). However, based on theoretical studies, the increased stock fluctuation leading to extinction cannot be solely, if at all, explained by fluctuations in harvesting pressure (Jonzén *et al.*, 2002; Braumann, 1999, 2002). This indicates there is some phenomenological process missing from our deterministic description of the natural world. However, stochastic models of populations subject to a random harvest process predict that harvesting can cause extirpation alone (Ridolfi *et al.*, 2011). These stochastic models indicate a noise-induced transition (NIT) is the cause of random harvesting related extirpation (Horsthemke & Lefever, 2006).

The ability for environmental stochasticity to re-shape the stability landscape, also known as a noise-induced transition (NIT), is a well established theory but has been given little attention in ecology (May, 1973). Before discussing stochastic models with NIT in ecology, I will briefly review deterministic stability using the ball-and-valley model. This model is the geometric equivalent of the potential function, and is useful when developing intuition about system stability (as reviewed by Nolting & Abbott, 2016). Simply, population size runs along the x-axis and the potential energy on the y. The current population size is represented by a ball, and moves with gravity to the lowest point. If there are multiple valleys, the current population is the outcome of initial conditions and external perturbations. External perturbations, if large enough, can push a system state uphill out of one valley to another passing through a peak. These valleys and peaks are stable and unstable equilibria, respectively (Strogatz, 2001). System state, population size, can also change if the underlying stability landscape changes. For example, if the harvest rate is larger than growth rate the landscape changes so that the only valley is at extinction. Noise-induced transitions also alter the number and/or location of peaks and valleys, but through a different mechanism (Ridolfi *et al.*, 2011; Nolting & Abbott, 2016). NITs are studied using stochastic differential equations (SDE). I will briefly review SDE stability analysis and the ODE analogs which will help in understanding the analysis method used in this paper. Unlike ODEs which have point equilibria or limit cycles, stochastic models inherently do not settle to a single point or set of points. Given this, stability within an SDE is defined by probabilistic terms in the form of the stationary probability distribution (SDP). The SDP can often be found by solving the Fokker-Planck equation of the SDE (Horsthemke & Lefever, 2006). When solving for the maxima of the SDP, the expression can be broken down into two terms. The first term is seen to be identical to the deterministic equilibria, while the second term is multiplied by the noise intensity. This means as the noise approaches zero, the SPD maxima approaches the deterministic equilibria. Alternatively, the distribution can be calculated numerically by fitting a curve to a histogram of population sizes from simulated population

time series (Horsthemke & Lefever, 2006). In either approach, the modes and antimodes (the least frequent value between two modes) of the probability distribution are analogous to stable and unstable equilibria of an ODE.

To this point, I have presented a subset of NITs, noise-induced extinction (NIE). Interestingly, under a subset of conditions environmental stochasticity can act as a stabilizing force leading to persistence, or bistability between extirpation and persistence (May, 1973; Ridolfi *et al.*, 2011). Returning to the ball-and-valley model, noise-induced persistence can be reached by multiple topographical changes. For example, bistability is produced by valleys at persistence and extinction but there is no requirement about the relative depths or slope gradients. In the simplest form, noise-induced persistence holds the stability landscape nearly constant while the persistence valley disappears in the noise-free equivalent ball-and-valley model. Of course, NIT does not always lead to equilibrium shifts between extirpation and persistence or vice versa (May, 1973). Noise-induced extinction or persistence are the extreme outcomes on the possible spectrum of NIT outcomes. We have chosen to study these extremes because they require less sensitivity to detect making them experimentally tractable.

The previous chapters demonstrated noise-induced extinctions within an algal mesocosm. The noise in the algal system is an example of the indirect effects of the Anthropocene. That is to say, increases in atmospheric carbon due to humans are predicted to change the mean and increase the variance of temperature and precipitation over time (Salinger, 2005; Karl & Trenberth, 2003). While photosynthetic radiation in nature is not expected to change as in the mesocosm experiments, it can constrain primary productivity just like temperature or precipitation. The time scale of indirect anthropogenic environmental noise is on the same order as climate change - decades, centuries, or longer.

However, that does not mean that the theory of noise-induced transitions should be tabled until it is *relevant*. The Anthropocene also includes population management practices that directly create environmental noise. Harvesting, culling, or other methods of reducing

population sizes can vary over time. For example, management practices based on effort (ie. hunting season, daily catch limits, etc.) have the potential to remove wildly different portions of the population from harvest to harvest (Parkinson *et al.*, 2004; Fukasawa *et al.*, 2020). Additionally, direct anthropogenic environmental noise can be modified on a much shorter time scale than indirect anthropogenic noise given the recurrent nature of harvesting. The plausibility of harvest noise-induced transitions has the potential to be a powerful tool for managers. In order to understand the potential for noise-induced transitions in ecological systems, we must explore more combinations of models with nonlinear feedback, and noise source (direct vs. indirect).

In the following quantitative and empirical paired chapters, I used a new experimental system to build on our understanding of noise-induced transitions in biological populations. Using a logistic model with discrete harvest events, I obtained the stationary distribution as a function of increasing harvest variability in the form of white shot noise, or harvests at random times and intensities. A noise-induced transition was defined as a qualitative difference between the stochastic stationary distribution and the deterministic equilibrium (Horsthemke & Lefever, 2006). Given the qualitative nature of defining the transition, I focused on parameter conditions that led to a critical transition from persistence to extinction or vice versa under stochastic but not fixed harvesting conditions. The parameter conditions bracketing the mismatched critical transition will be used to inform the experimental design of the bench experiments in the next chapter.

4.2 Methods

The density dependent growth of *Saccharomyces cerevisiae* populations were characterized by a logistic model (4.1). The population size (N) was rescaled by carrying capacity (K) so the population size ($N' = N/K$) is bounded between zero and one (4.1). For simplicity, I have dropped the prime notation going forward but always mean the population size

as a proportion of carrying capacity. After rescaling, the only density dependent growth parameter is the intrinsic rate of increase (r).

$$\frac{dN}{dt} = rN(K - N) \tag{4.1a}$$

$$\frac{dN}{dt}\frac{1}{K} = r\frac{N}{K}(\frac{K}{K} - \frac{N}{K}) \tag{4.1b}$$

$$\frac{dN'}{dt} = rN'(1 - N') \tag{4.1c}$$

4.2.1 Model Parameterization

Model parameterization was based on *S. cerevisiae* (strain BY4741 SUC2:YFP ; Gore *et al.*, 2009). This strain was used because because populations have a strong Allee effect when grown with sucrose as carbon source in well mixed broth Dai *et al.* (2012). An Allee effect, positive density dependence, increases the range of population sizes that result in extinction, increasing experimental tractability. However, the presence of an Allee effect when grown on agar as opposed to broth had not previously demonstrated. The per capita growth rate and Allee effect strength on an agar matrix were quantified to parameterize a dynamical model. In two parameterization experiments, initial populations were seeded with a known number of cells by individually sorting cells onto agar media with either a control carbon, glucose, or the Allee effect treatment carbon, sucrose, via flow cytometery.

The growth rate was estimated by seeding 8 populations with 5 viable cells each into the wells of a μ-Slide (Ibidi cat. no 80826) filled with the agar medium. Starting at 15 hours of growth, 2 populations were destructively sampled by flooding the well with broth media and mixing by pipette to suspend all cells in the colony. Complete colony suspension was verified through microscopy before collecting samples to be counted using a hemocytometer. This process was repeated at 20, 22.5, and 23.75 hours. The geometrically decreasing sampling schedule was based on previous observations of the exponential growth period. Growth rate

(r) was calculated using an exponential growth formula, $r = ln(N_t/N_0)/t$, where N_0 and N_t is the population size at time zero and t, respectively.

The strength of an Allee effect when grown on an agar matrix was estimated by fitting a Weibull function to the probability of establishment as a function of initial population sizes (Kaul *et al.*, 2016). This relationship changes shape from an inverse exponential curve to sigmoidal in the presence of a strong Allee effect. A Weibull function ($y = 1 - exp^{(-x/\lambda)^k}$) can take on both shapes. The function is sigmoidal when the shape parameter, k, is greater than one and the scale parameter, λ, is the inflection point of the sigmoid. A strong Allee effect is present if $k \geq 1$. The parameter λ is the critical population density needed to escape the effect. The probability of establishment was measured by seeding 20 populations with one to five cells and then geometrically increasing from 8 to 128 cells onto agar media-filled Petri dishes. This process was repeated for media with sucrose and glucose, where glucose is a negative control for the Allee effect. Populations were visually scored (0/1) after 23.75 hours of growth. The Weibull function was fit to the raw binary data, not the average of the 20 binary outcomes per inoculum size.

All simulations used an intrinsic rate of increase of 0.36 hr^{-1}, and lacked an Allee effect.

4.2.2 Model Simulation and Analysis

The presence of a noise-induced transition was detected by a comparison of three proportional harvest regimes: mean field constant harvest, fixed discrete harvest, and stochastic discrete harvest. The three way comparison is needed to determine the effect of noise within the harvest process (fixed vs. stochastic discrete harvest) rather than the effect of a discrete harvest process (mean field constant harvest vs. discrete harvest). These three harvest regimes were added to non-dimensional logistic models (4.2).

$$\frac{dN}{dt} = rN(1-N) - hN \tag{4.2a}$$
$$\frac{dN}{dt} = rN(1-N) - \alpha\lambda N \tag{4.2b}$$
$$\frac{dN}{dt} = rN(1-N) - \xi_{wsn}N \tag{4.2c}$$

The mean field harvest regime consists of a single parameter representing a constant harvest rate (h, 4.2a). The discrete harvest regimes are characterized by two parameters; one representing the harvest frequency (λ) and the other representing the proportion of the population removed during the harvest (α). In the case of the fixed discrete harvest, these parameter values were held constant during a model simulation (4.2b). The stochastic discrete harvest regime follows white shot noise, ξ_{wsn}, which was created by drawing events from a compound Poisson distribution ($\langle\xi_{wsn}\rangle = \lambda\alpha$) where the expected interarrival time is an exponential distribution ($T \sim Exp(1/\lambda)$; 4.2c). For each harvest event, the proportional harvest was drawn from a truncated exponential distribution ($H \sim Exp(\alpha)$). The compound Poisson process allows for easy comparison between the fixed and stochastic discrete harvesting process since they have the same expected value of $\alpha\lambda$

The harvest regimes were further modified to accommodate bench experimental restraints. *Saccharomyces cerevisiae* population harvest events and transfer of cells to a fresh agar media matrix occurred at the same time, and required a minimum proportional harvest of 0.5. With this modification, the mean and variance of the proportional harvest random variable α changes ($E[\alpha] = (0.5+\alpha*0.5)$; $V[\alpha] = 0.25\alpha^2$) such that it no longer has an exponential distribution. Previous published steady state analytical solutions are not applicable since they assume an exponential distribution. For this reason, only numerical solutions were explored.

In the case of the continuous harvest rate, h is modified to $(0.5 + h * 0.5)$.

We studied the model over a range of initial conditions and harvest rates by varying N_0,

h, α, and λ from zero to one. In the case of the stochastic harvest regime, 100 populations for each parameter combination were simulated. All simulations ran for ∼600 generations under ideal conditions (500 hours). The solutions to the models were calculated in 'R' using the 'lsoda' function in the deSolve package, which automatically switches between stiff and non-stiff methods (Soetaert *et al.*, 2010). Discrete harvests were incorporated through the 'events' argument (See Appendix A for code).

The mean field constant harvest and the fixed discrete harvest models have equilibrium point values while the stochastic discrete harvest model has a stationary distribution of probable population sizes. For this work, I will be treating the mode(s) of the stationary distribution as analogous to the equilibrium point values of the deterministic models. The stationary distribution was calculated by converting the trajectories of population sizes post burn-in into a histogram with a bin size of 0.01. The bin with the highest frequency is the mode. The stationary distribution is considered bimodal if the second highest frequency bin is more than 0.05 away from the mode. The equilibrium point values for the deterministic models were calculated by averaging the final population size across all initial conditions for a given harvest parameter set. Extinction was defined as $N < 10^{-6}$ or approximately 1 cell assuming a carrying capacity of 10^7 cells. A phase transition can be detected by looking for harvest parameter space were the stationary distribution mode and point equilibrium values qualitatively differ. To this end, heatmaps of mode(s) or point values over the harvest parameter space were created. They were then compared to identify any regions where one model transitioned from persistence to extinction, while the other model did not.

4.3 Results

The intrinsic per capita growth rate (r) was estimated to be 0.360 ± 0.021 hr^{-1} which is similar to previously measured values in well mixed broth by Dai *et al.* (2012). An Allee effect was detected when populations were grown with a sucrose carbon source ($\hat{k} > 1$; Fig.

4.1). The estimated critical density, or the scale parameter, is just over one cell. Despite detecting a strong Allee effect, biologically, the populations grown under a sucrose carbon condition are unlikely to experience substantial positive density dependence. These results lead to the removal of positive density dependence from model simulations used to select treatments. In the case of the glucose media, we fail to reject the null hypothesis of no Allee effect due to the confidence interval for the shape parameter including values above and below the threshold of $k \geq 1$.

Population persistence in the continuous harvest and fixed discrete harvest models occurs while harvesting (h, or $\alpha \times \lambda$) is less than the intrinsic rate of increase (r). The critical harvesting threshold is clearly defined in the numeric solutions (Fig. 4.3A). As the number of harvested individuals decreases, the population is able to persist under more frequent harvesting. However, no population is able to persist when the interarrival time of harvests is 60% of the intrinsic rate of increase (Fig. 4.2).

Persistence in the noisy harvest model differed qualitative and quantitatively from the noise-free harvest model. Rather than an abrupt change in the stable equilibrium (first order discontinuity), the population mode gradually declines to extirpation as the harvesting frequency increases (Fig. 4.3B). Interestingly, the noisy harvest model indicates population persistence at a larger range of harvesting conditions than the noise-free harvest model . The divergence in the stability landscape between the fixed and noisy harvest models demonstrate an example of noise-induced persistence.

The noise-induced persistence is also reflected in the probability of extinction. Populations subject to subcritical noise-free harvests persist indefinitely. At the critical harvesting threshold, the probability of extinction jumps to unity. In the case of populations subject to noisy harvests, the probability of extinction gradually increases (Fig. 4.4B)

4.4 Discussion

I simulated the growth of *S. cerevisiae* on agar when harvested at a continuous constant rate, fixed discrete events, and stochastic discrete events. The models with continuous and fixed discrete harvests did not differ dynamically from each other, but the dynamics of the stochastically harvested populations did differ from the other two harvest regimes. Simulated populations with stochastic harvesting were able to persist at an increased harvest intensity (as measured by both α and λ) when compared to the fixed harvesting regime. This is a theoretical demonstration of variability in the harvesting process causing population persistence despite an unsustainable mean harvesting rate, also known as a noise-induced persistence.

This work suggests that another layer of model complexity could be needed to fully capture harvested fisheries dynamics. Harvests often remove the largest and oldest individuals from the population (Kuparinen & Merilä, 2007; Lewin *et al.*, 2006). Exploited fish populations experiencing this selective pressure shift to a 'fast' life history leading to increased growth rates (Uusi-Heikkilä *et al.*, 2015; Enberg *et al.*, 2012; Matsumura *et al.*, 2011). There is potential for these observed shifts to interact with NIS in interesting ways. First, exploited fish populations that have a 'fast' life history related to increased growth rate are hypothesized to be viable and highly productive because of this life history shift (Zimmermann & Jørgensen, 2015). When this phenomenon simultaneously occurs with a transitioned stability landscape, there could be a multiplicative effect on sustainable harvest rates compared to when only one phenomenon is present. Alternatively, NIS could be mistaken as an increased growth rate if only deterministic processes are considered. A NIS in a stochastic model and a deterministic model with increased growth rate would have similar dynamical properties- an increase in the maximum sustainable yield. The second area of exploration is when the harvesting pressure is released. Fishing-induced evolution, as opposed to a phenotypic shift, is most likely species and stock dependant (Darimont *et al.*, 2009). When the harvesting

pressure is released, one might expect the return time of the population to pre-harvesting characteristics to be faster under phenotypic, instead of genotypic, changes. The destabilizing effect of a rapidly decreasing growth rate due to phenotypic adaptations, rather than genotypic evolution, could be offset by the legacy of a larger stable population size given NIS.

Storage effect theory focuses on understanding species coexistence as a response to environmental stochasticity (Chesson, 2000). For example, climatic variability allows for plants to maintain higher growth rates leading to coexistence (Adler *et al.*, 2006). Coexistence time in two species storage effect models have a non-monotonic relationship such that coexistence time increases with environmental stochasticity to some intermediate maximum before declining (Adler & Drake, 2008). This intermediate unimodal relationship between environmental stochasticity and maximum stable number of species maps onto the work presented here, replacing species with individuals. Given these similarities, we should look to the storage effect literature when choosing the next experimental noise-induced transition.

The Weibull function fit to the probability of population establishment grown under sucrose sugar carbon conditions was sigmoidal ($k > 1$). This sigmoidal relationship would be evidence for an Allee effect. However, the inflection point of the sigmoid λ, or the critical density, is near one cell. The estimated near zero critical densities indicate that an Allee effect is not a driving force in the population dynamics when grown on agar and is orders of magnitude less than previous work in broth cultures (Dai *et al.*, 2012). The mechanism of the Allee effect can explain the difference in the positive density dependence importance between broth and agar cultures. Sucrose, a disaccharide, must first be cleaved into monosaccharides before moving from the periplasmic space into the cytoplasm (Carlson & Botstein, 1982; Dickinson & Schweizer, 2004). Gore *et al.* (2009) reported that when this strain of *S. cerevisiae* is grown in broth culture a majority of the monosaccharides diffuse out of the periplasm space before the cell can import the sugar. At low cell densities cleaving disaccharides is energetically costly given the inefficient capture process. As the cell density

increases, the extracellular monosaccharide concentration increases, offsetting the cost of inefficient capture and allowing the population to escape the Allee effect. It is reasonable to expect the capture process to be more efficient on an agar substrate than in a well mixed broth because the diffusion of the newly cleaved glucose away from the cell is much slower on agar than in broth.

Noise within the discrete harvesting process increases the population's tolerance for harvesting. As a point of reference, in the fixed harvesting model the harvest parameters are also bifurcation parameters and can push the system through a fold catastrophe at the critical point of the harvesting rate equal to the intrinsic rate of increase ($\alpha\lambda = r$). In the stochastic harvesting model the probability distribution function, the inverse of the system's quasi-potential, maintains a non-zero mode at mean harvesting rates above the growth rate. The region of parameters in which the deterministic harvesting model predicts population persistence is a subset of the persistence parameter region of the stochastic harvesting model. Specifically, the stochastic harvesting model predicts population persistence at higher proportional harvesting rates given the same frequency, and higher harvesting frequencies given the same proportional harvest rate. The expanded harvest parameter space for population persistence in the stochastic model as compared to the deterministic model is indicative of a noise-induced transition. In this case, noise within the harvest process acts as a stabilizing effect leading to noise-induced persistence. This work contradicts the common view that environmental variability is a destabilizing force, and puts forth predictions to test the plausibility of noise-induced persistence within a microcosm.

4.5 Figures

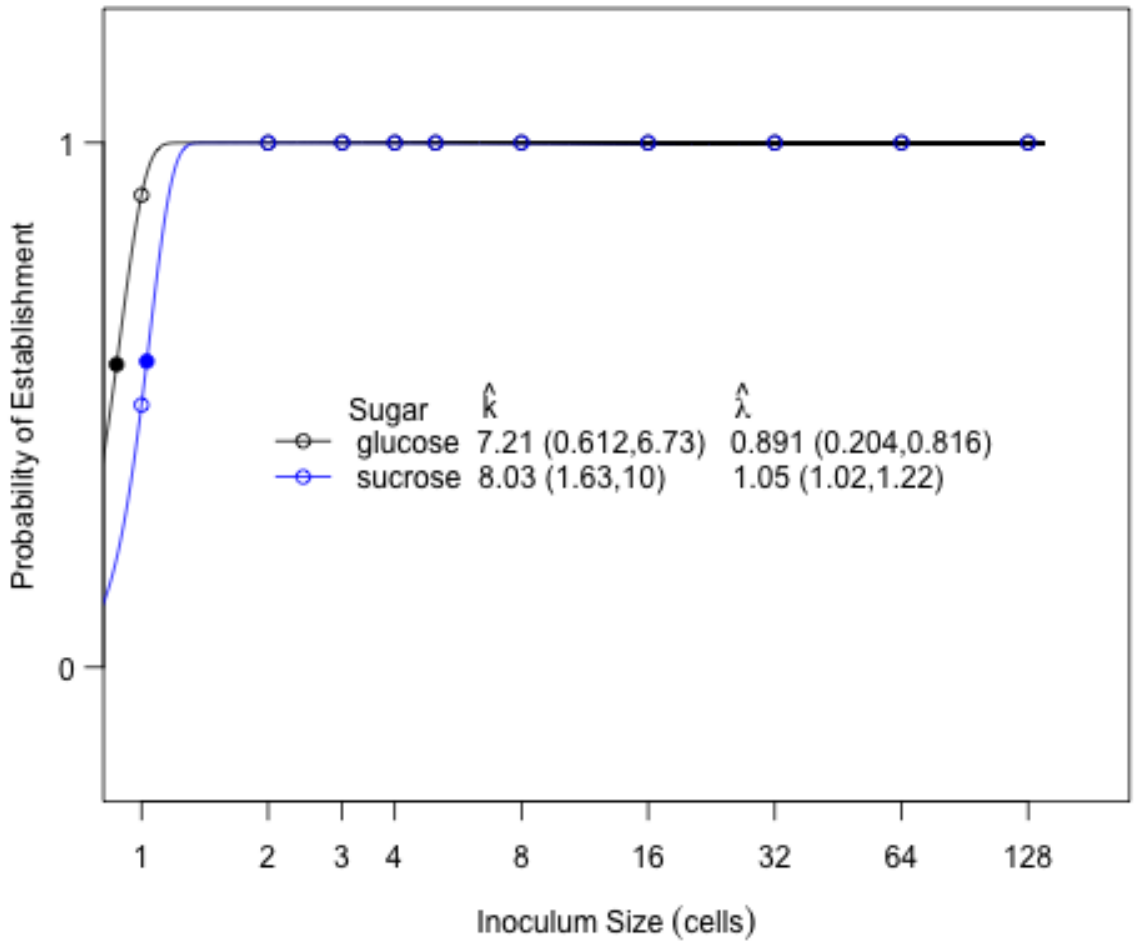

Figure 4.1: An Allee effect was detected by fitting establishment vs. inoculum size. The mean of the binary outcomes by inoculum size are plotted with open circles. A sigmoidal fitted line ($k \geq 1$) indicates an Allee effect in sucrose (blue line). No conclusions of the absence of presence of an Allee effect can be made about populations grown in glucose (black line). The critical densities of cells needed to overcome the Allee effect (λ) when grown in sucrose is near one cell. The point estimate of λ is plotted with a closed circle. The parameter estimates are printed with their 95% confidence interval.

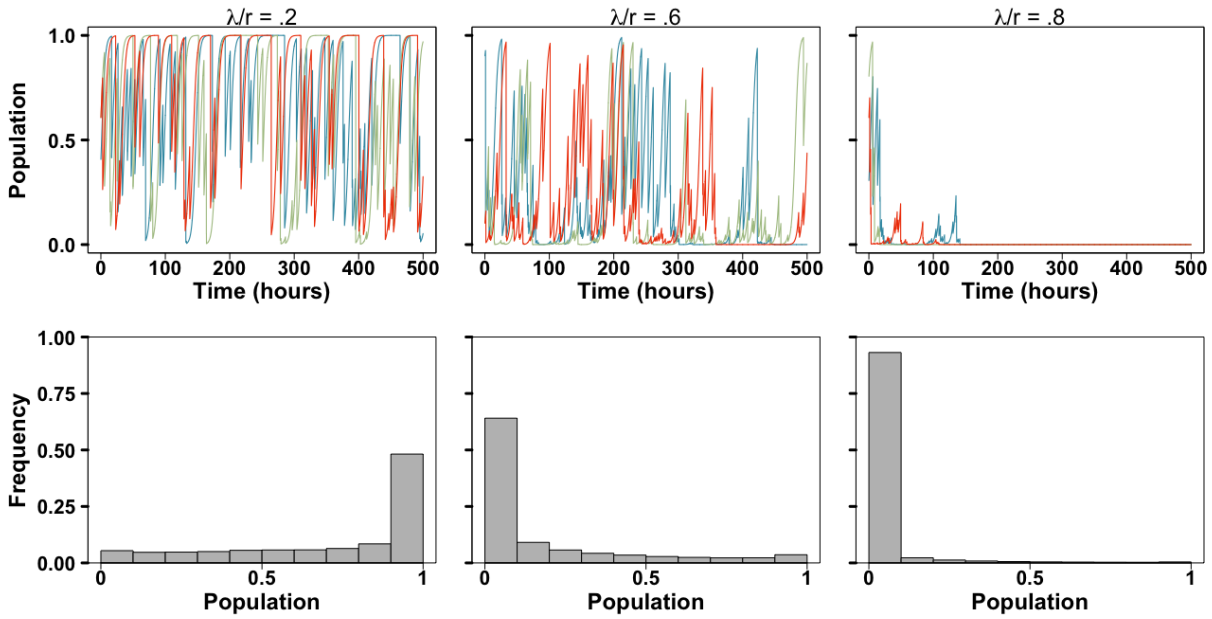

Figure 4.2: Example of simulated populations and corresponding probabilistic distribution of population size. The top row are examples of simulated population with the same mean proportional harvest ($\alpha = 0.8$) and decreasing interarrival time from left to right. Simulations were initialized with a range of population densities, and were used to calculate the steady state of the stochastic model shown in the bottom row after removing a 24 hour burn-in period.

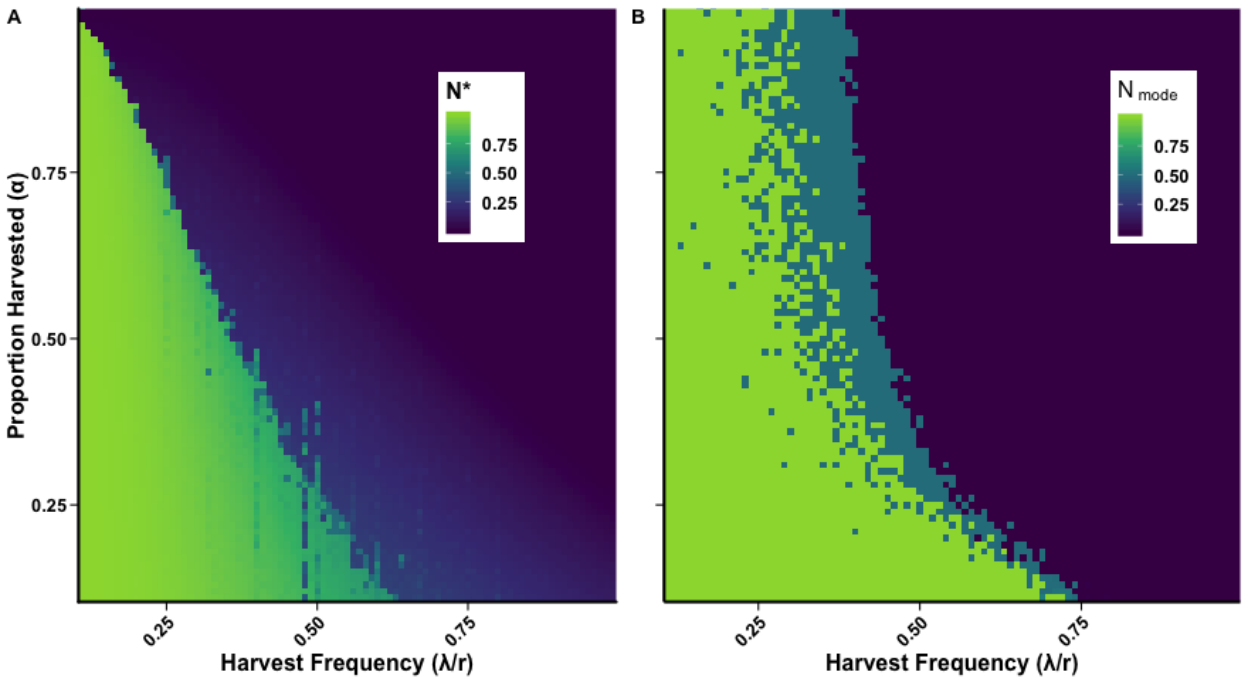

Figure 4.3: Simulated final population size under fixed and stochastic harvest regimes. The deterministic equilibrium (A) was calculated by averaging the final population size starting from different initial conditions. The most probable population size under stochastic harvesting (B) was based on the mode(s) of the stationary distribution. Regions with a mode of 0.5 should be interpreted as bimodal with peaks near carrying capacity (1) and extinction.

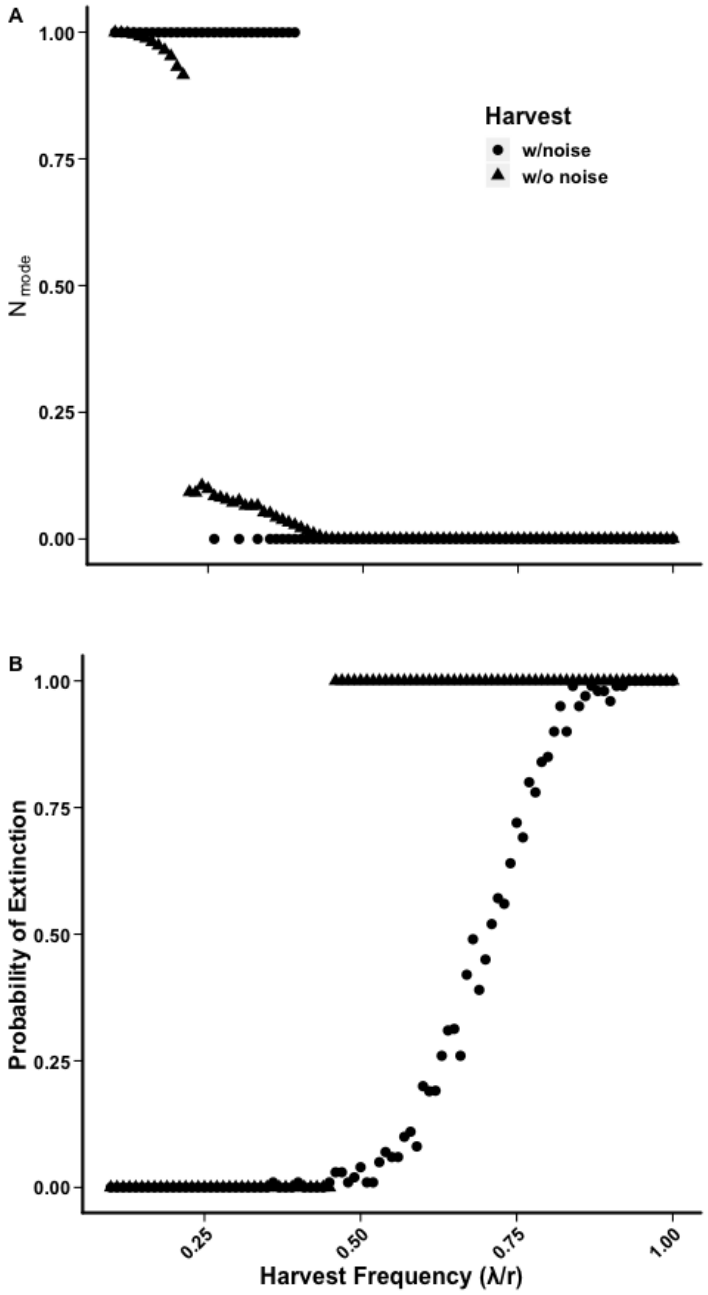

Figure 4.4: Impact of harvesting frequency on final population size at a proportional harvest of $\alpha = 0.8$. (A) The equilibrium value of the deterministic (w/o noise; ▲) and stochastic (w/noise;●) harvest models. The bimodal region for the stochastic model ranges between a harvest frequency 0.25 and 0.4 λ/r. The probability of extinction (B) calculated as the proportion of simulations ending in extinction for the deterministic (w/o noise; ▲) and stochastic (w/noise;●) harvest models. Noise-induced persistence ranges from 0.5 to 0.8 λ/r

Bibliography

Adler, P. B. & Drake, J. M. (2008). Environmental Variation, Stochastic Extinction, and Competitive Coexistence. *The American Naturalist*, 172, E186–E195.

Adler, P. B., HilleRisLambers, J., Kyriakidis, P. C., Guan, Q. & Levine, J. M. (2006). Climate variability has a stabilizing effect on the coexistence of prairie grasses. *Proceedings of the National Academy of Sciences*, 103, 12793–12798.

Anderson, C. N. K., Hsieh, C.-h., Sandin, S. A., Hewitt, R., Hollowed, A., Beddington, J., May, R. M. & Sugihara, G. (2008). Why fishing magnifies fluctuations in fish abundance. *Nature*, 452, 835–839.

Braumann, C. A. (1999). Variable effort fishing models in random environments. *Mathematical Biosciences*, 156, 1–19.

Braumann, C. A. (2002). Variable effort harvesting models in random environments: Generalization to density-dependent noise intensities. *Mathematical Biosciences*, 177-178, 229–245.

Carlson, M. & Botstein, D. (1982). Two differentially regulated mRNAs with different 5' ends encode secreted with intracellular forms of yeast invertase. *Cell*, 28, 145–154.

Chesson, P. (2000). Mechanisms of Maintenance of Species Diversity. *Annual Review of Ecology and Systematics*, 31, 343–366.

Dai, L., Vorselen, D., Korolev, K. S. & Gore, J. (2012). Generic Indicators for Loss of Resilience Before a Tipping Point Leading to Population Collapse. *Science*, 336, 1175–1177.

Darimont, C. T., Carlson, S. M., Kinnison, M. T., Paquet, P. C., Reimchen, T. E. & Wilmers,

C. C. (2009). Human predators outpace other agents of trait change in the wild. *Proceedings of the National Academy of Sciences*, 106, 952–954.

Dennis, B., Munholland, P. L. & Scott, J. M. (1991). Estimation of Growth and Extinction Parameters for Endangered Species. *Ecological Monographs*, 61, 115–143.

Dickinson, J. R. & Schweizer, M., eds. (2004). *The Metabolism and Molecular Physiology of Saccharomyces Cerevisiae*. 2nd edn. CRC Press, Boca Raton. ISBN 978-0-415-29900-8.

Enberg, K., Jørgensen, C., Dunlop, E. S., Varpe, Ø., Boukal, D. S., Baulier, L., Eliassen, S. & Heino, M. (2012). Fishing-induced evolution of growth: Concepts, mechanisms and the empirical evidence. *Marine Ecology*, 33, 1–25.

Fukasawa, K., Osada, Y. & Iijima, H. (2020). Is harvest size a valid indirect measure of abundance for evaluating the population size of game animals using harvest-based estimation? *Wildlife Biology*, 2020, wlb.00708.

Gore, J., Youk, H. & van Oudenaarden, A. (2009). Snowdrift game dynamics and facultative cheating in yeast. *Nature*, 459, 253–256.

Griffen, B. D. & Drake, J. M. (2008). A review of extinction in experimental populations. *Journal of Animal Ecology*, 77, 1274–1287.

Horsthemke, W. & Lefever, R. (2006). *Noise-induced transitions: theory and applications in physics, chemistry, and biology*. No. 15 in Springer series in synergetics, 2nd edn. Springer, Berlin. ISBN 978-3-540-11359-1.

Jonzén, N., Ripa, J. & Lundberg, P. (2002). A Theory of Stochastic Harvesting in Stochastic Environments. *The American Naturalist*, 159, 427–437.

Karl, T. R. & Trenberth, K. E. (2003). Modern Global Climate Change. *Science*, 302, 1719–1723.

Kaul, R. B., Kramer, A. M., Dobbs, F. C. & Drake, J. M. (2016). Experimental demonstration of an Allee effect in microbial populations. *Biology Letters*, 12, 20160070.

Kuparinen, A. & Merilä, J. (2007). Detecting and managing fisheries-induced evolution. *Trends in Ecology & Evolution*, 22, 652–659.

Lewin, W.-C., Arlinghaus, R. & Mehner, T. (2006). Documented and Potential Biological Impacts of Recreational Fishing: Insights for Management and Conservation. *Reviews in Fisheries Science*, 14, 305–367.

Lewontin, R. C. & Cohen, D. (1969). On Population Growth in a Randomly Varying Environment. *Proceedings of the National Academy of Sciences*, 62, 1056–1060.

Matsumura, S., Arlinghaus, R. & Dieckmann, U. (2011). Assessing evolutionary consequences of size-selective recreational fishing on multiple life-history traits, with an application to northern pike (Esox lucius). *Evolutionary Ecology*, 25, 711–735.

May, R. M. (1973). Stability in Randomly Fluctuating Versus Deterministic Environments. *The American Naturalist*, 107, 621–650.

Nolting, B. C. & Abbott, K. C. (2016). Balls, cups, and quasi-potentials: Quantifying stability in stochastic systems. *Ecology*, 97, 850–864.

Parkinson, E. A., Post, J. R. & Cox, S. P. (2004). Linking the dynamics of harvest effort to recruitment dynamics in a multistock, spatially structured fishery. *Canadian Journal of Fisheries and Aquatic Sciences*, 61, 1658–1670.

Ridolfi, L., DOdorico, P. & Laio, F. (2011). *Noise-Induced Phenomena in the Environmental Sciences*. Cambridge University Press, Cambridge. ISBN 978-0-511-98473-0. URL `http://ebooks.cambridge.org/ref/id/CBO9780511984730`.

Salinger, M. J. (2005). Climate Variability and Change: Past, Present and Future — an Overview. In: *Increasing Climate Variability and Change: Reducing the Vulnerability of*

Agriculture and Forestry (eds. Salinger, J., Sivakumar, M. & Motha, R. P.). Springer Netherlands, Dordrecht. ISBN 978-1-4020-4166-2, pp. 9–29.

Soetaert, K., Petzoldt, T. & Setzer, R. W. (2010). Solving Differential Equations in R: Package deSolve. *Journal of Statistical Software*, 33, 1–25.

Strogatz, S. H. (2001). *Nonlinear Dynamics and Chaos: With Applications to Physics, Biology, Chemistry, and Engineering*. Studies in Nonlinearity, 2nd edn. Perseus Books, Cambridge, Mass. ISBN 978-0-7382-0453-6.

Tuljapurkar, S. & Orzack, S. H. (1980). Population dynamics in variable environments I. Long-run growth rates and extinction. *Theoretical Population Biology*, 18, 314–342.

Uusi-Heikkilä, S., Whiteley, A. R., Kuparinen, A., Matsumura, S., Venturelli, P. A., Wolter, C., Slate, J., Primmer, C. R., Meinelt, T., Killen, S. S., Bierbach, D., Polverino, G., Ludwig, A. & Arlinghaus, R. (2015). The evolutionary legacy of size-selective harvesting extends from genes to populations. *Evolutionary Applications*, 8, 597–620.

Zimmermann, F. & Jørgensen, C. (2015). Bioeconomic consequences of fishing-induced evolution: A model predicts limited impact on net present value. *Canadian Journal of Fisheries and Aquatic Sciences*, 72, 612–624.

4.6 Appendix A: R Code

The functions used to simulate populations are listed below. The harvesting treatments were created and saved prior to running population simulations. The last two functions, OdeHarvestSim and ParaHarvestLogSim, are the parallel version of the previous functions.

- ScaleLogGrowth
- HarvestingSeries

- OdeHarvestSimAndSoln
- OdeHarvestSim
- ParaHarvestLogSim

```
library(deSolve)
library(foreach)
library(dplyr)
library(truncdist)

# Logistic growth ODE
ScaleLogGrowth <- function(t, y, params) {

  # Computes the rate of change of the variable y over time
  #
  # Args:
  #   t: vector of time points in the integration
  #   y: vector of variables in the differential equation
  #   params: vector of parameter values
  #
  # Returns:
  #   The rate of change of the variable y.

  N<-y #create local variable N

  with(as.list(c(params)), {
    dN <- r*N*(1-N)
    res <- c(dN)
    list(res)
  }
  )
```

```
}



#Simulate Harvest Time Series
HarvestingSeries = function(lam, #lambda vector
                            alp,  #alpha vector
                            explength = 10, #length of experiment in same
                               units of r (hours)
                            events = TRUE, # return in format for ODE
                               events
                            noreps = 2 # number of replicate series for
                               each alpha X lambda
){
    #make combination of a parameter values
    al <-  data.frame(cbind(lambda=rep(lam, each= length(alp)), alpha =
       alp, treatment = c(1:(length(lam)*length(alp)))))
    alplam <- data.frame(apply(al, 2, rep, each = noreps))
    alplam <- alplam %>% mutate(rep=rep(1:noreps, length=nrow(alplam)),
       simNo = c(1:nrow(alplam)))

    foreach(i = 1:nrow(alplam), .combine ='rbind') %do% {
       treatset <- alplam[i,]
      # interarrival times
        waitingtime <- NULL
        while(sum(waitingtime) < explength){
          waitingtime <- c(waitingtime, rexp(1, rate = alplam$lambda[i]))
        }
        #pull heights for each event from truncated exponential fnc
           between (0,1)
        height  <- data.frame(height= rtrunc(n=length(waitingtime),a=0,b
           =1,spec="exp", rate = 1/alplam$alpha[i]))
        # assemble event times and intensity
        harvesting <- as.data.frame(cbind(waitingtime, height))
```

```
        if(events == TRUE) {
          harvesting <- harvesting %>%
            mutate(contTime = cumsum(waitingtime)) %>%
            mutate(height) %>%
            mutate(event = seq(1,length(contTime), by=1)) %>%
            filter(contTime < explength) %>%
            mutate(var = "N", time=contTime, value = (1-height), method="
               mult",alpha=treatset$alpha, lambda =treatset$lambda ,
               treatment = treatset$treatment, rep =treatset$rep, simno =
               i) %>%
            select(var,time,value,method, treatment,alpha, lambda, rep,
               simno)
        } else {
          harvesting <- harvesting %>%
            mutate(contTime = cumsum(waitingtime)) %>%
            mutate(height) %>%
            mutate(event = seq(1,length(contTime), by=1), treatment =
               treatset$treatment, alpha=treatset$alpha, lambda =treatset$
               lambda, rep =treatset$rep, simno = i) %>%
            filter(contTime < explength)
        }

        return(harvesting)
      }
    }


#simulate noise and OSE solution
OdeHarvestSimAndSoln = function(lambda, alpha, length, params=c(r=0.36),
   Ninitial=c(N=0.5), plotit = TRUE){
  #create noise
  simulatedNoise <- HarvestingSeries(lam=lambda,alp = alpha, explength =
```

```
    length)
  #create events df
  sN <-simulatedNoise %>%
    mutate(var= "N", time=contTime, value = (1-height), method="mult") %>%
    select(var,time,value,method)
  # obs times for lsoda including event times
  times <- sort(c(sN$time, seq(0,length,1/60)))
  outTemp <-  as.data.frame(lsoda(Ninitial, times, ScaleLogGrowth, params,
      events = list(data = sN)))
  if(plotit == TRUE) {plot(outTemp, ylim=c(0,1))}

  return(list(outTemp,simulatedNoise))
}

## Parallel scripts

#simulate OSE solution given event df, eventsdf is one parameter
   combination treatment, with max(simno) replicates
OdeHarvestSim = function(params=c(r=0.36), Nstart=c(N=0.5), explength,
   eventsdf, resolution){
  # when interarrival time is very small the times values become too close
      to start integration despite using unique() [issue with floating
     point]. So I round the event times to 7 significant digits. The
     number of significant digits was based on the number of digits
     displayed in the console, not any analytical reason.

  require(dplyr)
  require(deSolve)

  merge.by.time <- function(a, b) {
    merge(a, b, by="time")
  }
```

```
  results <- foreach(i=unique(eventsdf$simno), .combine = 'merge.by.time'
     ) %do% {
        #eventsdf is output of HarvestingSeries which includes treatment
           and rep columns that need to be removed
        eventnames <- eventsdf %>% filter(simno == i)
        event <- eventnames %>%
          mutate(time = signif(time, digits=7)) %>%
          select(c(var, time, value, method))
          # obs times for lsoda including event times
          times <- unique(sort(c(event$time, seq(0,explength,resolution)))
             )
          outTemp <-  as.data.frame(lsoda(Nstart, times, ScaleLogGrowth,
             params, events = list(data = event)))
          #standardize time
          out <- outTemp[outTemp$time %in% seq(0,explength, resolution),]
          #rename N so has unique name when parallelized
          names(out)[2] <- paste("T",max(eventnames$treatment),"r",max(
             eventnames$rep),"N",Nstart,"_sim",max(eventnames$simno), sep=
             "")
          return(out)

      }
  return(results)
}


#Function to simulate logistic growth with compound Poisson harvest in
   parallel
ParaHarvestLogSim=function(alleventsdf, #output of HarvestingSeries
   function
                        N0.seq = c(N=0.5), #initial condition
                        parameters=c(r=0.360), #ODE
                        maxtime = 100, #max length of experiment in same
```

```
                          units of r (hours); same value used in noise
                          sim
                        cores=2, #number of cores to use in parallel
                        res = (5/60), #time interval to  return in hours
                        folder = '' #where to save simulations
) {

  require(dplyr)
  require(doParallel)
  require(foreach)


  merge.by.time <- function(a, b) {
    merge(a, b, by="time")
  }



  #
  # make cluster
  cl <- makeCluster(cores, outfile=paste(folder,"Log.txt"))
  registerDoParallel(cl)
  #results <-
  foreach(i = unique(alleventsdf$treatment),.export = c("OdeHarvestSim","
     ScaleLogGrowth","merge.by.time"), .packages = c("foreach", "dplyr", "
     deSolve")) %dopar% { #default returns each iteration as an entry in a
      list

    results <- foreach(j = 1:length(N0.seq), .combine = 'merge.by.time') %
       do% { #add back in when want to start from different initial
       conditions.
                  OdeHarvestSim(
                    Nstart = c(N=N0.seq[j]),
                    params=parameters,
```

```
                    eventsdf = alleventsdf %>% filter(treatment == i),
                    explength=maxtime,
                    resolution = res)
                }
  saveRDS(results, file = paste(folder,"T",i,".RDS",sep=""))

    }

  stopCluster(cl)
  #return(results)
}
```

R session information.

```
sessionInfo()
R version 4.0.4 (2021-02-15)
Platform: x86_64-apple-darwin17.0 (64-bit)
Running under: macOS Catalina 10.15.7

Matrix products: default
BLAS:   /System/Library/Frameworks/Accelerate.framework/Versions/A/
   Frameworks/vecLib.framework/Versions/A/libBLAS.dylib
LAPACK: /Library/Frameworks/R.framework/Versions/4.0/Resources/lib/
   libRlapack.dylib

locale:
[1] en_US.UTF-8/en_US.UTF-8/en_US.UTF-8/C/en_US.UTF-8/en_US.UTF-8

attached base packages:
[1] parallel  stats4    stats     graphics  grDevices utils     datasets
[8] methods   base

other attached packages:
```

```
[1] doParallel_1.0.16 iterators_1.0.13  truncdist_1.0-2   evd_2.3-3
[5] dplyr_1.0.5       foreach_1.5.1     deSolve_1.28

loaded via a namespace (and not attached):
 [1] Rcpp_1.0.6          pillar_1.5.1        compiler_4.0.4     plyr_1.8.6
 [5] bitops_1.0-6        tools_4.0.4         digest_0.6.27      evaluate_0.1
    4
 [9] lifecycle_1.0.0     tibble_3.1.0        pkgconfig_2.0.3    rlang_0.4.10
[13] yaml_2.2.1          xfun_0.22           stringr_1.4.0      knitr_1.31
[17] generics_0.1.0      vctrs_0.3.8         gtools_3.8.2       caTools_1.18
   .1
[21] tidyselect_1.1.0    glue_1.4.2          R6_2.5.0           fansi_0.4.2
[25] rmarkdown_2.7       purrr_0.3.4         reshape2_1.4.4     magrittr_2.0
   .1
[29] gplots_3.1.1        codetools_0.2-18    ellipsis_0.3.2     htmltools_0.
   5.1.1
[33] utf8_1.2.1          KernSmooth_2.23-18 stringi_1.5.3       crayon_1.4.1
```

Experimental demonstration of harvest noise-induced transition

5.1 Introduction

Finding sustainable harvesting practices is a driving application for population ecology. Overexploitation can lead to population collapse or anthropogenic extinction, and sustainable harvesting practices are one solution to this. An illustration of this is the extinction of the passenger pigeon of North America over less than 100 years of intense hunting (Brooks, 1955). Modern commercialized harvesting still struggles with overexploitation as demonstrated by the 1990s collapse of the Atlantic ground fisheries spanning from New England to Newfoundland and Labrador, which is just one of the estimated 366 harvest related fisheries collapses from 1955 to 2005 (Hutchings & Myers, 2011; Mullon *et al.*, 2005). These collapsed fisheries represent roughly one fourth of global fisheries, and can take decades to recover if at all (Mullon *et al.*, 2005).

Before collapse, the harvest targets for these fisheries were based on the theoretical concept of the maximum sustainable yield (MSY), or harvesting only enough individuals from the population to limit negative density dependent feedback and maintain the population's maximum growth rate (May *et al.*, 1978; Roughgarden & Smith, 1996). There are many potential reasons why MSY failed to maintain viable populations, including that harvest-

ing itself magnifies variance in the population size and increases the chance of extinction (Beddington & May, 1977; May *et al.*, 1978; Anderson *et al.*, 2008). However, harvesting does not always lead to reduced population stability or size. In discrete population models, harvesting can increase population stability or size by reducing the growth rate below the bifurcation point on the logistic map, or reducing overcompensatory dynamics (May, 1976; Jiménez López & Liz, 2021; Seno, 2008). To date, there has been little research into processes that could lead to similar results in continuous time models.

Most harvesting theory to date has assumed a constant stability landscape. Stability and equilibria can be visualized by plotting the potential function, known in ecology as a ball-in-cup or ball-and-valley model (as reviewed by Nolting & Abbott, 2016). Within this model, the stable equilibria are at the bottom of valleys, while the unstable equilibria are the inflection points on the peaks. The system, or ball, follows gravity to the closest valley. Changes in the system state are either due to a parameter change that shifts the valley accessible by the ball, or perturbations pushing the ball into another valley (Beisner *et al.*, 2003). For example, harvesting-related population collapse can act as a perturbation by pushing the ball into another valley near extinction, while in other systems a change in the harvesting rate parameter can cause the stability to switch such that peaks become valleys and vice versa. However, the theory of noise-induced transitions (NIT) provides an alternative mechanism for changes in equilibria. The NIT framework acknowledges that variability within the system can lead to qualitative changes in the stability landscape (Horsthemke & Lefever, 2006). Stability in deterministic and stochastic systems can be written in an expression. In the case of a deterministic system, linear stability analysis will result in point equilibria or limit cycles. However, stochastic systems by nature will never settle to a single point equilibria, but rather must be expressed in probabilistic terms. Equilibria in stochastic systems are defined by a stationary probability distribution (SPD) which can be found by solving the Fokker-Planck equation of the SDE (Horsthemke & Lefever, 2006). A transition occurs when the SPD goes through a qualitative change. This can be detected by tracking a

single metric, the SPD extrema. The expression for the SPD extrema consists of two terms. The first term is the deterministic equilibria, while the second term is multiplied by the noise intensity, meaning that as noise approaches zero the SPD extrema approach the deterministic equilibria. This is a key property that allows experimental detection of NITs, and is justification for treating the SPD extrema as equivalent to the deterministic equilibrium.

Noise-induced transitions are further categorized by the outcome. Proposed classifications include noise-induced extinction (NIE), noise-induced recovery (NIR), and noise-induced stability (NIS) (Ridolfi *et al.*, 2011; Bashkirtseva & Ryashko, 2018; Meng *et al.*, 2020a; Meyer & Shnerb, 2018). NIE follows ecologists' general dogmatic understanding of noise as a destabilizing force on system stability (Dennis *et al.*, 1991; Tuljapurkar & Orzack, 1980; Lewontin & Cohen, 1969) . There are many examples of noise-induced recovery or stability in community ecology, even if using a noise-induced framework is uncommon. Exceptions to the competitive exclusion principles like the paradox of the plankton, or more general competitor co-existence can be explained by variability in an environmental condition (Gause, 2003; D'Odorico *et al.*, 2005; Benincà *et al.*, 2008). Within mutualistic plant-pollinator networks, restoring degraded networks with species approaching near zero abundances is extremely difficult due to the hysteresis loop created by a saddle-node bifurcation at the critical mutualistic interaction strength value (Meng *et al.*, 2020b). However, these networks can be restored by increasing variability in species abundance and bypassing the hysteresis properties of the network (Meng *et al.*, 2020a). In the case of intertidal species assemblages in the Mediterranean, increases in the variance of stress due to air exposure time offset the negative impacts of sole increases in mean exposure time (Benedetti-Cecchi *et al.*, 2006). All of these examples are of communities, but is NIS possible in a single species system?

Harvesting noise-induced transition is an alternate explanation for the mismatch between MSY theory and application and has yet to be empirically explored. D'Odorico *et al.* (2006) has theoretically shown variability in the harvesting rate led to extirpation despite having a

sustainable mean harvesting rate.

To investigate this idea, I conducted experiments using populations of *Saccharomyces cerevisiae* (strain BY4741 SUC2:YFP). However, computer simulations parameterized for *S. cerevisiae* have shown variable harvesting to act as a stabilizing force (See Ch. 4). Here, I report on an empirical study designed to detect a harvesting noise-induced transition in experimental populations of *S. cerevisiae*. Harvesting noise was introduced into the microcosms by discrete proportional harvesting events of randomly drawn times and proportions, or white shot noise. The comparison of these populations to populations subject to a constant discrete proportional harvesting rate was used to demonstrate the causal link between harvesting noise and extinction. This study shows that a harvesting process with otherwise unsustainable mean harvesting rates can allow population persistence when the harvesting is characterized by stochastic noise.

5.2 Methods

The possibility of a harvest noise-induced transition was examined using spatially structured microcosms of *Saccharomyces cerevisiae* (strain BY4741 SUC2:YFP; Gore *et al.*, 2009). White shot noise within the discrete harvest process was introduced in the harvest frequency (λ) and the proportion of the population removed at a harvest(α; Ridolfi *et al.*, 2011).

Populations were subjected to either a fixed or stochastic harvest regime along a 4-point harvest frequency (λ) gradient at a single proportional harvest ($\alpha = 0.8$) as informed by the system model (Ch 4). Unique stochastic harvest series were created by drawing the time between harvests from an exponential distribution ($T \sim Exp(1/\lambda)$). For each stochastic harvest event, the proportional harvest was drawn from an exponential distribution with the upper bound truncated to one ($H \sim Exp(\alpha)$). In the case of the fixed harvest regimes, which act as a control, the harvest frequency and proportion harvested was set to the mean value of the stochastic harvest regime.

5.2.1 Culture & Harvesting Methods

Populations were grown on yeast synthetic media with complete supplement, 2% sucrose, and 2% agar in 100mm Petri dishes, and incubated at 30°C in a humidified chamber. The experiment was executed in replicate blocks of 12 populations. Each block contained 2 replicates, and a control fixed discrete harvest of the four λ ($\lambda/r = 0.12,0.28,0.44,0.60$) and α ($\alpha = 0.8$) treatments. All populations were started by plating $200\mu L$ of an overnight broth culture diluted to an OD_{600} of 0.03 ($\approx 500 cells/\mu L$) with fresh media. At a harvest event, the Petri dish was flooded with 1mL of sugar free media broth and cells were manually resuspended with a plate spreader. The suspended cells were transferred, and diluted to a total volume of 500 μL according to the proportional harvest treatment. Populations were censused at this point by a replicate spot plate assay using aliquots of 3 μL. The remaining volume of the newly diluted cells was then plated on pre-warmed agar plates. Once the plates were completely dry, they were sealed with parafilm and returned to the incubator. The extinction detection limit was set at 0.3 $cells\ \mu L^{-1}$ and was defined by no growth in the spot plate assay within 48 hours. The difference between the cell suspension volume (1mL) and the final dilution volume (0.5mL) allowed for some liquid to absorb into the agar without compromising the harvest treatment. This difference also means that populations were diluted at least 1:2 at every harvest event. Populations were maintained until extinction or 144 hours.

5.2.2 Data Analysis

The spot plate assay was used to score populations as present (0) or extinct (1) at each harvesting event. This binary outcome was used to fit a general linear model with a binomial family. The effect of the noisy harvest regime was tested using an ANOVA (type I sum of squares). A pairwise test for significance was done using a two sided Fisher's exact test given the small sample size.

5.3 Results

We found that noise within the harvest process increased the range of viable harvest frequencies (Fig. 5.1). The mean binomial outcome by treatment did not differ between the control and treatment harvest regime for three of the harvest frequency treatments. However, at harvest frequency 0.44, the control harvest regime was significantly more likely to go extinct when compared to the noisy harvest treatment (Fisher's; p-value = 0.001). Additionally, we found qualitative agreement between the model predictions and experimental results. Two contaminated populations within the same experimental block were removed. The contaminant was easily identifiable by color and mobility. The removals reduced the total number of harvest regime treatment replicates to 13 for harvest frequencies of 0.28, and 0.44. The control populations were not effected.

5.4 Discussion

This study provides the first experimental demonstration of noise-induced persistence in a biological system. These findings are contrary to the paradigm of noise as a destabilizing force. In the case of this system, the mean harvesting frequency could be increased by $\approx 16\%$ (from 28% to 44% of r) without increasing the probability of extinction. The increased range in sustainable harvesting frequency could be substantial enough to meaningfully change the total harvested individuals over a period of time. The D'Odorico *et al.* (2006) model characterized tree-grass dynamics in savannas. In savannas, fire can push the system to one of two states, tree or grass dominated, depending on frequency and intensity. If fire is modeled as a stochastic process, the system develops an intermediate state of tree-grass coexistence in a subset of harvesting by fire parameters, while in an other parameter space bistability between the tree and grass dominated states arise. These new stability patterns are unique to the stochastic model, when compared to the deterministic equivalent, which has

a single stable state at a proportion of the carry capacity dictated by the harvest frequency and intensity.

Given these previous findings, we expected our model to predict regions of harvest parameters that led to bistability, and regions where the preferential state lies between extinction and carrying capacity (D'Odorico *et al.*, 2006; Ridolfi *et al.*, 2011). This was the case in our model with the standard harvest process, but not in the model including the harvesting modifications needed to accommodate experimental logistics. Essentially, the modified harvesting protocol almost doubled the mean (2α) and reduced the variance by 75% ($0.25\alpha^2$) of the harvest intensity, α parameter. After the harvesting modifications were incorporated into simulations, the regions of bistability and suppressed carrying capacity in the harvesting parameter space disappeared. Instead, the region of harvesting parameters that led to a non-zero preferred population size increased. The difference in outcomes of the standard and modified harvesting regime indicate the importance of the noise distribution as related to the transition. While the modified harvest regime may be unlikely in practice, this theoretical analysis created predictions that can now be experimentally tested in *S. cerevisiae* populations. The phenomenon of noise-induced persistence is not unique to our study system, and has been observed in theoretical models of tumor cell growth and mutual interaction networks (Meng *et al.*, 2020b; Zeng & Wang, 2010; Yang *et al.*, 2014). Outside of the biological literature, this increased stability has arisen in many models, and an experimental electrical system (Dayan *et al.*, 1992; Mantegna & Spagnolo, 1996; Fiasconaro *et al.*, 2005).

While the generality of noise-induced persistence within biological systems must be established by future research, this experimental demonstration has provided clear support that noise can act as a stabilizing force allowing populations to persist despite unsustainable mean conditions. The possibility of noise-induced transitions stresses the need to move from a deterministic to stochastic paradigm for population management. This result requires ecologists to re-examine the assumption that extirpation of a managed population was due to overexploitation, and has the potential to alter management practices.

5.5 Figures

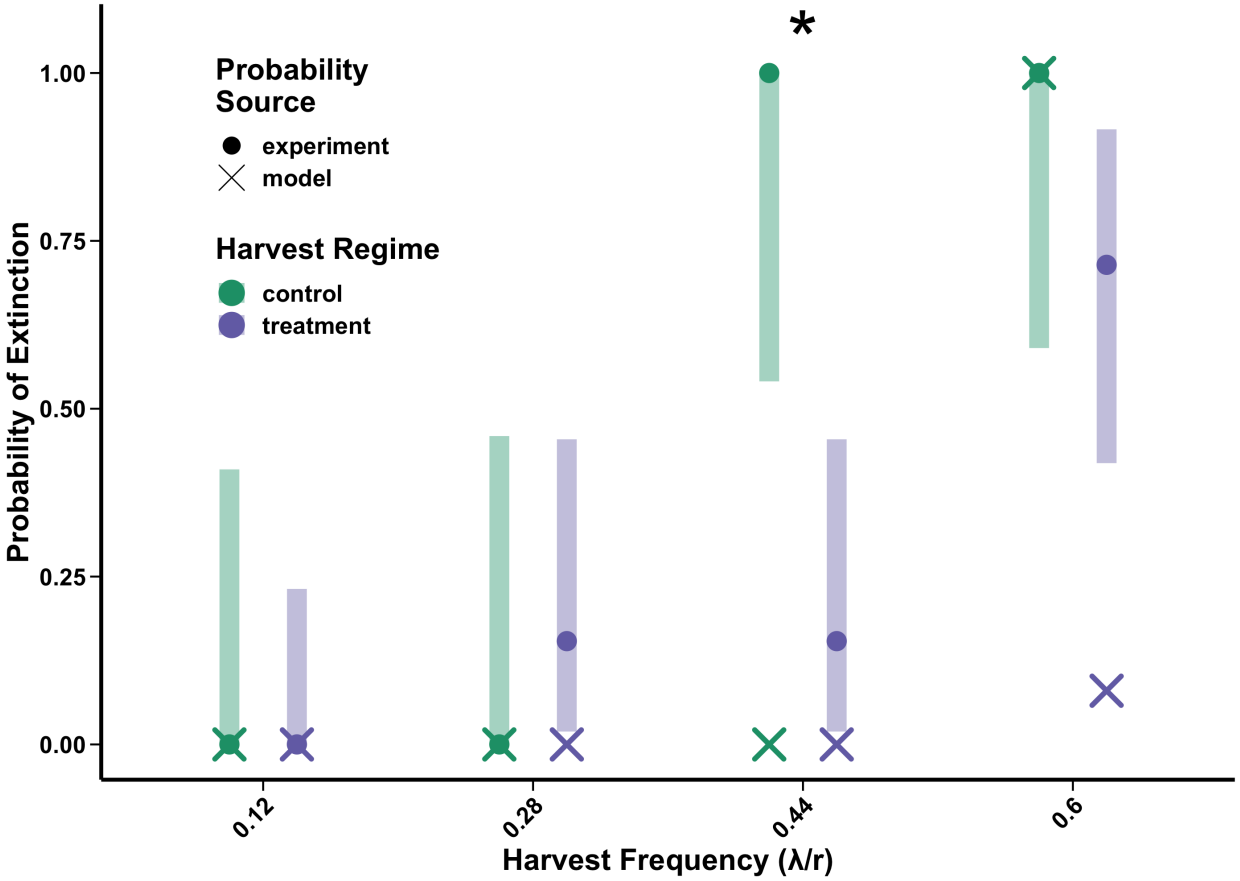

Figure 5.1: The probability of extinction for the noisy and fixed harvest regimes is plotted as a function of harvest frequency. The point estimates are from model simulations (x), and the experimental mean ($\circ$) of the binary outcome of each population for the control (n=7) and treatment (n=14) populations and the binomial confidence interval which was calculated using the exact method. An ANOVA of a generalized linear model using a binomial family indicated an effect of the harvest regime and frequency (λ/r). Significant difference between the control and harvest regimes is indicated with an asterisk ($*$; p-value = 0.001).

Bibliography

Anderson, C. N. K., Hsieh, C.-h., Sandin, S. A., Hewitt, R., Hollowed, A., Beddington, J., May, R. M. & Sugihara, G. (2008). Why fishing magnifies fluctuations in fish abundance. *Nature*, 452, 835–839.

Bashkirtseva, I. & Ryashko, L. (2018). Stochastic Sensitivity Analysis of Noise-Induced Extinction in the Ricker Model with Delay and Allee Effect. *Bulletin of Mathematical Biology*, 1–19.

Beddington, J. R. & May, R. M. (1977). Harvesting Natural Populations in a Randomly Fluctuating Environment. *Science*, 197, 463–465.

Beisner, B. E., Haydon, D. T. & Cuddington, K. (2003). Alternative stable states in ecology. *Frontiers in Ecology and the Environment*, 1, 376–382.

Benedetti-Cecchi, L., Bertocci, I., Vaselli, S. & Maggi, E. (2006). Temporal Variance Reverses the Impact of High Mean Intensity of Stress in Climate Change Experiments. *Ecology*, 87, 2489–2499.

Benincà, E., Huisman, J., Heerkloss, R., Jöhnk, K. D., Branco, P., Van Nes, E. H., Scheffer, M. & Ellner, S. P. (2008). Chaos in a long-term experiment with a plankton community. *Nature*, 451, 822–825.

Brooks, M. (1955). Review of The Passenger Pigeon: Its Natural History and Extinction. *The Wilson Bulletin*, 67, 228–230.

Dayan, I., Gitterman, M. & Weiss, G. H. (1992). Stochastic resonance in transient dynamics. *Physical Review A*, 46, 757–761.

Dennis, B., Munholland, P. L. & Scott, J. M. (1991). Estimation of Growth and Extinction Parameters for Endangered Species. *Ecological Monographs*, 61, 115–143.

D'Odorico, P., Laio, F. & Ridolfi, L. (2005). Noise-induced stability in dryland plant ecosystems. *Proceedings of the National Academy of Sciences of the United States of America*, 102, 10819–10822.

D'Odorico, P., Laio, F. & Ridolfi, L. (2006). A Probabilistic Analysis of Fire-Induced Tree-Grass Coexistence in Savannas. *The American Naturalist*, 167, E79–E87.

Fiasconaro, A., Spagnolo, B. & Boccaletti, S. (2005). Signatures of noise-enhanced stability in metastable states. *Physical Review E*, 72, 061110.

Gause, G. (2003). *The Struggle for Existence*. Dover Books on Biology Series. Dover Publications. ISBN 978-0-486-49520-0.

Gore, J., Youk, H. & van Oudenaarden, A. (2009). Snowdrift game dynamics and facultative cheating in yeast. *Nature*, 459, 253–256.

Horsthemke, W. & Lefever, R. (2006). *Noise-Induced Transitions: Theory and Applications in Physics, Chemistry, and Biology*. No. 15 in Springer Series in Synergetics, 2nd edn. Springer, Berlin. ISBN 978-3-540-11359-1.

Hutchings, J. A. & Myers, R. A. (2011). What Can Be Learned from the Collapse of a Renewable Resource? Atlantic Cod, Gadus morhua, of Newfoundland and Labrador. *Canadian Journal of Fisheries and Aquatic Sciences*.

Jiménez López, V. & Liz, E. (2021). Destabilization and chaos induced by harvesting: Insights from one-dimensional discrete-time models. *Journal of Mathematical Biology*, 82, 3.

Lewontin, R. C. & Cohen, D. (1969). On Population Growth in a Randomly Varying Environment. *Proceedings of the National Academy of Sciences*, 62, 1056–1060.

Mantegna, R. N. & Spagnolo, B. (1996). Noise Enhanced Stability in an Unstable System. *Physical Review Letters*, 76, 563–566.

May, R. M. (1976). Simple mathematical models with very complicated dynamics. *Nature*, 261, 459–467.

May, R. M., Beddington, J. R., Horwood, J. W. & Shepherd, J. G. (1978). Exploiting natural populations in an uncertain world. *Mathematical Biosciences*, 42, 219–252.

Meng, Y., Jiang, J., Grebogi, C. & Lai, Y.-C. (2020a). Noise-enabled species recovery in the aftermath of a tipping point. *Physical Review E*, 101, 012206.

Meng, Y., Lai, Y.-C. & Grebogi, C. (2020b). Tipping point and noise-induced transients in ecological networks. *Journal of The Royal Society Interface*, 17, 20200645.

Meyer, I. & Shnerb, N. M. (2018). Noise-induced stabilization and fixation in fluctuating environment. *Scientific Reports*, 8, 9726.

Mullon, C., Fréon, P. & Cury, P. (2005). The dynamics of collapse in world fisheries. *Fish and Fisheries*, 6, 111–120.

Nolting, B. C. & Abbott, K. C. (2016). Balls, cups, and quasi-potentials: Quantifying stability in stochastic systems. *Ecology*, 97, 850–864.

Ridolfi, L., DOdorico, P. & Laio, F. (2011). *Noise-Induced Phenomena in the Environmental Sciences*. Cambridge University Press, Cambridge. ISBN 978-0-511-98473-0.

Roughgarden, J. & Smith, F. (1996). Why fisheries collapse and what to do about it. *Proceedings of the National Academy of Sciences*, 93, 5078–5083.

Seno, H. (2008). A paradox in discrete single species population dynamics with harvesting/thinning. *Mathematical Biosciences*, 214, 63–69.

Tuljapurkar, S. & Orzack, S. H. (1980). Population dynamics in variable environments I. Long-run growth rates and extinction. *Theoretical Population Biology*, 18, 314–342.

Yang, T., Zhang, C., Zeng, C., Zhou, G., Han, Q., Tian, D. & Zhang, H. (2014). Delay and noise induced regime shift and enhanced stability in gene expression dynamics. *Journal of Statistical Mechanics: Theory and Experiment*, 2014, P12015.

Zeng, C. & Wang, H. (2010). Colored Noise Enhanced Stability in a Tumor Cell Growth System Under Immune Response. *Journal of Statistical Physics*, 141, 889–908.

Conclusion

Ecologists have long been interested in understanding population dynamics, especially catastrophic changes (Lewontin & Cohen, 1969; May, 2001; Scheffer, 2020). These catastrophic changes, or disproportionately large state shifts in response to a changing kinetic parameter or perturbation, are often explained using an alternative stable states framework (Nolting & Abbott, 2016). Returning to the ball-in-valley model, there are two paths to these large shifts. Either the system moves into another valley due to an external push, or the valley itself moves due to a change in a kinetic parameter. However, May (1973) proposed a third path to a substantial change in the populations' stable states. This third path, noise-induced transitions, takes into account the stochasticity found in the natural world. When this noise is incorporated into population models, equilibria can move similar to a kinetic parameter change or new equilibria can arise and/or disappear. This work experimentally demonstrates two sub-types of NITs in biological systems; noise-induced extinctions and noise-induced persistence. Noise-induced extinctions fall within ecologists' dogmatic understanding of environmental stochasticity (Lewontin & Cohen, 1969; Dennis *et al.*, 1991; Tuljapurkar & Orzack, 1980). However, noise-induced persistence within a single population challenges our understanding of environmental noise and its impact on systems. Depending on the prevalence of NITs in biological systems, this could be a shaping force in the natural world that has been ignored until now.

The possibility of a noise-induced extinction was explored using *Aphanizomenon flos-*

aqua algal chemostats. Environmental noise was introduced by continuously varying the incident light which is akin to the random normal carrying capacity example presented by May (1973). The constant incident light parameter was replaced with a random normal variable in a mechanistic algal growth model originally published by Huisman & Weissing (1994). Simulated populations with sufficiently large variance in light conditions went extinct despite an ideal mean light condition. This model prediction was used to guide the chemostat experimental design. Unfortunately, the experimental set up proved to be too unpredictable to identify where the stability transition takes place along a noise gradient, just that it exists. This experimental system and contrived source of environmental variability is useful for model-based reasoning and reasoning by analogy to natural systems (Drake & Kramer, 2012). The combined theoretical and empirical approach used for this work could be especially useful when estimating the indirect anthropogenic effect of increased environmental stochasticity due to climate change (Thornton *et al.*, 2014).

Noise-induced persistence was demonstrated in populations of *Saccharomyces cerevisiae* subject to variable discrete harvesting events (strain BY4741 SUC2:YFP ; Gore *et al.*, 2009). White shot harvesting events were drawn from a Poisson process ($T \sim Exp(1/\lambda)$, and the proportion of the population removed at a harvest event was drawn from a truncated exponential distribution with an expected value of α. Previous theoretical studies of stochastic harvesting predicted a transition to extinction rather than persistence (Ridolfi *et al.*, 2011). The difference between past studies and the one presented here is caused by harvesting modifications required to accommodate bench limitations. These modifications reduced variance in the proportional harvest variable by 75% creating a condensed distribution when compared to the original exponential distribution. The transect of harvest frequencies used in the bench experiments were based on model predictions of the transition to persistence threshold. The transition to persistence was captured in the experimental data, where populations harvested at a frequency of half the growth rate $\lambda/r = 0.44$ under a white shot harvest regime were significantly less likely to go extinct when compared to fixed harvest populations. This

work suggests the need for noise-induced transitions to be incorporated into harvest theory, especially as applied to fisheries, given humans' direct control of harvesting practices (Anderson *et al.*, 2008; Jonzén *et al.*, 2002; Braumann, 1999; Parkinson *et al.*, 2004; Fukasawa *et al.*, 2020).

This dissertation first presents the implications of destabilizing effects of environmental noise as expected under ecological dogma of stochasticity. Then, I present the surprising result of noise-induced persistence in stochastically harvested populations. These are just two vignettes of the possible nonlinear dynamics and environmental stochasticity observed in natural populations. By building a concept map of the noise-induced outcomes of different combinations of nonlinear dynamics and types of environmental noise, we can develop a heuristic understanding of how and when a stochastic rather than deterministic model is a more appropriate description of the natural world. With this understanding in hand, we can start to build a more nuanced NIT framework that incorporates other stability related phenomena like fishing induced evolution (Uusi-Heikkilä *et al.*, 2015). Over the last century, community ecologist have sought to develop a holistic understanding of stability in a changing world (Chesson, 2000). It is time for population ecologists to follow by moving from a deterministic representation of the world to one which incorporates multiple sources of stochasticity and thinks of stability in quasi-stationary terms.

Bibliography

Anderson, C. N. K., Hsieh, C.-h., Sandin, S. A., Hewitt, R., Hollowed, A., Beddington, J., May, R. M. & Sugihara, G. (2008). Why fishing magnifies fluctuations in fish abundance. *Nature*, 452, 835–839.

Braumann, C. A. (1999). Variable effort fishing models in random environments. *Mathematical Biosciences*, 156, 1–19.

Chesson, P. (2000). Mechanisms of Maintenance of Species Diversity. *Annual Review of Ecology and Systematics*, 31, 343–366.

Dennis, B., Munholland, P. L. & Scott, J. M. (1991). Estimation of Growth and Extinction Parameters for Endangered Species. *Ecological Monographs*, 61, 115–143.

Drake, J. M. & Kramer, A. M. (2012). Mechanistic analogy: How microcosms explain nature. *Theoretical Ecology*, 5, 433–444.

Fukasawa, K., Osada, Y. & Iijima, H. (2020). Is harvest size a valid indirect measure of abundance for evaluating the population size of game animals using harvest-based estimation? *Wildlife Biology*, 2020, wlb.00708.

Gore, J., Youk, H. & van Oudenaarden, A. (2009). Snowdrift game dynamics and facultative cheating in yeast. *Nature*, 459, 253–256.

Huisman, J. & Weissing, F. J. (1994). Light-Limited Growth and Competition for Light in Well-Mixed Aquatic Environments: An Elementary Model. *Ecology*, 75, 507–520.

Jonzén, N., Ripa, J. & Lundberg, P. (2002). A Theory of Stochastic Harvesting in Stochastic Environments. *The American Naturalist*, 159, 427–437.

Lewontin, R. C. & Cohen, D. (1969). On Population Growth in a Randomly Varying Environment. *Proceedings of the National Academy of Sciences*, 62, 1056–1060.

May, R. M. (1973). Stability in Randomly Fluctuating Versus Deterministic Environments. *The American Naturalist*, 107, 621–650.

May, R. M. (2001). *Stability and Complexity in Model Ecosystems*. Princeton Landmarks in Biology, 1st edn. Princeton University Press, Princeton. ISBN 0-691-08861-6.

Nolting, B. C. & Abbott, K. C. (2016). Balls, cups, and quasi-potentials: Quantifying stability in stochastic systems. *Ecology*, 97, 850–864.

Parkinson, E. A., Post, J. R. & Cox, S. P. (2004). Linking the dynamics of harvest effort to recruitment dynamics in a multistock, spatially structured fishery. *Canadian Journal of Fisheries and Aquatic Sciences*, 61, 1658–1670.

Ridolfi, L., DOdorico, P. & Laio, F. (2011). *Noise-Induced Phenomena in the Environmental Sciences*. Cambridge University Press, Cambridge. ISBN 978-0-511-98473-0.

Scheffer, M. (2020). *Critical Transitions in Nature and Society*. Princeton University Press. ISBN 978-1-4008-3327-6.

Thornton, P. K., Ericksen, P. J., Herrero, M. & Challinor, A. J. (2014). Climate variability and vulnerability to climate change: A review. *Global Change Biology*, 20, 3313–3328.

Tuljapurkar, S. & Orzack, S. H. (1980). Population dynamics in variable environments I. Long-run growth rates and extinction. *Theoretical Population Biology*, 18, 314–342.

Uusi-Heikkilä, S., Whiteley, A. R., Kuparinen, A., Matsumura, S., Venturelli, P. A., Wolter, C., Slate, J., Primmer, C. R., Meinelt, T., Killen, S. S., Bierbach, D., Polverino, G., Ludwig, A. & Arlinghaus, R. (2015). The evolutionary legacy of size-selective harvesting extends from genes to populations. *Evolutionary Applications*, 8, 597–620.